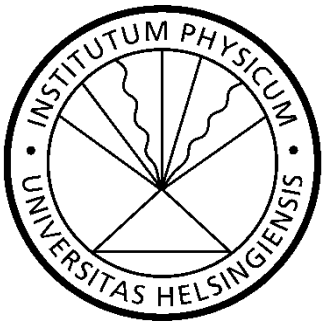

Master's Thesis

Materials and nanophysics

^{14}C - CO_2 Measurements with Accelerator Mass Spectrometry

Tomi Vuoriheimo

17.9.2017

Supervisor: Vesa Palonen, Pertti Tikkanen

Examiners: Pertti Tikkanen, Jyrki Räisänen

UNIVERSITY OF HELSINKI
DEPARTMENT OF PHYSICS

P.O. Box 64 (Gustaf Hällströmin katu 2)
00014 University of Helsinki

HELSINGIN YLIOPISTO – HELSINGFORS UNIVERSITET – UNIVERSITY OF HELSINKI

Tiedekunta/Osasto – Fakultet/Sektion – Faculty/Section	Laitos – Institution – Department	
Faculty of Science	Department of Physics	
Tekijä – Författare – Author		
Tomi Vuoriheimo		
Työn nimi – Arbetets titel – Title		
14C-CO2 Measurements with Accelerator Mass Spectrometry		
Oppiaine – Läroämne – Subject		
Physics		
Työn laji – Arbetets art – Level	Aika – Datum – Month and year	Sivumäärä – Sidoantal – Number of pages
Master's thesis	September 2017	68

Tiivistelmä – Referat – Abstract

Accelerator mass spectrometry (AMS) is a technique developed from mass spectrometry and it is able to measure single very rare isotopes from samples with detection capability down to one atom in 10^{16}. It uses an accelerator system to accelerate the atoms and molecules to break molecular bonds for precise single isotope detection.

This thesis describes the optimization of University of Helsinki's AMS system to detect the rare radioactive isotope ^{14}C from CO_2 gas samples. Using AMS to detect radiocarbon is a precise and fast way to conduct radiocarbon dating with minimal sample sizes. Solid graphite samples have been in use before but as the ion source has been adopted to use also gaseous CO_2 samples, optimizations must be made to maximize the carbon current and ionization efficiency for efficient ^{14}C detection.

Parameters optimized include cesium oven temperature, CO_2 flow, carrier gas helium flow and their dependencies with each other. Both carbon current and ionization efficiency is looked at in the optimizations. The results are analyzed and discussed for further optimizations or actual measurements with gas. Ionization occurring in the ion source can be understood better with the results.

Standard samples of CO_2 were measured to determine the background and precision of the AMS system in gas use by comparing the results with literature. The current system was found to have tolerable background of 1.5% of the standard and the Fraction modern value of actual sample was 2.4% higher than values from literature. Ideas to improve background were discussed.

A new theory of negative-ion formation in a cesium sputtering ion source by John S. Vogel is reviewed and taken into account in the discussion of optimization. Utilizing the theory, possible future upgrades to improve the ionization efficiency are presented such as cathode material choices to reduce competitive ionization and cesium excitation by laser.

Avainsanat – Nyckelord – Keywords

Accelerator Mass Spectrometry, AMS, Radiocarbon, CO2 ion source, Optimization

Säilytyspaikka – Förvaringställe – Where deposited

Muita tietoja – Övriga uppgifter – Additional information

HELSINGIN YLIOPISTO – HELSINGFORS UNIVERSITET – UNIVERSITY OF HELSINKI

Tiedekunta/Osasto – Fakultet/Sektion – Faculty/Section	Laitos – Institution – Department	
Matemaattis-luonnontieteellinen tiedekunta	Fysiikan laitos	
Tekijä – Författare – Author		
Tomi Vuoriheimo		
Työn nimi – Arbetets titel – Title		
14C-CO2 Measurements with Accelerator Mass Spectrometry		
Oppiaine – Läroämne – Subject		
Fysiikka		
Työn laji – Arbetets art – Level	Aika – Datum – Month and year	Sivumäärä – Sidoantal – Number of pages
Pro gradu -tutkielma	Syyskuu 2017	68

Tiivistelmä – Referat – Abstract

Kiihdytinmassaspektrometria (AMS) on massaspektrometriasta jatkokehitetty tekniikka, joka pystyy mittaamaan yksittäisiä harvinaisia isotooppeja näytteistä havaintotarkkuudella yksi atomi 10^{16} atomista. AMS käyttää kiihdytinsysteemiä kiihdyttääkseen atomit ja molekyylit. Törmäyttämällä molekyylit jalokaasuun molekyylien sidokset voidaan hajottaa tarkkaa yhden tietyn isotoopin mittaamista varten.

Tämä tutkielma kuvaa Helsingin yliopiston AMS-systeemin optimointia CO_2 -kaasunäytteillä tehtäviä harvinaisen radioaktiivisen ^{14}C isotoopin mittauksia varten. AMS:n käyttäminen radiohiilen mittaamiseen on tarkka ja nopea tapa tehdä radiohiiliajoituksia hyvin pienistäkin näytteistä. Kiinteitä grafiittinäytteitä on käytetty mittauksissa aiemmin, mutta koska ionilähde on muunnettu käyttämään myös CO_2-kaasunäytteitä, täytyy laitteistoa optimoida mahdollisimman suuren hiilivirran sekä ionisaatiotehokkuuden saavuttamiseksi tehokasta ^{14}C-havaitsemista varten.

Optimoituja parametrejä ovat esimerkiksi kesium-uunin lämpötila, CO_2 -virtausnopeus, kuljetuskaasu heliumin virtausnopeus ja näiden riippuvuudet keskenään. Sekä hiilivirta että ionisaatiotehokkuudet on huomioitu optimoinnissa. Tulokset on analysoitu ja pohdittu jatko-optimointeja tai oikeita kaasumittauksia varten. Ionisaatiota ionilähteessä pystyy ymmärtämään paremmin tulosten kanssa.

Standardinäytteet mitattiin CO_2 -kaasulla taustan ja AMS-systeemin tarkkuuden määrittämiseksi kaasukäytössä vertaamalla tuloksia kirjallisuusarvoihin. Tämänhetkisellä systeemillä havaittiin 1,5 % tausta standardiin verrattuna ja oikean näytteen Fraction modern –tulos oli 2,4 % korkeampi kuin kirjallisuudessa. Ideoita taustan parantamiseen pohdittiin.

Uusi John S. Vogelin ionisaatioteoria cesiumionilähteessä käytiin läpi, ja teoriaa hyödynnettiin optimoinnin tuloksien pohdinnassa. Tulevia mahdollisia ionilähteen päivityksiä on esitetty teoriaan perustuen. Näihin päivityksiin kuuluvat esimerkiksi katodin materiaalivalinnat kilpaillun ionisaation vähentämiseksi ja cesiumin virittäminen laserilla.

Avainsanat – Nyckelord – Keywords

Kiihdytinmassaspektrometria, AMS, Radiohiili, CO2 ionilähde, Optimointi

Säilytyspaikka – Förvaringställe – Where deposited

Muita tietoja – Övriga uppgifter – Additional information

Acknowledgements

I would like to thank my thesis supervisor Dr. Vesa Palonen for helping with the measurements and for good discussion about the subject. With his help I was able to do all the measurements in time, analyze the results, and write the thesis without problems, and Dr. Pertti Tikkanen for helping writing and improving the thesis and being the examiner. I would also like to thank Professor Jyrki Räisänen for introducing me this subject for the thesis and being the second examiner. I also want to thank all the other staff at the accelerator mass spectrometry research group, Pietari Kienanen and Mikko Mannermaa, for helping and teaching with the measurements. With their participation I was able to learn more about handling the equipment.

Finally I want to express my gratitude to my friends for discussing about writing the thesis, to my parents for supporting me throughout the university and to my girlfriend Makana for supporting and encouraging me writing this thesis. Thank you.

Contents

1 Introduction

Determining the age of organic material by using the radioactive isotope of carbon, ^{14}C, has been one of the most reliable and used methods during past several decades [1]. This method is called radiocarbon dating. Taking advantage of 5730 year half-life of ^{14}C isotope, it is possible to determine the age of carbon containing materials. As the radioactive carbon isotope slowly decays, it is difficult to measure carbon from materials with the age of several tens of thousands of years. With samples older than this, there is not enough ^{14}C isotope left for accurate measurements as the background of the measurement becomes too high. Possible samples include not only archeological objects but also carbon containing gases and liquids such as oil.

For several decades since 1950's the only way to determine the age of ^{14}C isotope was to measure the number of decays within a given amount of carbon. Comparing this to the number of decays from a modern carbon containing material, it was possible to find out how large portion of the carbon had decayed, thus giving an approximation of the age. Measurements relying on decay events were slow and often required large masses of samples for accurate measurements. In 1970's, accelerator mass spectrometry (AMS) was developed as a faster and more precise way to measure the amount of ^{14}C isotope [2].

AMS measurements do not rely on decay events. Instead, the exact ratio of number of ^{14}C, ^{13}C and ^{12}C isotopes can be measured. This allows measurements to be made with higher precision, shorter measurement times, and samples with smaller masses, for example allowing measurements of older or smaller samples than it was possible before.

Conventional AMS techniques measure the carbon from graphite which is prepared from CO_2 gas. Newer techniques allow measurements directly from the CO_2 gas, eliminating the slow graphite preparation phase and making it possible to measure even smaller samples down to 1 µg [3]. Even though first measurements with CO_2 were done in 1980's [4], handling gas instead of solid samples causes new problems to be solved though, such as storing the gas, transferring it and suitable gas flow, making solid graphite to be the more used sample. Hybrid AMS systems which can measure both solid and gas samples are becoming more popular and therefore the problems within the gas system need to be solved

and the ion source optimized for gas. This also requires further knowledge of the ionization procedures inside the ion source.

This thesis explains the basics behind radiocarbon dating starting from the original decay measurements. After this the AMS is presented with ways how it has affected the way to measure ^{14}C. The newly built gas injection system for University of Helsinki is introduced and its operation explained for the hybrid AMS. The main part of the thesis is about optimizing the ion source for efficient gas usage. A theory about negative-ion formation of carbon in plasma is presented and the results of measurements are discussed to see how they support the theory. Different parameters affecting the ionization rate for gas are explained, measured and results analyzed. Finally, standard gases are measured and analyzed for actual future measurements.

2 Radiocarbon dating

Carbon has three different isotopes that can be observed in atmosphere: $^{12}\mathrm{C}$, $^{13}\mathrm{C}$ and $^{14}\mathrm{C}$. Two of these isotopes are stable, $^{12}\mathrm{C}$ and $^{13}\mathrm{C}$, with the corresponding atomic abundance of 98.9% and 1.1% in the atmosphere. $^{14}\mathrm{C}$ is a radioactive and rare isotope. Its concentration is only 10^{-12} in the atmosphere and it is being constantly produced by cosmic rays . [5]

Being able to determine the age of items from their atomic composition has greatly affected archeology. Having a chronological order of events is very important and the discovery of the radioactive carbon isotope $^{14}\mathrm{C}$ made it possible to develop radiocarbon dating. $^{14}\mathrm{C}$ has a half-life of 5730 years which means that its decaying is easy to see for the past few tens of thousands of years, ideal for many archeological events.

$^{14}\mathrm{C}$ is mostly produced in upper atmosphere by cosmic radiation. Neutrons formed by the cosmic radiation hit the nitrogen atoms in the atmosphere, causing a nuclear reaction in which the nitrogen emits a proton and becomes radioactive carbon isotope:

$$\mathrm{n} + {}^{14}_{7}\mathrm{N} \rightarrow {}^{14}_{6}\mathrm{C} + \mathrm{p} \qquad (1)$$

Production of $^{14}\mathrm{C}$ and therefore its concentration in the atmosphere is usually constant within short time scales. This combined with the radioactive decay of the isotope causes a dynamic equilibrium in the atmosphere where the production and decay are in balance, giving us a constant concentration which is only changed by other events such as nuclear bomb testing or additional radiation from supernovas. The exact production mechanisms and production rates are poorly known but for the actual radiocarbon measurements only the radiocarbon concentration in the atmosphere is needed, making it possible to get precise results even without understanding the actual production process. Other things affecting the production rate are solar cycles and the magnetic field of Earth. These changes are affecting the production greatly in larger timescales so knowledge about them is also needed for better accuracy in measurements. [6]

Once the radiocarbon has been produced in the atmosphere, it rapidly forms CO and $\mathrm{CO_2}$. Measurements show that most of the radiocarbon forms CO and only a small portion forms $\mathrm{CO_2}$ instantly. There have been results that show the $\mathrm{CO_2}$ portion to be 7% [7] or in more recent studies up to 23% [8]. From the atmosphere the radiocarbon enters into living

organisms through photosynthesis. This causes a certain fraction of carbon inside plants to be $^{14}\mathrm{C}$. This fraction is the same as in the atmosphere at that time. Changes in local $^{12}\mathrm{C}/^{14}\mathrm{C}$ ratio can cause differences in different areas but these are usually very local. Changes include for example higher CO_2 production near coal plants after industrial revolution or areas with high volcanic activity for increased $^{12}\mathrm{C}$ or nuclear power plants for increased $^{14}\mathrm{C}$. [6]

As the CO_2 gets incorporated to plants' cells through photosynthesis, it passes along to animals through food chain. It is possible to see even yearly changes in radiocarbon in trees that have annual tree rings because the cells in older rings are no longer getting new carbon from the atmosphere inside them. This causes only the newest rings to be in equilibrium with environment. With animals, most carbon inside them has been incorporated to plants recently because most animals eat newer, fresh parts of plants such as leaves and not the old woody material. This helps with radiocarbon dating as the intake of radiocarbon stays approximately constant. [6,9]

In water environments such as oceans and lakes the concentration of radiocarbon is different from that in the atmosphere. Oceans and lakes function as CO_2 reservoirs, taking some from atmosphere and releasing some back. Water currents mix the water in oceans but there are some areas in which water is moving less, causing large differences in $^{12}\mathrm{C}/^{14}\mathrm{C}$ ratio. This occurs especially within deep seas. The difference in $^{12}\mathrm{C}/^{14}\mathrm{C}$ ratio needs to be taken into account when measuring samples from marine environments as organisms living in surface waters have less radiocarbon than organisms on land but more than organisms living in deep waters. [1,9]

2.1 Decay measurements

Radiocarbon decays through beta decay:

$$^{14}_{6}\mathrm{C} \rightarrow {}^{14}_{7}\mathrm{N} + \mathrm{e}^{-} + \bar{\nu}_{\mathrm{e}} \qquad (2)$$

In general, radioactive decay happens exponentially:

$$A = A_0 e^{-\lambda t} = A_0 e^{-\frac{\mathrm{t}*\ln 2}{t_{1/2}}} \qquad (3)$$

When considering a material containing carbon, the radiocarbon inside it starts to decay as presented in equation (3), in which A_0 is the activity of radiocarbon in atmosphere and $t_{1/2}$ is the half-life of $^{14}\mathrm{C}$ isotope. This half-life was originally estimated to be 5568 $\pm$ 30 years, first measurements done in 1949 by Libby [10]. Later experiments gave an estimate of 5730 $\pm$ 40 years which is still often used as the more standard half-life [11]. Because the original half-life had been in use for some time before more accurate times were calculated, the 5568 years became the standard in radiocarbon dating. [6]

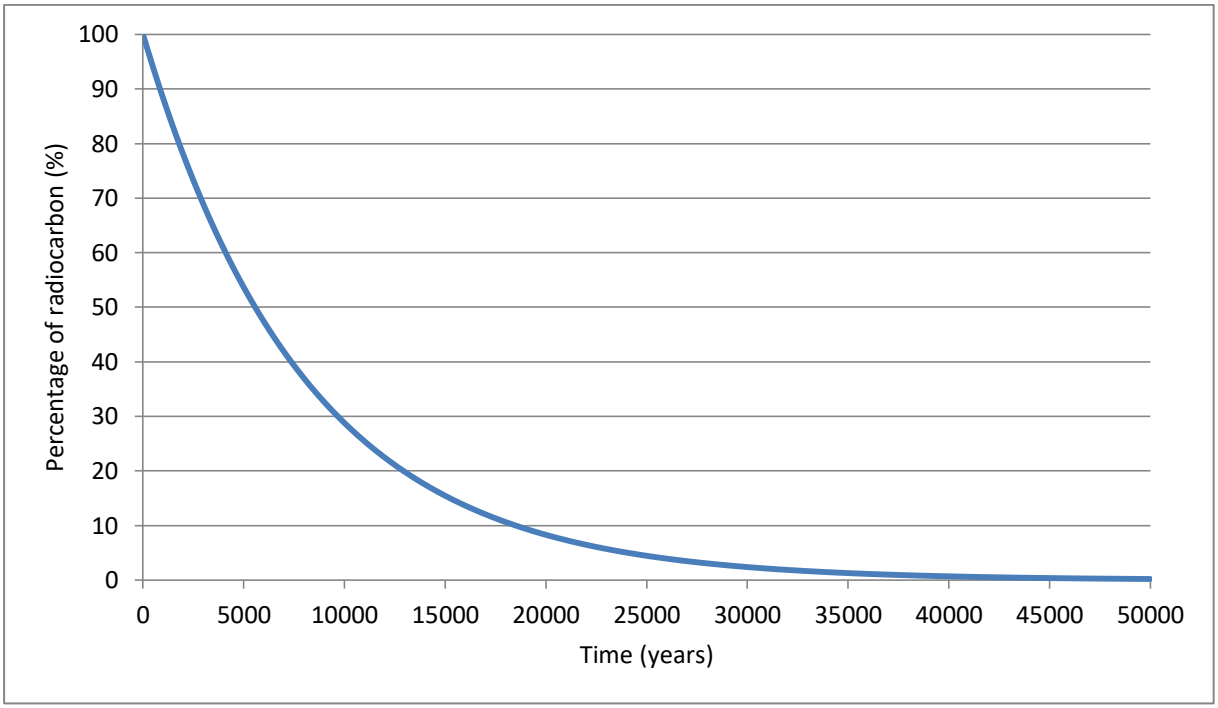

Figure 1: *The amount of radiocarbon remaining in a sample counting back from modern atmosphere values. The original half-life of 5568 years is used with equation (3) to get these results. It can be seen that the amount of radiocarbon is reduced to very small amounts after 30 000 years and very little remains after 50 000 years.*

There was a need for standard activity to measure and compare results done in different laboratories. Because industrialization and nuclear tests were affecting the amount of $^{14}\mathrm{C}$ greatly, a standard was made to fit the value of the natural atmospheric concentration of the year 1950. This value was not however the isotopic ratio in the atmosphere. The standard was calculated to correspond to the ratio when there was no effect from CO_2 emissions from industrialization. Therefore a wood sample from 1890 was used to calculate the natural isotopic ratio for the year 1950. All radiocarbon dating results are compared to this standard value and the age is presented in units of Before Present (BP) which is the number of years

calculated back from year 1950. More about standards and age calculations is in chapter 2.2. [12,13]

The first radiocarbon measurements were done by Libby in 1940's [10] with carbon extracted from a sample and converted to solid carbon. A special Geiger counter had its inner walls coated with the solid carbon and it had to be well shielded from ionizing cosmic radiation. Beta radiation coming from the radiocarbon ionizes gas inside the Geiger counter and the ions and electrons are accelerated to the detectors by applying an electric field between the sample and the detector. These decay events are then detected and counted by registering the electric current from the electrons and ions as each pulse represents a decay event. This type of counter registers the number of decays happening in certain time, giving a value of sample activity. With the known mass of carbon sample, it is possible to calculate the fraction of radiocarbon in it. [12]

Gas proportional counters quickly replaced the original radiation counters using solid samples. These types of counters can detect beta radiation more easily as the ionizations are multiplied by avalanche effect in which the original ionization caused by the first electron causes more ionizations and this large pulse is then detected. The gas inside the detector is different compared to a normal Geiger meter because it needs to be able to cause the avalanche ionizations but also to inhibit the ionization so that they will eventually stop when hitting the detectors. Gas proportional counters made it possible to use CO_2 gas samples, which also made the sample preparation easier by skipping the solidification of carbon from CO_2. [14]

Later, liquid scintillation counting type of detectors were developed and optimized for radiocarbon dating. These types of detectors use liquid samples such as benzene in which the sample material is dissolved. Beta radiation from the radiocarbon excites phosphors in the liquid. Phosphors are molecules that emit light when they receive energy from the beta radiation. The emitted photons can then be detected by photocathodes as electric pulses as the photons leave the liquid, thus allowing counting of decay events. Producing samples takes longer time compared to gas proportional counters but this detection technique allows measurements for smaller samples, reducing the minimum mass of carbon from around 8 grams to about 2 grams. [14]

2.2 Measurement of isotopic ratios

As the measurements of decay events were slow and unefficient, scientists started to develop devices that could measure the relation of the stable isotope of ^{12}C and the radiocarbon ^{14}C as this could reveal the remaining amount of radiocarbon more accurately than counting the decay events. In addition to faster measurements and more reliable results, the sample sizes could be even smaller because the sample size is no longer affecting the amount of decays. [14]

Measuring the isotopic ratio of ^{12}C and ^{14}C is not easy because of all the carbon in atmosphere, only 10^{-10}% is ^{14}C compared to 98.9% of ^{12}C. The ratio gets even lower in old samples in which the radiocarbon has partly decayed. Because of this low amount of radiocarbon in samples, the number of atoms often sets a limit to the minimum mass of carbon that needs to be measured, even with 100% detection rate. For example, to get a precision of 0.3% there must be 10^5 atoms of radiocarbon which means 2 µg of carbon even for modern samples and about 10 µg for older ones. [6]

Accelerator mass spectrometry, which will be explained in more detail in chapter 3, was developed to count individual atoms of radiocarbon. As the efficiencies of AMS are usually at the scale of 1%, the minimum mass needed for measurements will be around 1 mg ideally. This is still much smaller amount than the few grams needed for decay measurements at minimum [6]. With improvements continuously happening with the AMS systems, there are also laboratories which are capable of measuring carbon down to tens of micrograms with solid samples [15] and down to 1 µg with gas samples [3]. Efficiencies are also getting better and the AMS used in this thesis's experiments can achieve precision better than 0.2% with solid graphite samples [16].

When measuring ratio of the isotopes instead of decay events, it is important not to let anything affect the natural ratio of the two isotopes. However, there are always some changes happening to the ratio of isotopes in chemical reactions and physical processes because of their different atomic masses. This phenomenon is called fractionation. In chemical reactions, it can be caused by different equilibrium constants for different isotopes. Some physical processes, such as evaporation, can have a slightly different effect for different isotopes. For example, the $^{14}C/^{12}C$ ratio after photosynthesis differs with the ratio

in atmosphere because larger and heavier isotopes $^{14}\mathrm{C}$ and $^{13}\mathrm{C}$ move more slowly through the photosynthesis reactions. [9,13]

Fractionation needs to be taken into account when doing the analysis for the radiocarbon ratio with corrections in the equations. Instead of calculating the fractionation from isotopic $^{14}\mathrm{C}/^{12}\mathrm{C}$ ratio, it is usually calculated from the more easily measurable $^{13}\mathrm{C}/^{12}\mathrm{C}$ ratio. The quantity which describes this ratio is $\delta^{13}\mathrm{C}$. It depends on the ratio but it is also compared to a standard material with known ratio. Originally the standard was a fossil PDB (Pee Dee Belemnite) with $^{13}\mathrm{C}/^{12}\mathrm{C}$ ratio of 1.12372% but as it was depleted, a new standard called VPDB (Vienna Pee Dee Belemnite) was manufactured from marble and is still in use [13].

The following steps to calculate the normalized activity of a sample are taken from *A guide to radiocarbon units and calculations* [13] and *Radiocarbon, Reporting of* ^{14}C *data* [17].

The equation for calculating $\delta^{13}\mathrm{C}$ is

$$\delta^{13}\mathrm{C} = \left(\frac{(^{13}\mathrm{C}/^{12}\mathrm{C})_S - (^{13}\mathrm{C}/^{12}\mathrm{C})_{VPDB}}{(^{13}\mathrm{C}/^{12}\mathrm{C})_{VPDB}} \right) \times 1000‰ \qquad (4)$$

In equation 4, $(^{13}\mathrm{C}/^{12}\mathrm{C})_S$ is the isotope ratio of the sample and $(^{13}\mathrm{C}/^{12}\mathrm{C})_{VPDB}$ is the ratio of the standard material.

Table 1: *$\delta^{13}C$ values for some typical materials from nature [17].*

Material	$\delta^{13}\mathrm{C}$ (‰)
Leaves	-27 (-22 to -32)
Recent wood, charcoal	-25 (-20 to -30)
Plants from arid environments	-13 (-9 to -17)
Fossil wood, charcoal	-24 (-20 to -27)
Peats, humus	-27 (-20 to -33)
Bone collagen, wood cellulose	-20 (-18 to -24)
Fresh water plants (submerged)	-16 (-4 to -24)
Marine plants (submerged)	-12 (-8 to -17)
Atmospheric CO_2	-9 (-6 to -11)
Marine carbonates (shells)	0 (4 to -4)

Using the age correction factor $\delta^{13}C$ the sample activity needs to be normalized. Normalization of the sample material is done by handling the material as if it was wood, meaning that normalization is made to change its $\delta^{13}C$ to -25‰. For this a fractionation factor is used.

$$\mathrm{Frac}_{13/12} = \frac{(^{13}C/^{12}C)_{[\delta^{13}C=-25‰]}}{(^{13}C/^{12}C)_S} \tag{5}$$

In equation (5) $(^{13}C/^{12}C)_{[\delta^{13}C=-25‰]}$ is the ratio of a standard material with $\delta^{13}C$ of $-25‰$ and $(^{13}C/^{12}C)_S$ is the ratio of the two isotopes in the sample. The ^{14}C fractionation factor can be estimated to be the square of $\mathrm{Frac}_{13/12}$ as

$$\mathrm{Frac}_{14/12} \approx \mathrm{Frac}_{13/12} * \mathrm{Frac}_{14/13} \approx \left(\mathrm{Frac}_{13/12}\right)^2 \tag{6}$$

With this, the normalized activity of the sample can be calculated with

$$A_{SN} = A_S * \mathrm{Frac}_{14/12} \approx A_S * \left(\mathrm{Frac}_{13/12}\right)^2 = A_S \left(\frac{\left(\frac{^{13}C}{^{12}C}\right)_{[\delta^{13}C=-25‰]}}{\left(\frac{^{13}C}{^{12}C}\right)_S} \right)^2 \tag{7}$$

Equation (7) can be expressed in a different way using equation (4).

$$A_{SN} = A_S \left(\frac{\left(1 - \frac{25}{1000}\right)((^{13}C/^{12}C)_{VPDB})}{\left(1 + \frac{\delta^{13}C}{1000}\right)((^{13}C/^{12}C)_{VPDB})} \right)^2 = A_S \left(\frac{0.975}{\left(1 + \frac{\delta^{13}C}{1000}\right)} \right)^2$$
$$\approx A_S \left(1 - \frac{2(25 + \delta^{13}C)}{1000}\right) \tag{8}$$

The last step of equation (8) is an approximation which causes a maximum error of 1‰ for values between -35‰ and 3‰.

To find out the age of a sample, its $^{14}C/^{12}C$ ratio, or activity, must be compared with a known standard. As mentioned before, the activity of the year 1950 was calculated and standard materials having this activity have been used since. Original standard material that has been in use is NIST oxalic acid ($C_2H_2O_4$), often named OxI. It was made from sugar beet in year 1955 but because of nuclear tests raising the radiocarbon levels in the atmosphere,

the sample had too much radiocarbon compared to the year 1950. This was taken into account in the calculations as the year 1950 had 95% activity compared to the standard material. The isotope correction $\delta^{13}\mathrm{C}$ was normalized to -19‰ with this standard. Equation (8) stated with this 95% activity and $\delta^{13}\mathrm{C}$ of -19‰ would then make the OxI normalized as

$$A_{ON} = 0.95 A_{OxI}\left(1 - \frac{2(19 + \delta^{13}\mathrm{C_{OxI}})}{1000}\right) \qquad (9)$$

This original standard is no longer in use and a newer version of the oxalic acid, OxII, is now commonly used with $\delta^{13}\mathrm{C}$ of -17.8‰. Equation (8) expressed with this standard makes it

$$A_{ON} = 0.7459 A_{OxII}\left(1 - \frac{2(25 + \delta^{13}\mathrm{C_{OxII}})}{1000}\right) \qquad (10)$$

When using these standards, they must be measured and normalized using these equations by inserting the activity found during the measurements.

As both the sample and the standard decay their $^{14}\mathrm{C}$ with the same rate, time of measurement does not affect the A_{SN}/A_{ON} ratio as they both have been normalized to the year 1950. If the original half-time of 5568 years is assumed, age of the sample, given in Before Present, can be calculated with

$$t = -8033 \ln\frac{A_{SN}}{A_{ON}} \qquad (11)$$

Result of the measurement can also be given in *percent Modern* (pM), which means how many percent there is left of the $^{14}\mathrm{C}$ compared to modern (year 1950) levels. But as the standard of the year 1950 keeps decaying, it is important to insert the absolute activity of the year 1950 to the calculations. This can be done with the following equation with the use of equation (3).

$$A_{ABS} = A_{ON} e^{\lambda(y-1950)} \qquad (12)$$

In equation (12), *y* is the year of measurement and $\lambda = \frac{1}{8267}\frac{1}{\mathrm{yr}}$, based on the corrected 5730 year half-life of $^{14}\mathrm{C}$. Using this, the percent Modern can be expressed with the following equation.

$$pM = \frac{A_{SN}}{A_{ABS}} \times 100\% = \frac{A_{SN}}{A_{ON} e^{\lambda(y-1950)}} \times 100\% \quad (13)$$

Downside of pM is that its value changes depending on the time of measurement. This is because the absolute value of the year 1950 does not change but the sample keeps decaying. To cover this change, corrections must be made to equation (13). One way to correct this is the use of pMC, which uses the decaying standard instead of its absolute value.

$$pMC = \frac{A_{SN}}{A_{ON}} \times 100\% \quad (14)$$

Another equation with corrected sample time is called *absolute international standard.* Instead of changing the absolute activity, it makes a correction to the activity of the sample to set it to the year 1950 levels. It however does not have correction for $\delta^{13}\mathrm{C}$ and therefore A_S is used instead of A_{SN}. It is defined as

$$\delta^{14}\mathrm{C} = \left(\frac{A_S e^{\lambda(y-x)}}{A_{ABS}} - 1\right) \times 1000‰ \quad (15)$$

In equation (15), *y* is the year of measurement and *x* is the year of growth. With normalization for $\delta^{13}\mathrm{C}$, equation (15) can be expressed as

$$\Delta = \left(\frac{A_{SN} e^{\lambda(y-x)}}{A_{ABS}} - 1\right) \times 1000‰ = \left(\frac{A_{SN} e^{\lambda(1950-x)}}{A_{ON}} - 1\right) \times 1000‰ \quad (16)$$

Nowadays, the result of a radiocarbon measurement is usually given as *Fraction Modern* *($F^{14}C_m$)* which compares the result value with the year 1950 value but also having background corrections in terms of $\delta^{13}\mathrm{C}$ applied. Fraction Modern is therefore expressed with both normalized sample activity A_{SN} and normalized standard activity A_{ON}. This also means that the results do not depend on measurement time.

$$F^{14}C_m = \frac{A_{SN}}{A_{ON}} = \frac{pMC}{100\%} = \frac{A_{SN}}{A_{ABS} e^{\lambda(1950-y)}} \quad (17)$$

In equation (17), *y* is again the year of measurement and $\lambda = \frac{1}{8267}\frac{1}{\mathrm{yr}}$. [13]

Most of the equations shown here require the activity of the radiocarbon. However, use of AMS gives the results as $^{14}\mathrm{C}/^{13}\mathrm{C}$ or $^{14}\mathrm{C}/^{12}\mathrm{C}$ ratio. When using this ratio instead of activity,

small changes need to be made to the equations for calculating Fraction Modern [13,18]. This is because the ratio of $^{14}C/^{12}C$ needs the fractionation correction twice. With $^{14}C/^{13}C$ there only needs to be one correction. This changes equation (8) and the equations derived from it to

$$\left(\frac{^{14}C}{^{12}C}\right)_{SN} = \left(\frac{^{14}C}{^{12}C}\right)_{S} \left(\frac{\left(1-\frac{25}{1000}\right)}{\left(1+\frac{\delta^{13}C}{1000}\right)}\right)^{2} \quad (18)$$

$$\left(\frac{^{14}C}{^{12}C}\right)_{ON} = 0.95\left(\frac{^{14}C}{^{12}C}\right)_{OxI} \left(\frac{\left(1-\frac{19}{1000}\right)}{\left(1+\frac{\delta^{13}C_{OxI}}{1000}\right)}\right)^{2} = 0.7459\left(\frac{^{14}C}{^{12}C}\right)_{OxII} \left(\frac{\left(1-\frac{25}{1000}\right)}{\left(1+\frac{\delta^{13}C_{OxII}}{1000}\right)}\right)^{2} \quad (19)$$

$$\left(\frac{^{14}C}{^{13}C}\right)_{SN} = \left(\frac{^{14}C}{^{13}C}\right)_{S} \left(\frac{\left(1-\frac{25}{1000}\right)}{\left(1+\frac{\delta^{13}C}{1000}\right)}\right) \quad (20)$$

$$\left(\frac{^{14}C}{^{13}C}\right)_{ON} = 0.95\left(\frac{^{14}C}{^{13}C}\right)_{OxI} \left(\frac{\left(1-\frac{19}{1000}\right)}{\left(1+\frac{\delta^{13}C_{OxI}}{1000}\right)}\right) = 0.7459\left(\frac{^{14}C}{^{13}C}\right)_{OxII} \left(\frac{\left(1-\frac{25}{1000}\right)}{\left(1+\frac{\delta^{13}C_{OxII}}{1000}\right)}\right) \quad (21)$$

$$F^{14}C_m = \frac{\left(\frac{^{14}C}{^{12}C}\right)_{SN}}{\left(\frac{^{14}C}{^{12}C}\right)_{ON}} = \frac{\left(\frac{^{14}C}{^{13}C}\right)_{SN}}{\left(\frac{^{14}C}{^{13}C}\right)_{ON}} \quad (22)$$

Measurements done in this thesis use the ratio of $^{14}C/^{13}C$ and therefore equations (20) and (21) are used.

From the measurements, two of the most important quantities are the $^{14}C/^{13}C$ ratios and number of ^{14}C atoms detected. By inserting the $^{14}C/^{13}C$ ratio of standard to equation (21) and the ratio of sample to equation (20) with their $\delta^{13}C$ values measured or from literature, the fractionation normalized $\left(\frac{^{14}C}{^{13}C}\right)_{SN}$ and $\left(\frac{^{14}C}{^{13}C}\right)_{ON}$ can be calculated. By inserting these values to equation (22), value of *Fraction Modern* can be calculated.

Background of the measurement is measured using for example a fossil fuel sample with very few ^{14}C atoms in it. Therefore most of the detected ^{14}C atoms are coming from the

equipment and can be classified as background. Background with the fossil fuel sample is measured as the normal sample and its Fraction Modern $F^{14}C_{bg}$ is calculated. With this value, the background reduced Fraction Modern $F^{14}C$ of the actual sample can be calculated with the following equation:

$$F^{14}C = F^{14}C_m \left[1 - F^{14}C_{bg}\left(\frac{1}{F^{14}C_m} - 1\right)\right] \quad (23)$$

Number of $^{14}\mathrm{C}$ atoms detected is used to calculate the relative error of the measured $^{14}\mathrm{C}/^{13}\mathrm{C}$ ratio. Longer measurements and more $^{14}\mathrm{C}$ counts make the error smaller. This is why long measurements and high number of $^{14}\mathrm{C}$ counts are preferred. Equation used for calculating the relative error is

$$err = \frac{1}{\sqrt{N}} \quad (24)$$

In equation (24), *N* is the number of detected $^{14}\mathrm{C}$ atoms. To calculate the full error, also the statistical dispersion of the measurement results is taken into account and for example the larger error of these is used.

3 Accelerator mass spectrometry

This chapter explains the basics of AMS and presents the equipment used in this thesis's measurements. Differences between solid and gas sample systems are also explained.

3.1 Overview

As explained in chapter 2.2, accelerator mass spectrometry was developed to measure the $^{14}\mathrm{C}/^{13}\mathrm{C}$ ratio instead of counting individual decay events. It was known that in theory measuring the $^{14}\mathrm{C}/^{13}\mathrm{C}$ ratio should be able to give much more precise results and faster than with decay measurements. Therefore research was made to be able to count the single $^{14}\mathrm{C}$ atoms. The way to do this was to further develop mass spectrometers.

When charged particles are moving in electromagnetic field, they are affected by Lorentz force:

$$\boldsymbol{F} = Q(\boldsymbol{E} + \boldsymbol{v} \times \boldsymbol{B}), \tag{25}$$

in which Q is electric charge, $\boldsymbol{E}$ is external electric field and $\boldsymbol{B}$ is magnetic field. This Lorentz force combined with Newton's second law (26) tells us how the carbon ions move in electric field.

$$\boldsymbol{F} = m\boldsymbol{a} \tag{26}$$

$$\left(\frac{m}{Q}\right)\boldsymbol{a} = \boldsymbol{E} + \boldsymbol{v} \times \boldsymbol{B} \tag{27}$$

Charged particles in perpendicular magnetic field move in circular motion according to equation (27). If the magnetic field $\boldsymbol{B}$, electric field $\boldsymbol{E}$ and the velocity of the incoming particles $\boldsymbol{v}$ are all assumed to be constants as in ideal mass spectrometer, then the radial acceleration $\boldsymbol{a}$ will only depend on the mass/charge ratio $\frac{m}{Q}$. This changes the path of ions inside mass spectrometer and lets us choose a certain $\frac{m}{Q}$ ratio to detector, meaning filtering of chosen momentum. Electric fields are used as kinetic energy filters. Even if the momentum of two ions is the same, one being slower is affected more by an electric field as the ion stays in the field longer time. This effect can accelerate ions with wrong energies so that they collide on the walls.

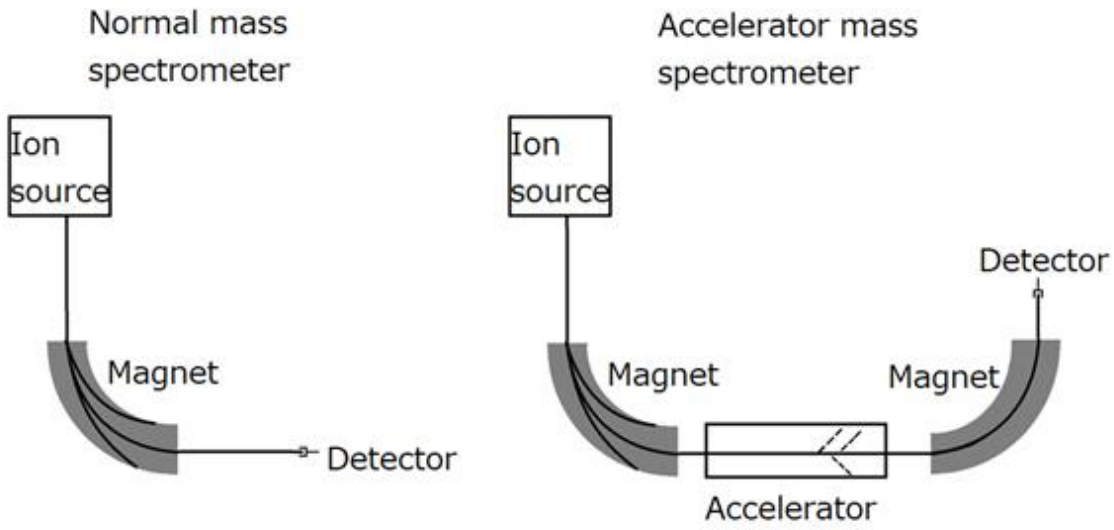

Figure 2: *Simplified comparison of normal mass spectrometer and accelerator mass spectrometer.*

As seen in Figure 2, normal mass spectrometers only have one magnet for separating different masses. This causes all the ions with the same $\frac{m}{Q}$ ratio to be detected and is the main reason why normal mass spectrometers cannot detect $^{14}\mathrm{C}$. As 1.1% of carbon in atmosphere is $^{13}\mathrm{C}$ and it is a stable isotope, it is measurable with mass spectrometers. But because of the very low number of $^{14}\mathrm{C}$ atoms, $10^{-10}\%$ at most, other atoms and molecules with similar mass, such as $^{14}\mathrm{N}$, $^{13}\mathrm{CH}$ and $^{12}\mathrm{CH}_2$, can easily affect the result more than the $^{14}\mathrm{C}$ itself, making normal mass spectrometers useless [12,19].

First successful AMS measurements were done in 1977 by several groups with high energy nuclear accelerators which used accelerating energies of several megavolts [20–22]. This way of separating $^{14}\mathrm{C}$ atoms had two important ideas. Using an ion source that produces negative ions from carbon can be used to eliminate $^{14}\mathrm{N}$ as nitrogen does not form negative ions. Then, using a high energy nuclear accelerator the negative ions are accelerated and guided through a stripper gas or a foil which takes electrons from the atoms and molecules passing it. Atoms get a high positive charge of +3 or +4 but as molecules lose many electrons, causing a Coulomb explosion which means that the bonds break in the molecule because of large Coulombic repulsion between different atoms. After the accelerator there is a second magnet which once again selects the correct mass from the ion beam from the accelerator. This allows precise selection of $^{14}\mathrm{C}$ atoms. [12]

3.2 Main equipment

There are two main parts in AMS machinery. One is the ion source in which ionization of carbon happens and the other is the actual spectrometer with the accelerator. Here ionization means the formation of a negative carbon ion. This chapter presents the equipment used in this thesis's experiments at University of Helsinki, Faculty of Science. Theory about the ionization is in more detail in chapter 5.

3.2.1 Ion source

Ion source used for the AMS measurements is a 40 sample multi-cathode sputter ion source MC-SNICS made by National Electrostatics Corporation. The ion source produces negative ions by sputtering the cathode with cesium. Schematic of the ion source is shown in Figure 3 and the ion source in use is shown in Figure 4.

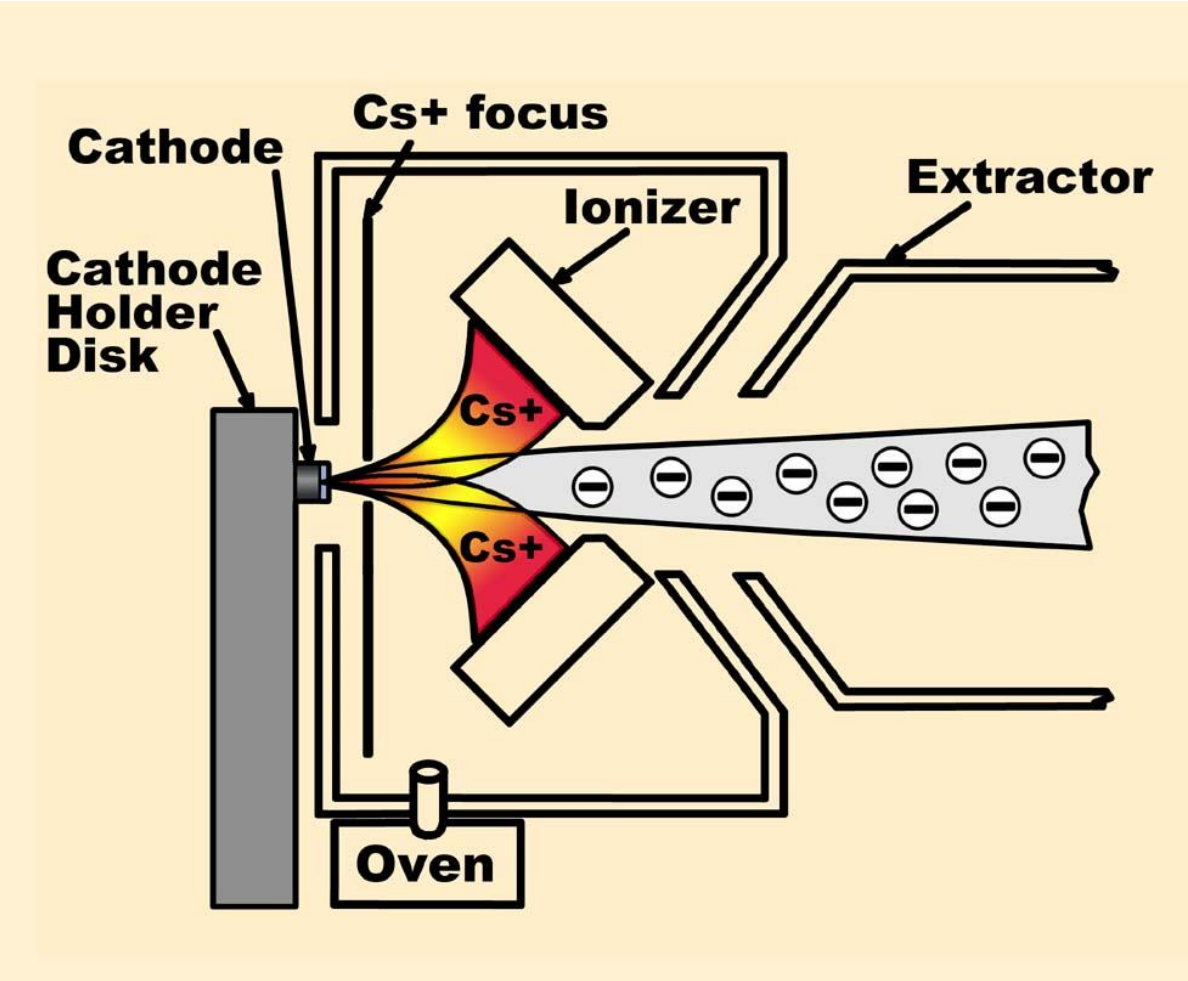

Figure 3: *Schematic of the 40 MC-SNICS ion source used in the measurements. Figure by National Electrostatics Corp.®. Taken from [23].*

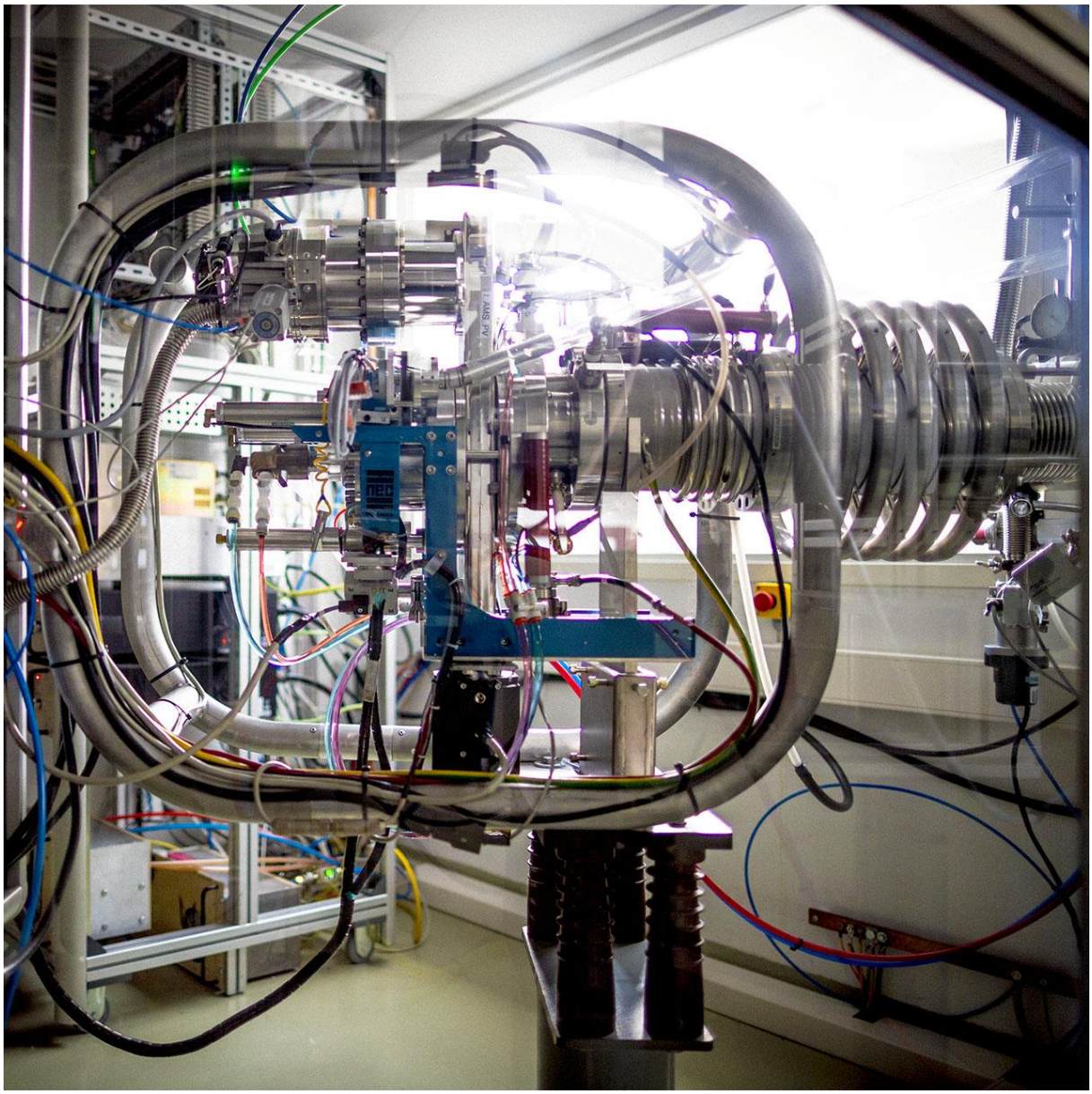

Figure 4: *The 40 MC-SNICS ion source used in the measurements. Photo taken by Alexandre Pirojenko.*

Cesium for sputtering comes from a cesium oven whose temperature can be controlled to choose the amount of cesium used for sputtering. The cesium comes as vapor to the space between the cold cathode and heated ionizer surface. Some of the cesium condenses on the cold cathode and some is ionized on the hot surface. The ionized cesium is accelerated towards the cathode with controllable voltage. Between the hot ionizer and cold cathode, there is also an immersion lens which is used to focus the ion beam to hit precisely to the cathode. As the accelerated cesium atoms hit the sample on the cathode, particles are sputtered from it. Negative ions are accelerated away from the cathode by extractor's

voltage. Positive and neutral particles can gain electrons near the surface from the cesium ions and are accelerated after this. [23]

The ion source is originally built for solid samples but modifications have been made to transform the ion source to a hybrid source which can ionize both solid and gas samples. Schematic of the modified ion source with the capillary tube for gas can be seen in Figure 5. Gas samples allow measurement of even smaller samples than with solid samples and also removes the slow phase of converting CO_2 to graphite as the CO_2 can be inserted to the ion source as gas. This again makes possible to measure more samples as the CO_2-to-graphite conversion is currently the bottleneck in sample preparation and measuring timewise.

For gas usage, special titanium gas cathodes are used. They have a hole for the carrier gas helium and CO_2 to flow from the back. Gas cathodes need to be inserted to the sample slots for gas measurements.

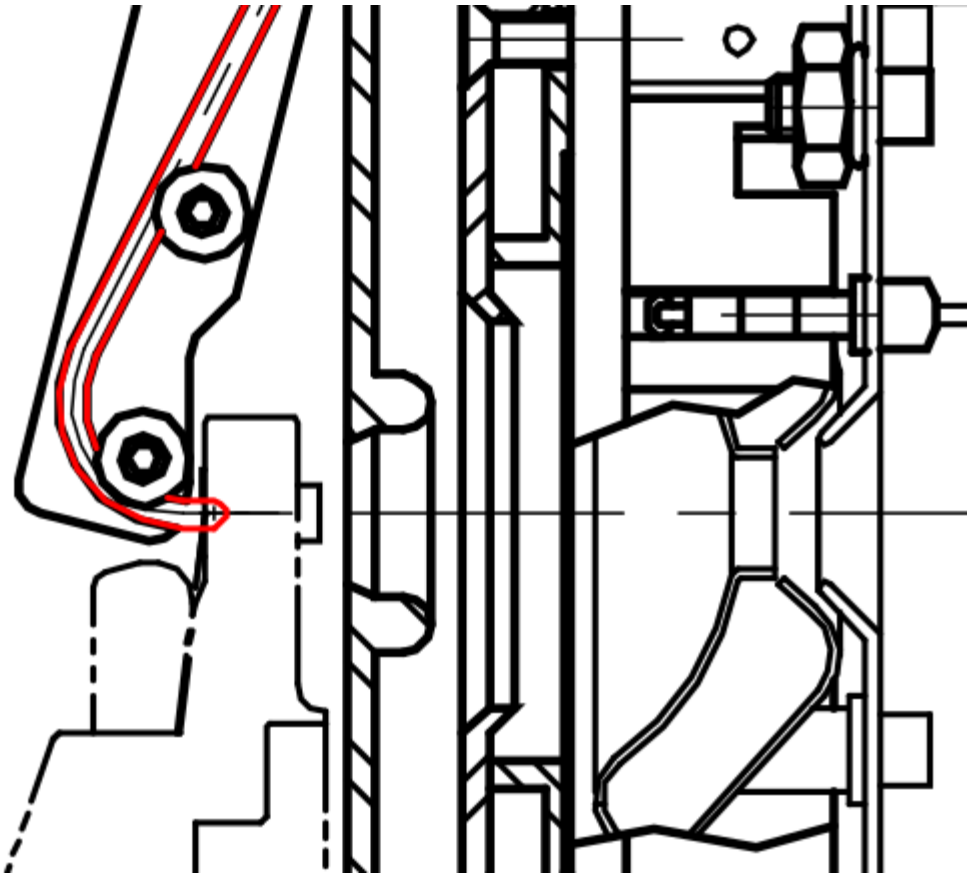

Figure 5: *Schematic of the gas injection to the gas cathode. Stainless steel tube connecting the capillary tube to the gas cathode is shown in red. Figure adopted from National Electrostatics Corp.®.*

3.2.2 Accelerator and beam transport

Accelerator used in the measurements and optimization is a 5-MV tandem accelerator TAMIA, which was originally installed in 1982 and decided to be converted to AMS usage in 1996 [24]. The adaptation was completed in 2003 but many new parts have been installed and improvements made continuously even after this. The schematic for the AMS system in 2004 is shown in Figure 6. Most of the information about the AMS equipment have been taken from *AMS facility at the University of Helsinki* [24] and *Accelerator mass spectrometry and Bayesian data analysis* [25].

C^- ions coming from the ion source are first focused by an einzel lens (EL) and accelerated by preacceleration tube (PAT). The preacceleration, including the acceleration done in the ion source, can accelerate the ions up to 80 keV but typically values of about 65 keV are used. After the acceleration, there is a cylindrical electrostatic energy analyzer (ESA) with radius of curvature of 0.5 m, effective bending angle of 40 ° and electrode separation of 53 mm. This

analyzer removes low energy particles from the ion beam. After this, a magnet analyzes particles with chosen momentum and turns them towards the accelerator. This injection magnet (IM) is a two-sided 90 ° magnet with radius of curvature of 0.3 m, ME/q^2 value of 13.3 u $\mathrm{MeV/e^2}$. Photo of IM and the equipment around it is shown in Figure 7. Different isotopes are selected with electrostatic plates for fast isotope switching. After choosing the particles with wanted momentum and energy, there is a faraday cup which can be moved on the beam's way to measure current before the accelerator. Carbon beam's current is usually adjusted to around 20 µA for solid samples and around 10 µA for gas samples. After choosing the wanted mass, there is an electrostatic triplet, X-Y steerer and X-deflector which are used to focus the beam into the accelerator. [24]

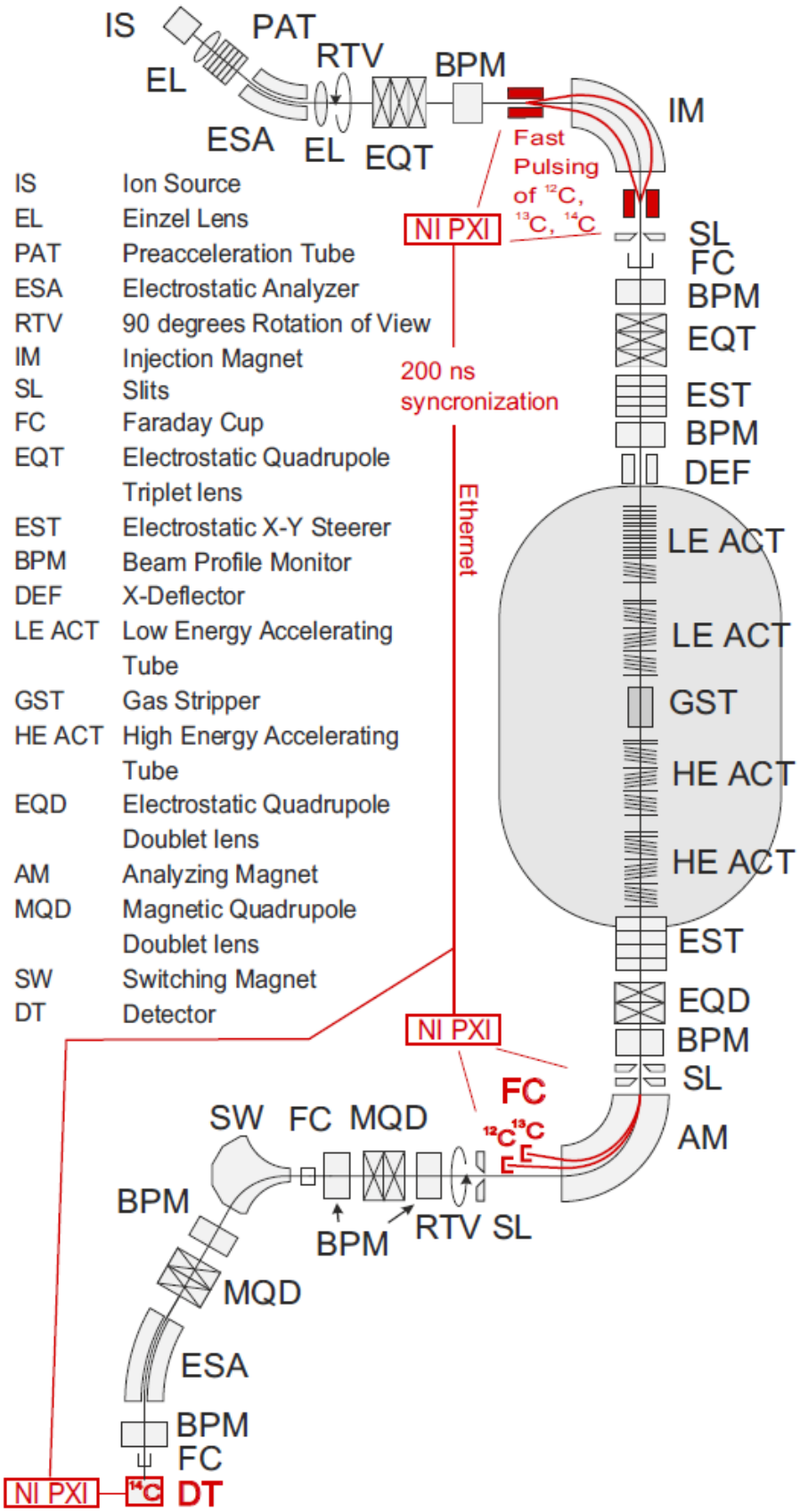

Figure 6: *Schematics diagram of the AMS system. Parts relevant for AMS measurements are listed and parts related to fast isotope switching are shown in red. Figure taken from* [16].

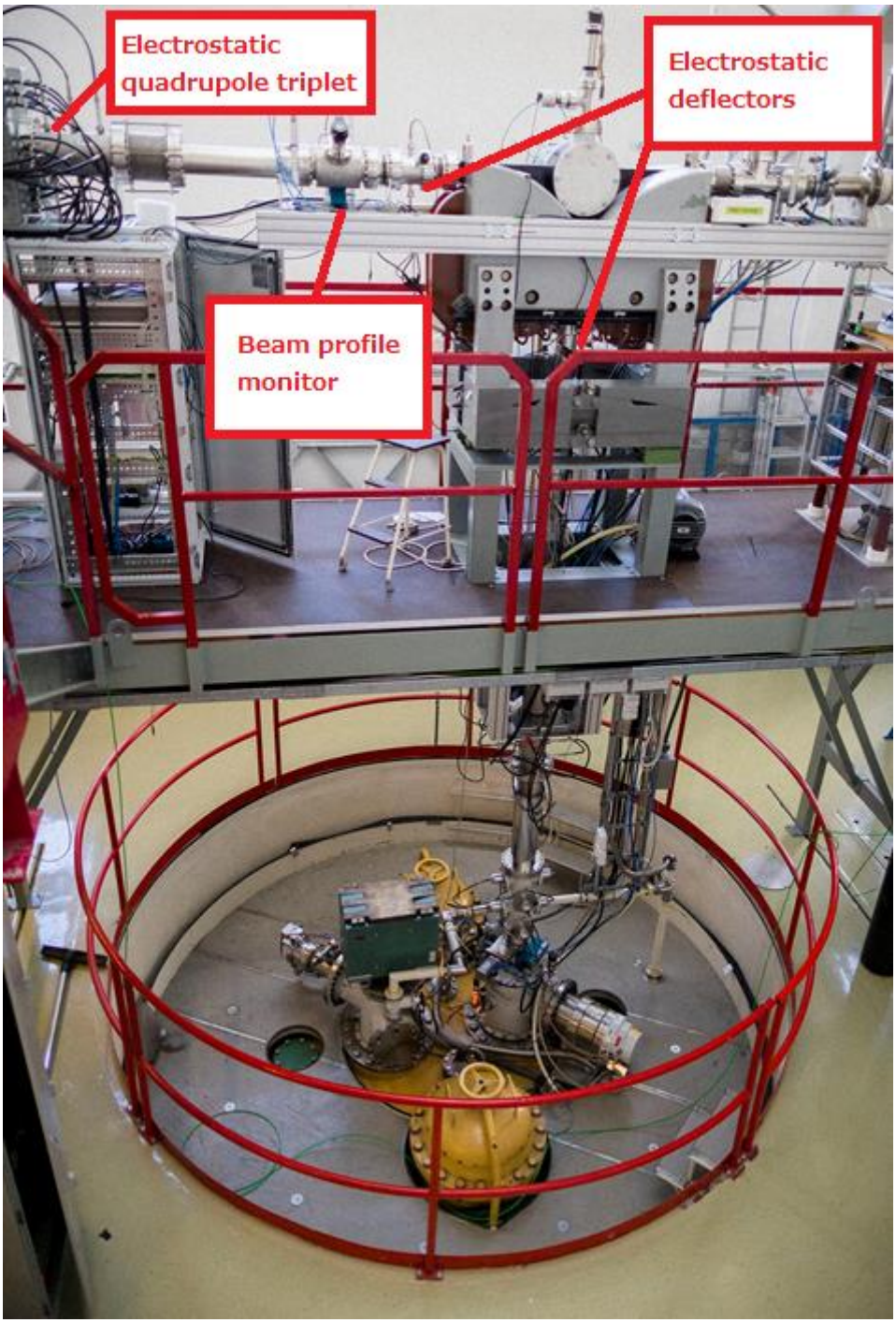

Figure 7: *Beam line to 90° injection magnet. The top of the accelerator can be seen in the bottom. Photo taken by Alexandre Pirojenko.*

The accelerator is a vertical belt-driven 5-MV tandem accelerator. It has four 2200 mm long inclined-field accelerating tubes. The first one also has an immersion lens and straight electrodes at the entrance. After two tubes there is a 545 mm long, 8 mm diameter gas stripper (GST) which uses either CO_2 or argon for ion exchange to change the negative ions in the beam to positive ones. For carbon, the accelerator is optimized to produce C^{+3} ions.

The final electric charge of the carbon ion depends on the velocity of the ions when entering the stripper. For $^{12}\mathrm{C}$, 2.6 MeV acceleration is the optimal for +3 charge [26]. This means that for $^{14}\mathrm{C}$ higher energy is needed and 3.0 MeV is expected to give the maximum yield and is therefore used in the accelerator.

The carbon ions are accelerated with terminal voltage of 3 MV which is more stable than 5 MV. After this the C^{+3} ions have been accelerated to 12 MeV total. After the accelerator there is an electrostatic quadrupole doublet lens (EQD) which focuses the ions to the second magnet, analyzing magnet (AM). It has radius of curvature of 1.5 m and ME/q^2 value of 240 u $\mathrm{MeV/e^2}$. The chamber after analyzing magnet has off-axis Faraday cups for measuring $^{12}\mathrm{C}$ and $^{13}\mathrm{C}$ currents simultaneously with the $^{14}\mathrm{C}$.

After the analyzing magnet there is a magnetic quadrupole doublet lens for focusing the beam into a switching magnet which turns the beam to the AMS beamline towards the detector. The switching magnet also functions as further momentum analyzer with angle of -60 °, radius of curvature of 1.2 m and ME/q^2 of 77 $\mathrm{MeV/e^2}$. There are three other lines in use for ion beam analyses and other research. In the AMS beam line there are a magnetic quadrupole doublet and an electrostatic analyzer with radius of curvature of 2.0 m and E/q value of 7.2 $\mathrm{MeV/e}$ as high resolution energy analyzer.

Single $^{14}\mathrm{C}$ ions are counted with an ion-implanted silicon detector with an active area of 100 $\mathrm{mm^2}$. It is located at the end of the beam line and is shown in Figure 8. A Faraday cup can be moved to the beam's way for optimization near the detector. Beam profile monitors are also used to help equipment optimization. [24]

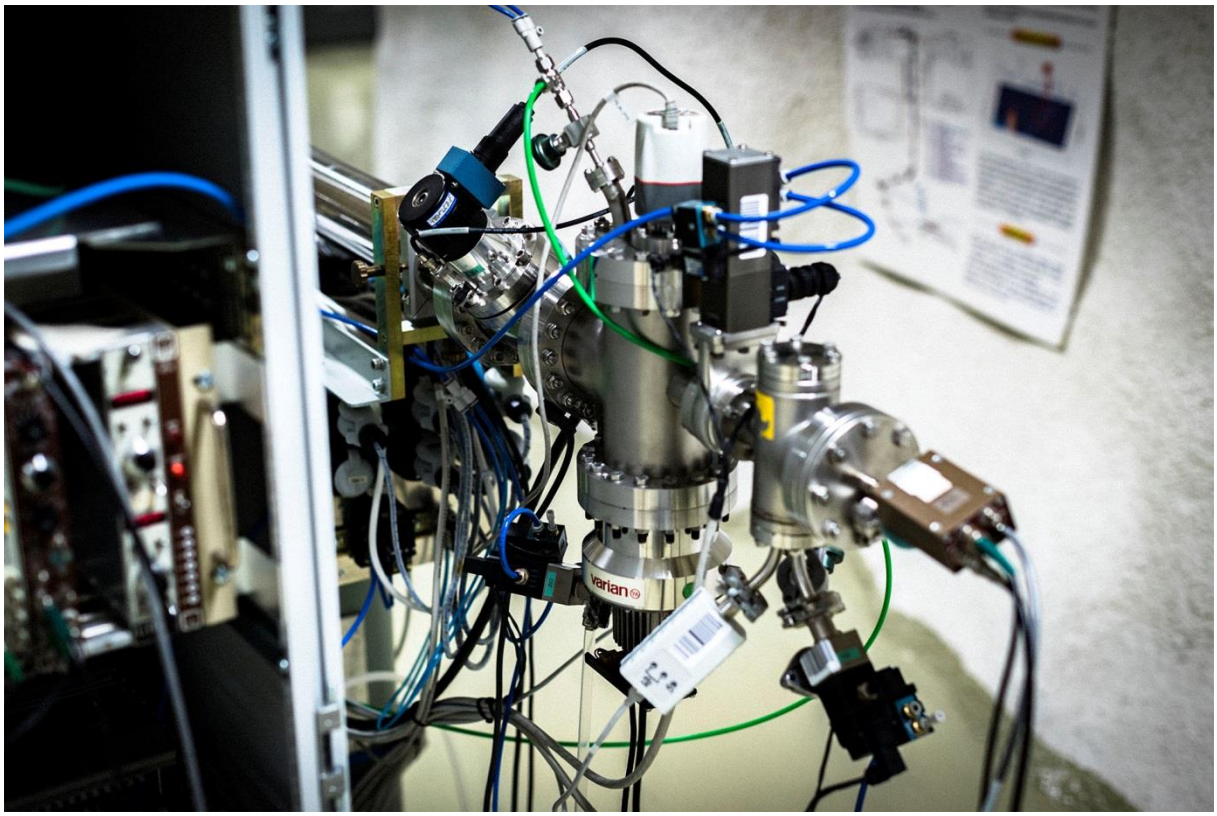

Figure 8: *Detector chamber at the end of AMS beamline for detecting single* ^{14}C *atoms. Photo taken by Alexandre Pirojenko.*

4 Gas system

Gas system was built when converting the ion source to hybrid source to measure not only solid graphite samples but also CO_2 as gas. This chapter describes the equipment in the gas system, how it functions and presents possible future improvements.

4.1 Overview

As the ion source can ionize carbon, another way instead of using solid graphite cathodes is the way of injecting carbon as CO_2 gas. Sample preparation for this is easy to do because the sample is burnt to CO_2 in the sample preparation when making solid samples. The slow process of converting the CO_2 to graphite can therefore be skipped. The gas system was built to handle storage and pumping of the CO_2 gas. Schematic can be seen in Figure 9.

The system uses helium as carrier gas to help CO_2 to flow through the capillary pipes towards the ion source in which the ionization occurs. With small samples helium carrier gas is essential for the CO_2 injection. There are two capillary tubes from the helium tank. One is to the main line to for example lower the pressure inside the capillary line with a vacuum pump if needed and the other capillary tube is to the CO_2 gas line for the helium to function as carrier gas. Once the CO_2 is flowing, it together with helium enters a longer capillary tube which leads to the gas cathode of the ion source. The pressure and thus the flow rate of helium can be adjusted.

Liquid nitrogen is used when CO_2 needs to be moved between places such as storages and the syringe utilizing the melting point of CO_2. Utilizing phase diagram of CO_2, the melting point is seen to be close to -120 °C at the low pressures of about 10 mbar used in the system. Boiling point of -196 °C of nitrogen allows the use of liquid nitrogen to crystallize gaseous CO_2 through deposition without liquid phase. When there is CO_2 in the main sample line, cooling a storage container with liquid nitrogen below the melting point of CO_2 in the low pressures causes CO_2 to crystallize inside the storage. After the deposition of CO_2 into the storage, the valve to storage is closed and the storage heated back to room temperature and the CO_2 becomes gas again through sublimation. As can be seen in Figure 9, liquid nitrogen cooling is used on all of the sample storages and on the syringe for sample transfer. All of them also have heaters to speed up the sublimation.

Samples are currently made in The Laboratory of Chronology in Helsinki and brought to the gas system with metal vials. By attaching the ampoules to the gas intake, the CO_2 can be moved from them to any of the 12 storages by cooling the storages. From the storages, the samples can be transferred to the syringe for AMS measurements. The transport of samples done with deposition and sublimation is very efficient in the system. By looking at the change of pressure in the system, it can be seen that less than 0.01% of the CO_2 is lost on every transport event.

In future the system is planned to be improved so that samples can also be prepared next to the gas system and the CO_2 can be extracted and transferred directly into the storages without sample handling in different facilities and moving samples in separate containers.

CO_2 gas in the syringe is pressurized to chosen pressure which is usually around 3 bar. The system was built that the pressure inside the syringe would always stay constant, even when releasing the gas into the capillary to ensure a constant flow of gas. Once pressurized to the chosen pressure, the valve from the syringe to the capillary line is opened and CO_2 can then flow into capillary tube with helium and eventually into the ion source. CO_2 flow can be controlled by changing the pressure in the syringe. The syringe is heated to 30 °C while pressurizing and pumping.

Gas valves, cooling and heating can all be controlled with a computer with a program made with LabVIEW. Manuals to use the program are on appendices A-D.

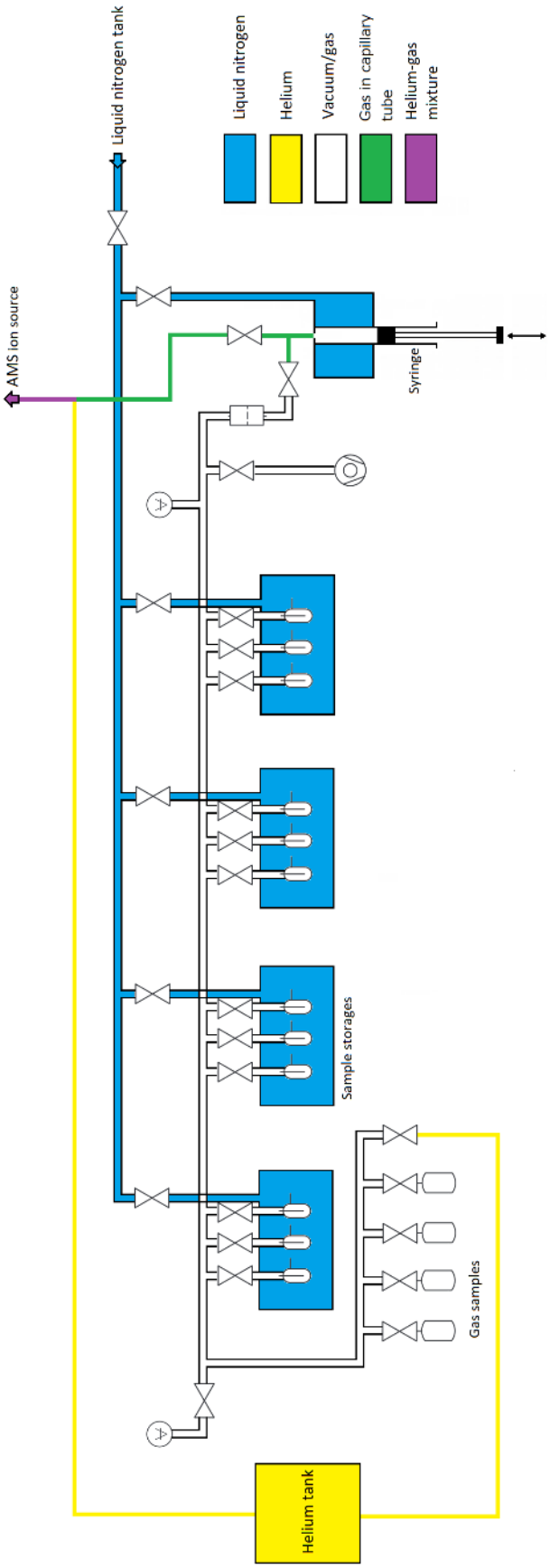

Figure 9: *Schematic of the gas system currently in use.*

4.2 Equipment

The gas system has been built during past years and is currently ready and functional for first actual measurements. No changes to the system have been done during this thesis. The system with valves, capillary tubes, storages and syringe has been built from different parts. The system is designed to hold 12 samples in their storages, a syringe to inject CO_2 to the ion source and capillary tubes for low volume transfer of the gas. There is also cooling and heating of storages and the syringe built into the system.

The capillary tubes used are fused silica. There are two sizes of tubes: inside diameter of 75 µm and 25 µm. Outside diameter is 363 µm on both of them. In the current system only the larger 75 µm capillary tubes are used. The smaller tubes require higher pressures to be able to transport as much CO_2 as the larger ones and can be used when improving the system.

Valves used to control the CO_2 flow are Rotarex Group SELFA M4S1V 316L and Swagelok 6LVV-DPMR4-P-C diaphragm valves. They are used on the storage containers and on the gas intakes and other parts inside the main gas line. There are two pinch valves used on the capillary tube line to stop the CO_2 flow by pinching the capillary tube. These pinch valves function properly and stop the flow with the pressures used but high pressures can cause leaking through small openings in the capillary tube. Liquid nitrogen line uses Swagelok SS-4UW-TW-TF-6C pneumatic valves to function properly even in the low temperatures. All the valves are remote controlled by computer with a LabVIEW program. [27]

Syringe used in the system is Hamilton Gastight 1001LTN (81317/02) with 1 ml volume. The needle of the syringe is stainless steel. To prevent cracking of the syringe by blocking direct contact of the syringe and stainless steel of the cooling parts, polytetrafluoroethylene (PTFE/Teflon) plug was made and attached to the end of the syringe. Piston of the syringe is controlled by a pneumatic linear drive. It can move the cylinder vertically for the required 60 mm.

Most of the current system can be seen in Figure 10. Future improvements should be focused on automated sample intake and to the syringe and capillary tubes to improve CO_2 flow and to reduce possible residue of previous samples that might be left inside the syringe and capillary tube, causing a memory effect and increased background in measurements.

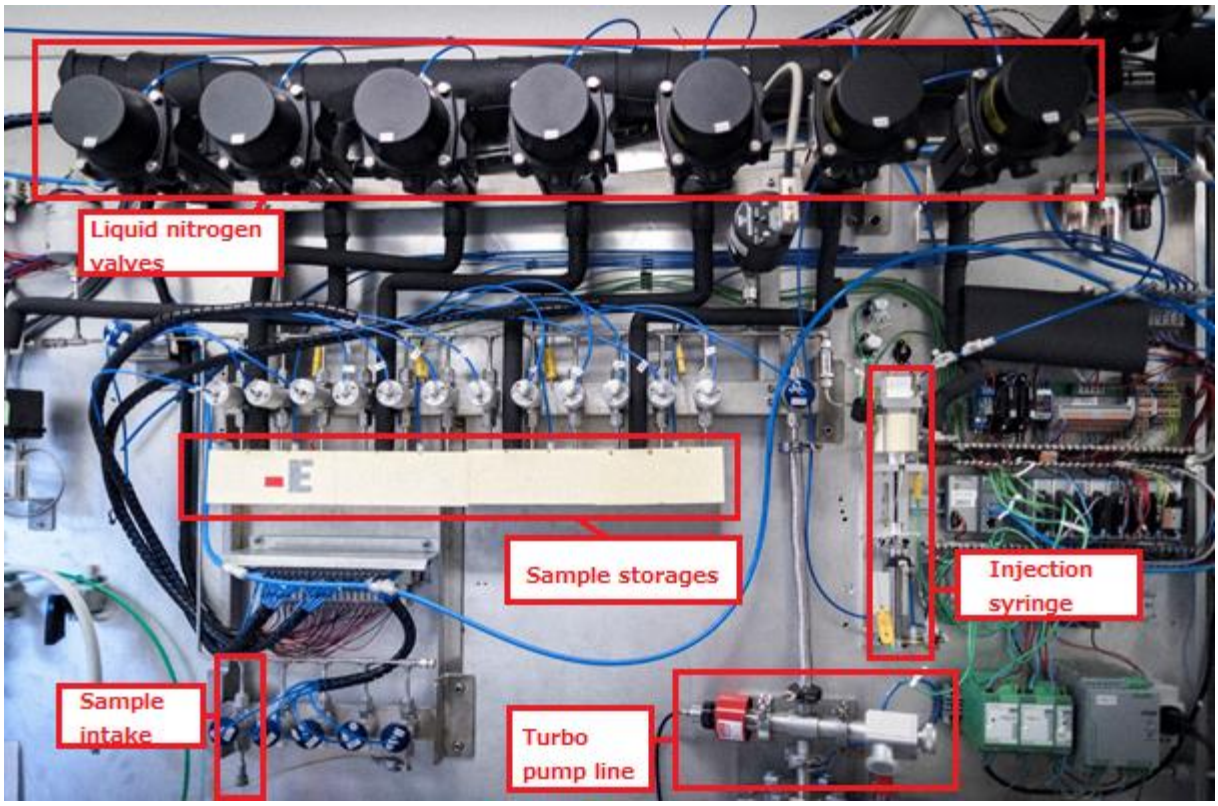

Figure 10: *The current gas system with its valves, storages and injection syringe. Photo taken by Alexandre Pirojenko.*

During the measurements the syringe was found to be unable to keep the pressure stable during injections. This might be because of the friction inside the syringe as the cylinder is moving. Having an unstable pressure does not affect the measurements much as all the CO_2 will eventually flow but it makes optimization difficult and makes it hard to keep the carbon current constant and high. A constant and stable pressure inside the syringe while injecting CO_2 would help with future improvements of the equipment. A possible fix to make the pressure more stable and pressurizing faster could be usage of even higher syringe pressures to reduce friction or by using a different syringe or a motorized linear drive instead of pneumatic drive. Higher pressures could be used by using a smaller capillary tube which would still keep the CO_2 flow the same as now. Knowing the gas flow speeds of both CO_2 and helium would help when trying to understand and improve the system.

5 Theory of carbon ionization

This chapter presents some theory of carbon ionization inside the ion source. Theories of past are compared with newer ones from different articles. Especially a theory by John S. Vogel is looked at more closely. Theory of laser improving the ionization process is explained and some calculations are done for future plans for a laser system to test the theory inside the ion source.

5.1 Theory of ionization inside the ion source

A theory which has often been used to describe the carbon ionization inside the cesium ion sources is that the cesium ionizes the carbon as it hits the carbon atoms on the surface of the cathode. This is called surface ionization as the atoms are ionized instantly as they are desorbed from the hot metal surface. The probability for an atom to desorb and ionize depends on its work function and cesium attaching to the metal lowers this work function, making it more probable for the sample to ionize [2]. With surface ionization, mass dependence is expected to occur, causing fractionation with carbon. AMS with cesium ion sources have however shown that $^{14}\mathrm{C}/^{13}\mathrm{C}$ ratio can be measured with accuracy of 0.22% of the sample, proving that there is barely no fractionation in the ionization procedure [28]. Normalizations are still done to remove the effect of even these small fractionations caused for example by acceleration, charge-exchange from negative to positive and accuracy of detectors [29].

The way for the ionization to happen in the surface ionization hypothesis is that the sputtered cesium atoms form a small crater to the cathode where the cesium ions transfer electrons to the carbon atoms, forming C^- ions [30]. This kind of alkali charge transfer requires energies of keV, while most of the sputtered atoms have the energy of electronvolts. As most of sputtered atoms are neutral, this process would only ionize a small portion of the carbon atoms at the cathode [29].

Vogel hypothesizes that most of the ionizations would occur in the neutral cesium plasma confined just above the sample [29]. There neutral carbon atoms would interact with neutral excited cesium atoms and charge transfer would happen. After charge-exchange, the carbon ions would leave the plasma accelerated by ion source voltage. Excited cesium atoms have

been found to ionize oxygen atoms better than ground state cesium atoms at low energies [31] which supports the hypothesis.

Other arguments that Vogel has to support his hypothesis are that the neutral cesium atoms stay in the recess of the cathode as plasma with positive cesium ions and secondary electrons coming from the sample and from the walls of the cathode. The cesium plasma density in this recess is about $10^{14}\ \mathrm{CS}^0/\mathrm{cm}^3$ which means that all the surface-ionized carbon atoms pass through this 1 mm length of plasma without any interactions thanks to their free path of several cm [29]. As the cesium plasma glows blue, Vogel also predicts that the excited cesium atoms rise from the 6s ground state up to 7p state because the decay from states $7\mathrm{p}_{1/2}$ and $7\mathrm{p}_{3/2}$ to ground corresponds to photon wavelengths of 459.3 nm and 455.5 nm respectively. These excitations would happen in the hot plasma as the moving neutral cesium atoms collide and interact with each other.

The exact way for the ionization to happen in Vogel's theory is called resonant electron transfer (RET). In RET, the donor atom is excited to some state in which it has a certain electron binding energy. In Vogel's theory the absolute value of the electron binding energy is called ionization potential. If the acceptor atom's ionization potential, which is the same as its electron affinity, is nearly equal to donor's ionization potential, the electron can be transferred from the donor to the acceptor. If the donor's ionization potential is lower than acceptor's, additional energy is required as kinetic energy of a collision or from a photon [32]. The $7\mathrm{p}_{1/2}$ and $7\mathrm{p}_{3/2}$ excitation states of cesium have ionization potentials of 1.17 eV and 1.20 eV which is very close to the electron affinity of carbon, 1.26 eV [33]. Figure 11 shows the electron excitation states of cesium with a likely path for an electron to reach the state 7p from the 6s ground state.

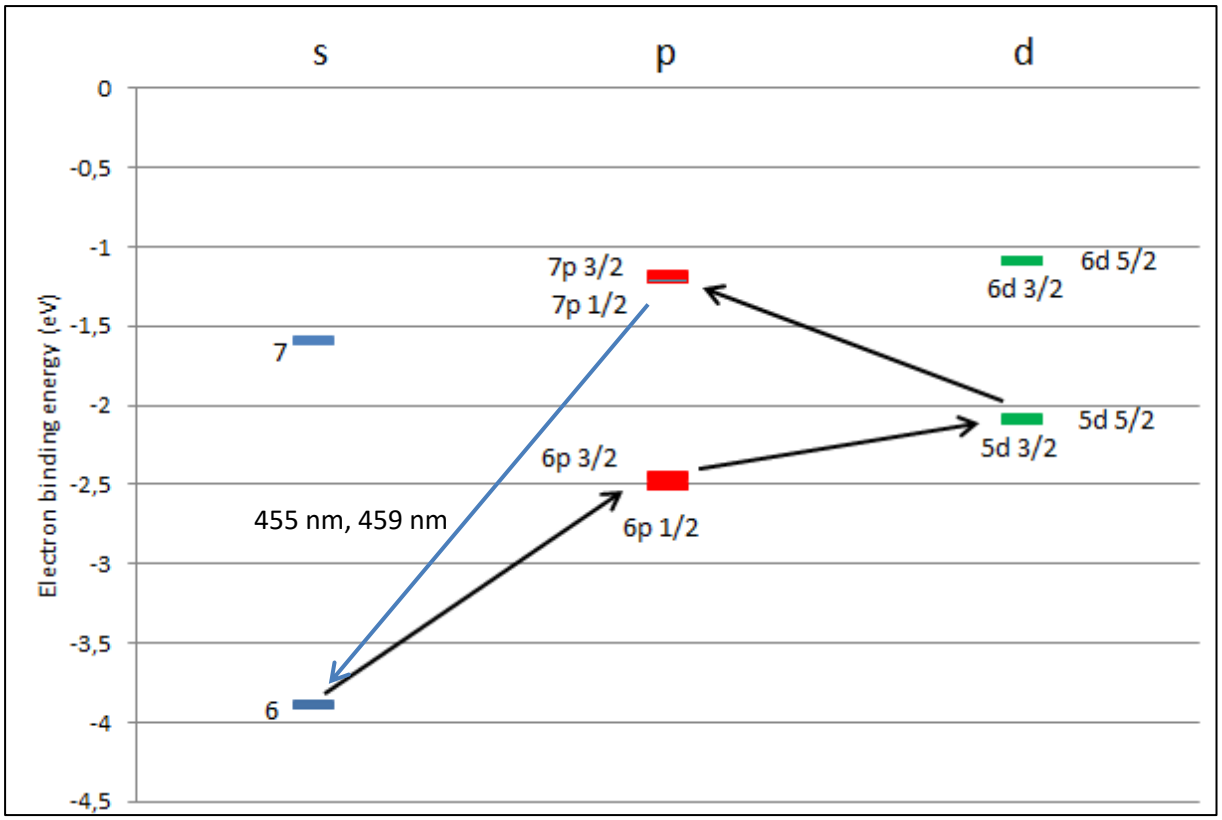

Figure 11: *Electron energy levels for a neutral cesium. The values for the energy levels are from Weber and Sansonetti* [34] *and NIST* [35] *and the path is an estimate by Vogel.*

Vogel shows results of a computer-calculated model of collision-radiation of neutral cesium plasma [29]. This model also shows that the high excitation states of 5d – 7p cause most of the carbon ionization with energies peaking at 2 eV. Model with stable plasma gives the highest ion currents, implying that most of the ionizations would happen in the plasma instead of the surface ionization. According to the model, the only visible-light photons emitted by the excited cesium are the 455.5 nm and 459.3 nm ones, matching the blue glow of the plasma [33]. As the cesium atoms can excite in collisions with other cesium atoms, having a small recess in the cathode increases cesium density and therefore the population of higher excitation states of cesium increases [36]. Using a smaller diameter recess can possibly improve the ionization capability of plasma greatly [37]. Small diameter recess cathodes are more recently tested especially for other elements with lower electron affinities such as aluminum but also for carbon to increase the amount of electrons on the high excited states on cesium.

Another result gained from the model was that other elements can hinder the ionization by reducing the number of electrons available by competing with the ionization. This is especially important with CO_2 because there are two oxygen atoms for every carbon atom. Other elements can take some of the electrons if their electron affinities are close to carbon's electron affinity of 1.26 eV. This can explain for example why copper with electron affinity of 1.23 eV and nickel with 1.16 eV have been noticed to greatly reduce carbon ionization if present in the cathode when compared to for example aluminum [33,36]. Electron affinity of oxygen is 1.40 eV which is also fairly close to electron affinity of carbon. Some electron affinity values of different elements are shown in Figure 12. Vogel presents a possibility to improve carbon ionization by reducing the amount of oxygen by reducing CO_2 to CO before injection into the cathode. This could be done for example with a zinc oven. Vogel also gives a possible way to enhance the carbon ionization by laser which is described in more detail in chapter 5.2. [33]

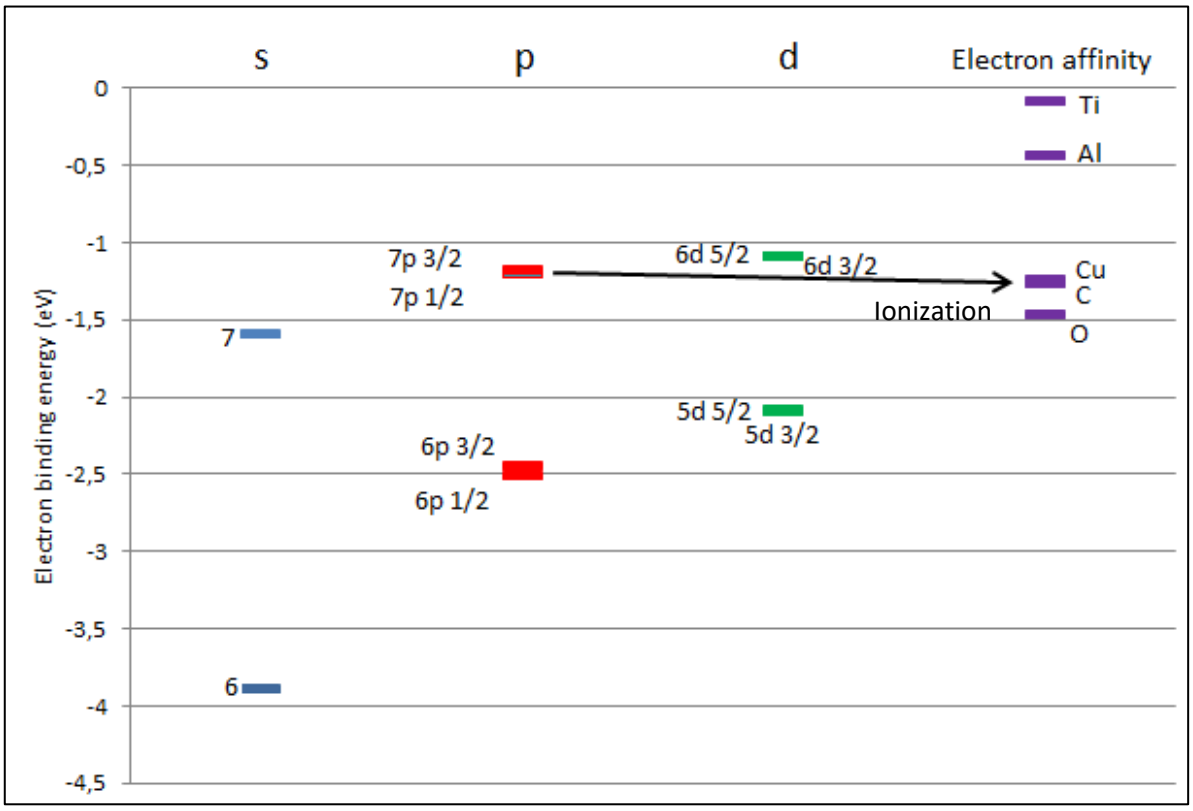

Figure 12: *Electron affinity values for some elements and RET ionization of carbon from 7p states of cesium shown with an arrow. Elements with electron affinities close to carbon compete to get the excited electrons of cesium according to Vogel.*

5.2 Improvement of ionization with laser

In the theory presented by Vogel, one possible way to improve carbon ionization would be to not only excite cesium with neutral collisions but also by using a laser [29,36]. By hitting the neutral ground state cesium atoms with a correct wavelength laser, the electrons can excite to wanted excitation states without collisions or without using the intermediate excited states. This can reduce the effect of oxygen because the highly competed 5d state is skipped.

To estimate the required laser power needed for efficient excitation of the ground state cesium atoms, the number of spontaneous emissions from the excited states and the number of photons emitted by the laser should be compared. Because no explicit value is needed, many assumptions are made to estimate the required power.

Photon energy for example for 455 nm wavelength can be calculated with equation

$$E = \frac{hc}{\lambda} = \frac{6.626 \times 10^{-34}\ \mathrm{J} \times \mathrm{s} \times 2.998 \times 10^{8}\,\frac{\mathrm{m}}{\mathrm{s}}}{455\ \mathrm{nm}} = 4.366 \times 10^{-19}\ \mathrm{J},$$

in which *h* is Planck constant, *c* is the speed of light and *λ* is the wavelength of the photon. Power for the laser is calculated with equation

$$P = \frac{E}{t},$$

in which *P* is the power, *E* is energy used and *t* is time in which the energy is used. This equation can be used to estimate how many photons of certain energy are emitted in certain time with equation

$$\frac{N_1}{t} = \frac{P}{E},$$

in which N_1 is the number of photons and *E* is the energy of the photons. To estimate the probability and number of emissions from the excited 7p state of cesium, Einstein's equation of spontaneous emission with Einstein coefficient must be used:

$$\left(\frac{dn_2}{dt}\right)_{spontaneous} = -A_{21}n_2,$$

in which $\frac{dn_2}{dt}$ is the change in excited state density per time, A_{21} is the Einstein A coefficient for an emission from excited state 2 to ground state 1 and n_2 is the density of the excited state. This equation can also be presented with the change of ground state density per time:

$$\frac{dn_1}{dt} = A_{21} n_2$$

Here density of states *n* is the number of atoms exited to the state in a certain volume:

$$n = \frac{N_i}{V},$$

in which *N* is the number of atoms on state *i* and *V* is the volume. Inserting this to the equation above gives us

$$\frac{dN_1}{dt} = n_2 \times A_{21} \times V$$

Einstein A coefficient values from National Institute of Standards and Technology NIST [38] are $A = 1.836 \times 10^6 \frac{1}{\mathrm{s}}$ for $7\mathrm{p}_{3/2}$ state with 455.5 nm wavelength photon emission and $A = 7.94 \times 10^5 \frac{1}{\mathrm{s}}$ for $7\mathrm{p}_{1/2}$ state with 459.3 nm wavelength photon emission. Volume of the cesium plasma can be estimated to be inside the gas cathode's recess which can be estimated to be about $3\ \mathrm{mm}^3$.

Density of excited states can be estimated to be the same as density of ground state if all of the atoms at ground state would get excited. Ground state density has been estimated by Vogel to be about $3 * 10^{11} \frac{1}{\mathrm{cm}^3}$ [29] and this value is assumed to be the same magnitude for the Helsinki AMS setup.

If the incoming photons are all assumed to excite one cesium atom, we can combine the equation for emitted photons from laser with the number of excitations in cesium. This gives us equation

$$n_2 \times A_{21} \times V = \frac{P}{E}$$

To find out the required power for the laser, *P* must be calculated. For 455 nm wavelength this gives us

$$P = n_2 \times A_{21} \times V \times E = 3 \times 10^{11} \frac{1}{\mathrm{cm}^3} \times 1.836 \times 10^6 \frac{1}{\mathrm{s}} \times 3\ \mathrm{mm}^3 \times 4.366 \times 10^{-19}\ \mathrm{J}$$
$$\approx 0.7\ \mathrm{mW}$$

Laser power needed for 459 nm is 0.3 mW with the same equation.

Calculations made here assume that all the power is emitted as photons which all hit the cesium and all cause excitations. This is of course not the case but allows estimation that the power needed is at least the magnitude of milliwatts. To reach a high enough density of 7p state, optimal laser power could be tens of milliwatts or a few hundred. Higher laser power increases the density of the higher states and should therefore make the effect easier to see. Possible usable lasers are for example 455 nm Blue Laser Diode NDB4216 with 100 mW from Nichia, a 445 nm WSLD-445-050m-1 laser with 50 mW from Wavespectrum Laser or a 455 nm TG455 or 460 nm TG460 with 50 mW from RPMC lasers.

There have also been measurements with two lasers using sequential excitation for cesium. In the experiment, 852 nm laser first excites an atom from the 6s ground state to a long-lasting intermediate state $6\mathrm{p}_{3/2}$ from which a 917 nm laser excites the electron to $6\mathrm{d}_{5/2}$ state. From there the electron falls to $7\mathrm{p}_{3/2}$ state, which has been confirmed to be usable with cesium lasers [39].

In the ion source, laser has been planned to be installed outside the vacuum chamber because of its size and ease of use. The laser is pointed into the chamber through a window if the laser power is low enough. To properly adjust the laser to hit the cathode, a mirror is needed inside the chamber. For this use, for example mirrors for argon ion lasers can be used to get a high reflectivity of 99.8% for the 455 – 460 nm wavelengths and durability for laser intensities. For example a 25 mm diameter TECHSPEC® laser line mirror sold by Edmund Optics can be used.

6 Optimization of equipment

This chapter describes the optimization of different parts of the AMS and gas system for CO_2 usage for maximum carbon ion current and for best efficiency calculated in both ^{12}C ionization efficiency and C/O_2 ratio for CO_2. Durability of the gas cathode was estimated with cesium current to the cathode. Practical issues about the gas usage of AMS are also discussed.

6.1 Optimization of AMS

Most of the optimization of the AMS equipment such as voltages for different parts of the equipment is done by an automated LabVIEW optimization program made for the AMS system. As some of the parameters have dependencies with each other, manual optimization of everything is time consuming. Using a program for it saves time and gives optimal parameters for each measurement. All parameters and results are saved to a real-time database for real-time optimizations and later query of previous settings and results for better repeatability. In measurements done for this thesis, the optimization of some parameters was done manually to find out the best values for high currents for most situations. During actual measurements of real samples, automatic optimization will be utilized more. The automated optimization system is presented with more detail by Palonen and Tikkanen [40].

The optimizations done in this thesis had most parameter values constant and only the ones being optimized were varied. Most AMS parameters were kept from a previous optimization or slightly manually optimized for highest possible carbon ion current with CO_2 gas. After first optimization, all the values were kept constant during the measurements to allow better comparison. Manually entered values are listed in Table 2.

Table 2: *Values of parameters which were manually optimized before starting other optimization measurements.*

Ionizer	68.0%
Cathode	5.900 kV
Immersion Lens	300 V
Extractor	14.000 kV
Focus Lens	0.900 kV
Accelerating	45.100 kV
Total Injection Energy	65 keV
IESA	11.210 kV
IESAEL	0 V
Quadrupole triplet Horizontal LE	7.300 kV, -0.500%
Injection Magnet	26.180 A (^{12}C), 30.350 A (^{16}O)

The main page of the AMS and ion source control system is seen in Figure 13. Most of the parameter changes cause instant changes to the carbon ion current and are therefore easy and fast to optimize for high current. Ionizer was always set to 68.0 % but during the measurements the carbon current was seen to improve with higher values at least up to 70.0 %. For possible future optimizations or actual measurements, higher ionizer values should be tested to achieve higher carbon currents when gas is being used.

Another manual optimization done to the AMS equipment was the angle of electrostatic energy analyzer (IESA) after the initial acceleration in the ion source. IESA can be rotated to work on two ion sources and it not being in a good angle for the ion source currently in use causes some of the beam not to get transported perfectly but to hit the IESA plates which causes a lot of noise during the gas measurements. The angle of IESA is written above it on the wheel which is used to rotate it. When this angle was set to 180° on the AMS ion source side and 36° on the other ion source side, noise during the measurements was noticed to be minimal. The original optimization done on the IESA angle was therefore correct and using those angles gave the least noise.

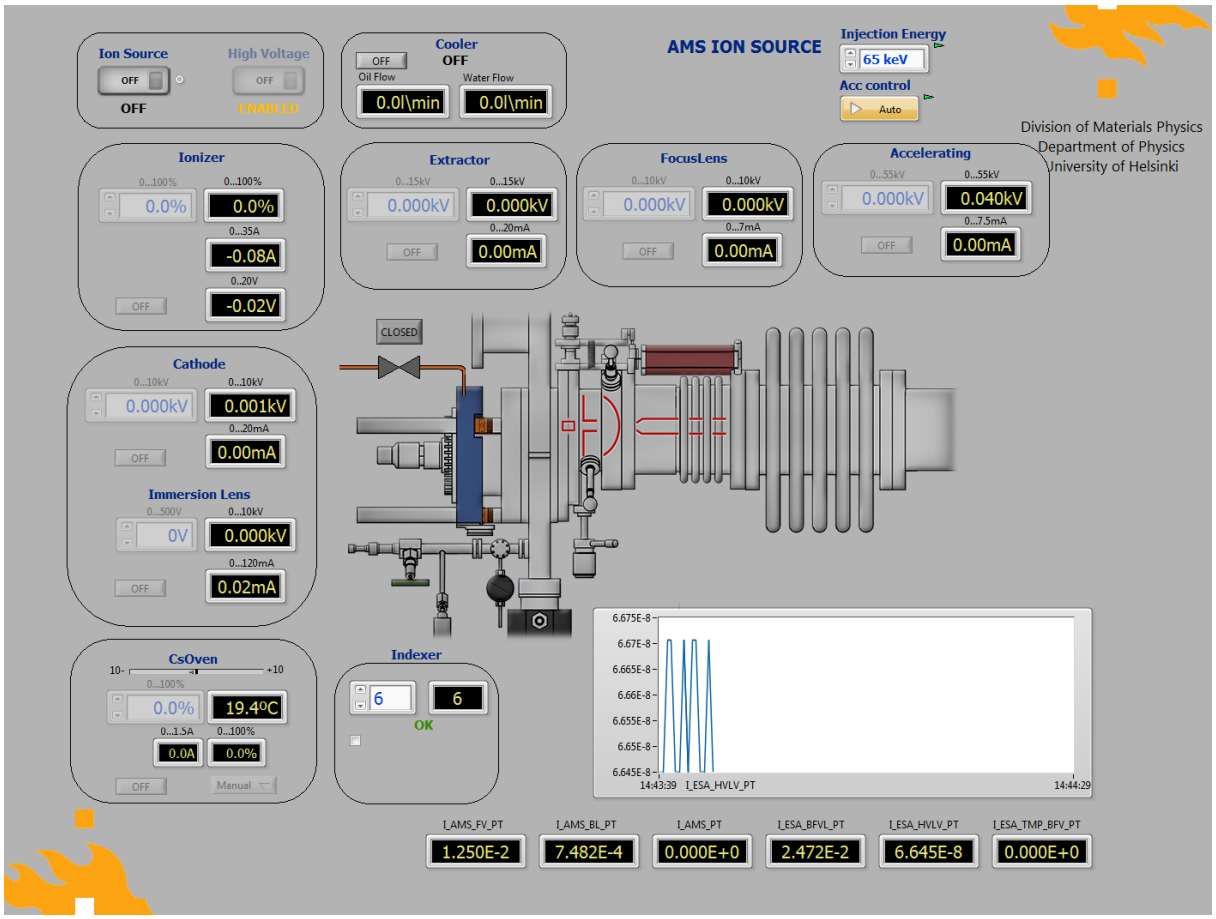

Figure 13: *AMS and ion source control page in the LabVIEW program. Different parameters for the ion source and AMS equipment can be manually input to the program. Parameter most focused on this page was the cesium oven temperature.*

6.2 Optimization of gas system

Parameters which were optimized in the gas system were the pressure of transfer gas helium (proportional to helium flow) and pressure of CO_2 in the syringe (linear to CO_2 flow with constant He pressure). These parameters were tested in different cesium oven temperatures and keeping all other parameters constant. Problems with unstable syringe pressure however caused some errors and inconsistencies to the results.

With low syringe pressure, helium pressure was noticed to have a very large impact on the measured carbon current. As seen in Figure 14, raising helium pressure greatly decreases the carbon current. Similar results have been reported on other similar CO_2 AMS systems [41]. In the measurement, movement of the syringe piston was not compared with different helium pressures so one possible reason to this might be that the carrier gas helium flows

too much and supersedes the CO_2, hindering its flow greatly and slowing the injection speed. This happens when helium pressure is close to or higher than CO_2 pressure at the joining T-piece. Another explanation could be that the carrier helium gas moves the CO_2 molecules away from the ionizing plasma at the gas cathode too fast for the ionization to occur. Raising the temperature of cesium oven causes the current to rise steadily, producing more carbon ionization with the same CO_2 flow.

For low syringe pressures, low helium pressure is preferable for maximum carbon ion current.

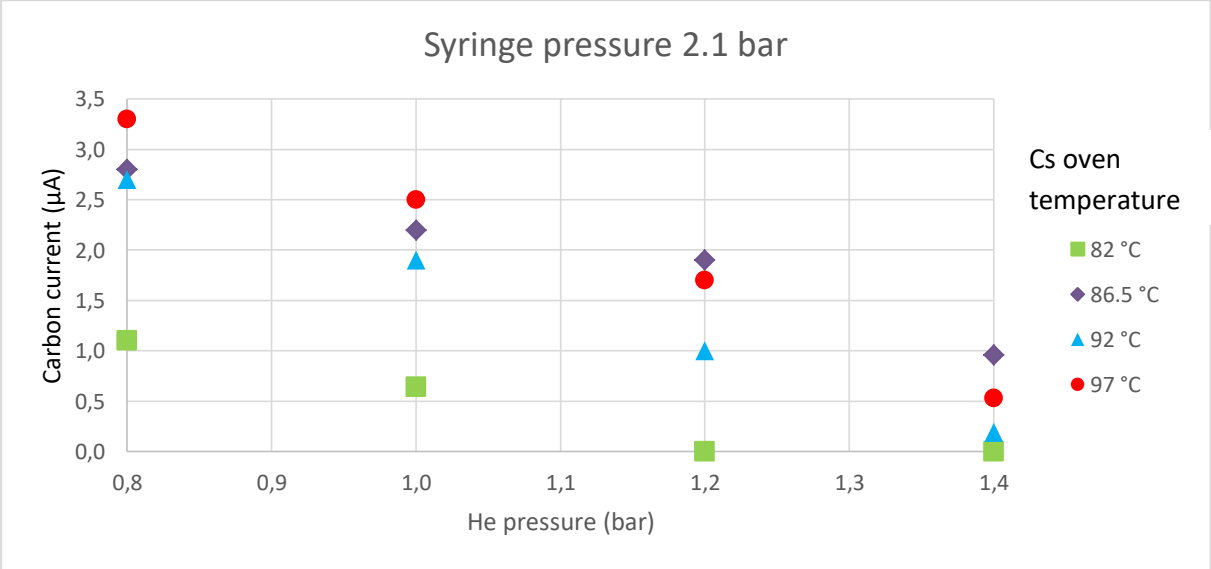

Figure 14: *Carbon ion current as function of pressure of carrier gas helium (proportional to helium flow) measured with different cesium oven temperatures with syringe pressure of 2.1 bar. Measurement with 86.5 °C might have had problems with pressure, which caused the difference to other measurements.*

With higher syringe pressures, pressure of helium affects the carbon current less. As seen in Figure 15, the maximum carbon current is no longer achieved with the lowest helium pressure. This means that the helium is helping the CO_2 flow and no longer hindering it. Maximum carbon current is achieved with around 1.0 – 1.2 bar helium pressure. Raising cesium oven's temperature steadily raises the carbon current.

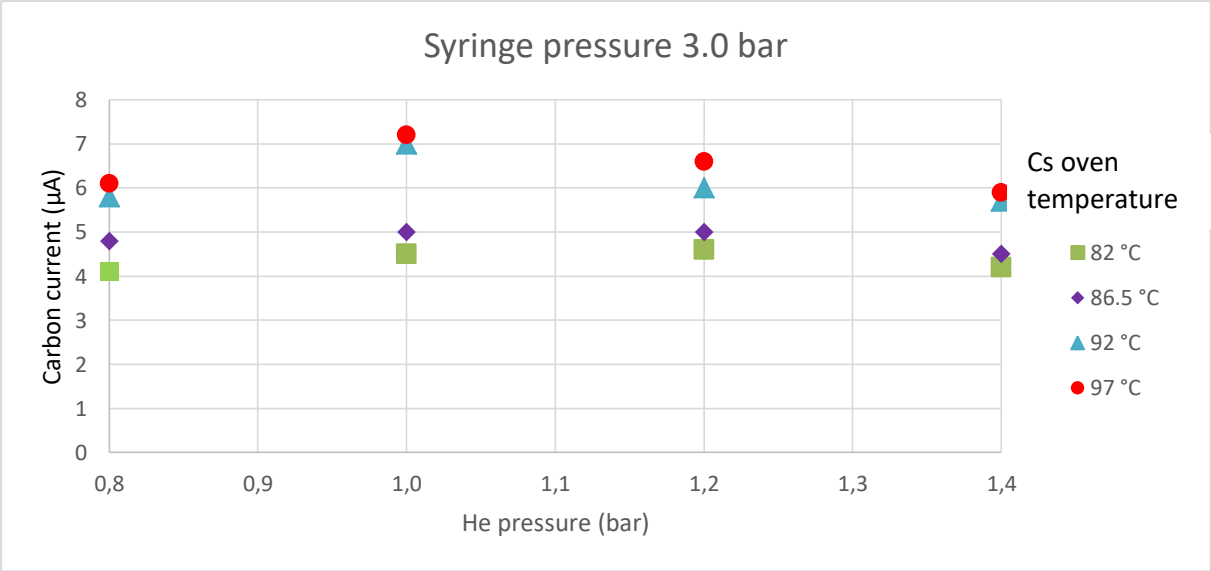

Figure 15: *Carbon current as function of pressure of carrier gas helium (proportional to helium flow) measured with different cesium oven temperatures with syringe pressure of 3.0 bar. Helium pressure does not affect the carbon current much, but it has a maximum point at around 1.0 – 1.2 bar.*

Another thing that is good to keep in mind is the ratio of carbon and oxygen with different syringe pressures. If the ion source would ionize both oxygen and carbon exactly the same way, ideally the amount of carbon should be exactly half of the amount of oxygen in CO_2. When less than half of carbon is ionized and detected, oxygen can be assumed to dominate the ionization process which can for example mean that there is not enough cesium to ionize the carbon as well as the oxygen or the populations of higher excitation states of cesium are not high enough. In Figure 16, carbon/oxygen ratio is shown as a graph in which ratio of 1 represents the ideal ratio of 1:2 for C:O. In this thesis the carbon/oxygen ratio is called relative carbon ionization efficiency which tells how efficiently the carbon is ionized compared to the oxygen, not compared to all the carbon in CO_2. It is meant to show the differences with the ionization of oxygen and carbon.

With 2.1 bar syringe pressure, the carbon current kept decreasing as helium pressure rose. The carbon/oxygen ratio however shows a maximum at around 1.0 – 1.2 bar helium pressure. With 2.1 bar pressure, the carbon current is very low so actual use of the very high carbon/oxygen ratio cannot be utilized easily. This should however be taken into account if very small samples are used with low syringe pressures. Aside from the 86.5 °C measurement which most likely has the most error in it, rising cesium oven temperature is

seen to improve the carbon/oxygen ratio. This implies that increase of cesium actually helps with the ionization of carbon when the helium and CO_2 flows are kept constant.

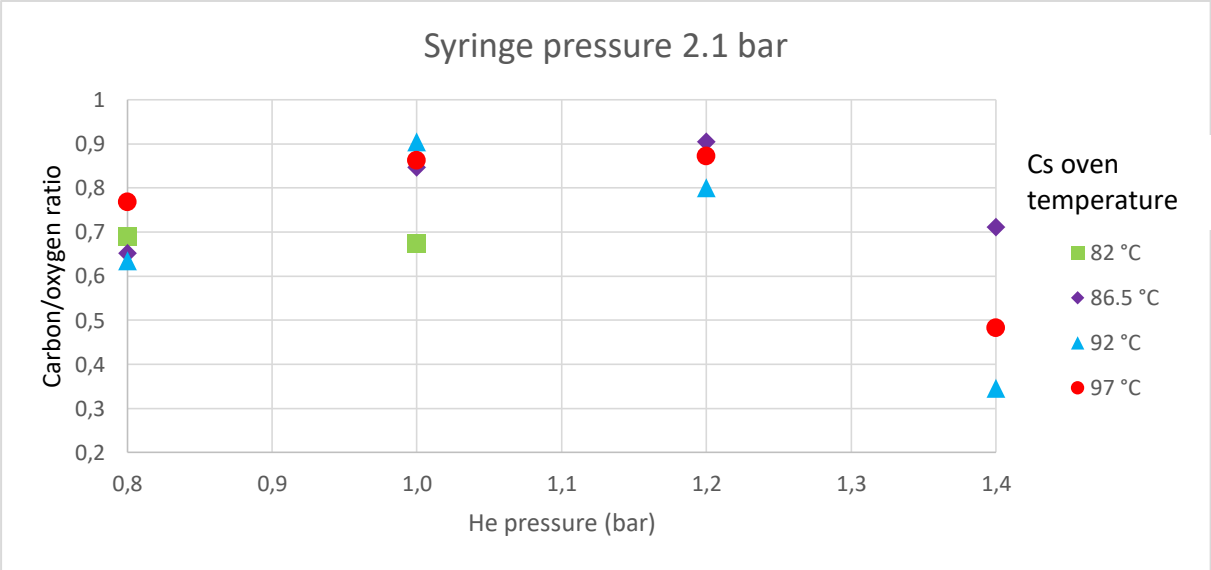

Figure 16: *Carbon/oxygen ratio as function of pressure of carrier gas helium (proportional to helium flow) measured with different cesium oven temperatures with syringe pressure of 2.1 bar. Ratio of 1 represents the ideal ratio of 1:2 for C:O. Measurement with 86.5 °C might have had an inconstant pressure, which caused the difference to other measurements.*

With higher syringe pressures, the behavior of carbon/oxygen ratio changes with different helium pressures. As can be seen in Figure 17, effect of helium on the ratio is much smaller than with low syringe pressures in Figure 16. The relative carbon ionization efficiency increases with higher helium pressures and is at its highest at 1.4 bar in the measurement. If the shape is assumed to be the same as with low pressures, the maximum point of efficiency is again at even higher helium pressures.

Temperature of cesium oven was again seen to have a significant effect on the carbon/oxygen ratio. With the syringe pressure being high and large amounts of CO_2 being injected, low temperature gave very low relative carbon ionization efficiency as expected.

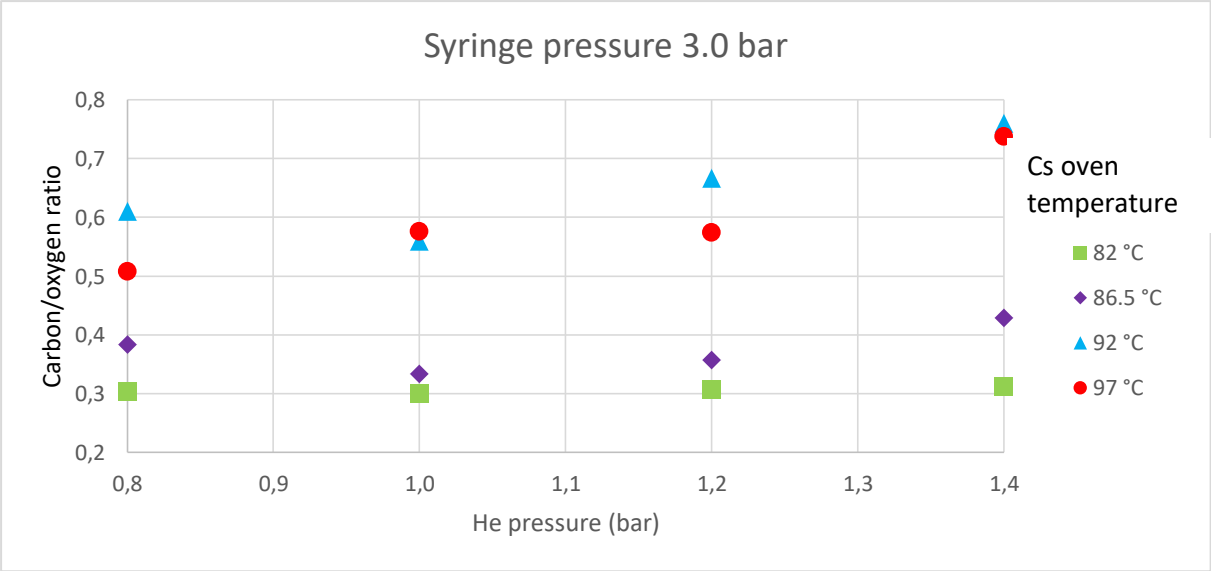

Figure 17: *Carbon/oxygen ratio as function of pressure of carrier gas helium (proportional to helium flow) measured with different cesium oven temperatures with syringe pressure of 3.0 bar.*

Overall when comparing the maximum carbon current and maximum relative carbon ionization efficiency, the maximum carbon current seems to be achievable with lower helium pressures and maximum relative carbon ionization efficiency with a little higher helium pressures. Role of helium as a carrier gas can easily explain the behavior with maximum current but is more complex when looking at the relative carbon ionization efficiency. One possible explanation might be that the efficiency increases just because the amount of CO_2 is decreased, therefore leaving more cesium to ionize the carbon. As a safe value, 1.0 bar helium pressure should be used so good values can be got from all syringe pressures. All the graphs and measurements after this use helium pressure of 1.0 bar.

When the helium pressure is chosen to be constant 1.0 bar, comparison of different syringe pressures (CO_2 flow) in different cesium oven temperatures is easy to make. In Figure 18, carbon current can be seen with different settings. Higher cesium oven temperatures seem to improve the current always on all syringe pressures. Higher syringe pressures also improve the current. This implies that when high currents are preferable and there is enough CO_2 gas to be used, a high syringe pressure with high cesium oven temperature should be used.

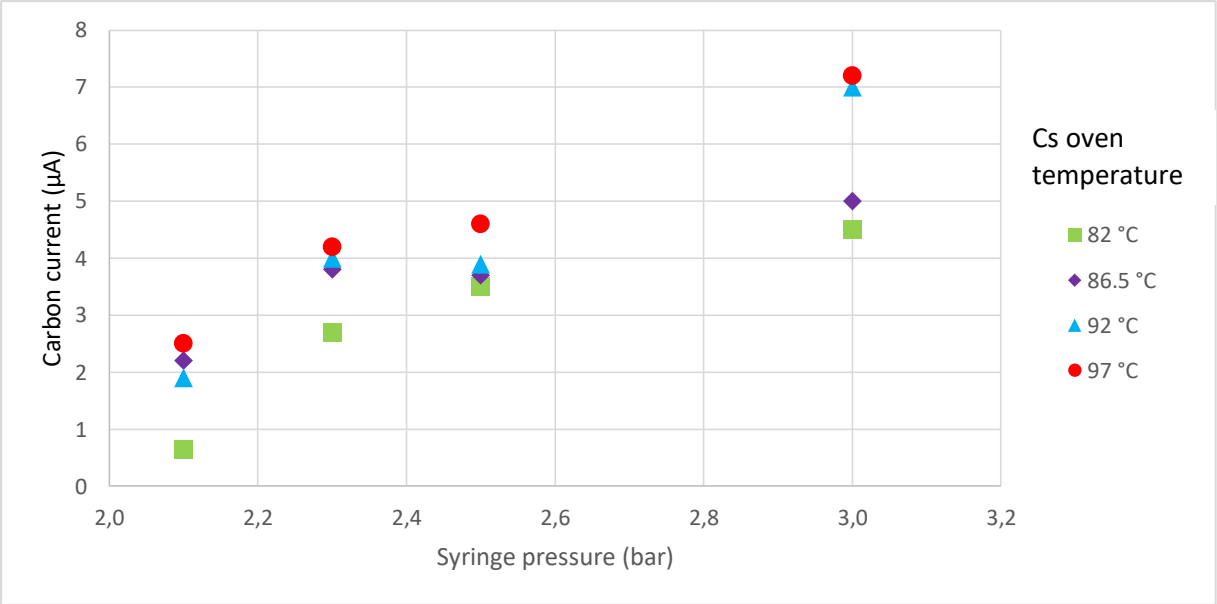

Figure 18: *Carbon current as a function of syringe pressure (proportional to CO_2 flow) in different cesium oven temperatures.*

With carbon/oxygen ratio, which is proportional to relative carbon ionization efficiency, the syringe pressure can be seen to have an opposite effect in Figure 19. High cesium oven temperature raises the relative ionization efficiency as more cesium is available to ionize carbon and the gas cathode temperature gets higher but also lower syringe pressure increases the ratio. This might be caused by the lower amount of CO_2 gas available, causing oxygen ionization to have a smaller impact on the carbon ionization and therefore increasing the ratio significantly.

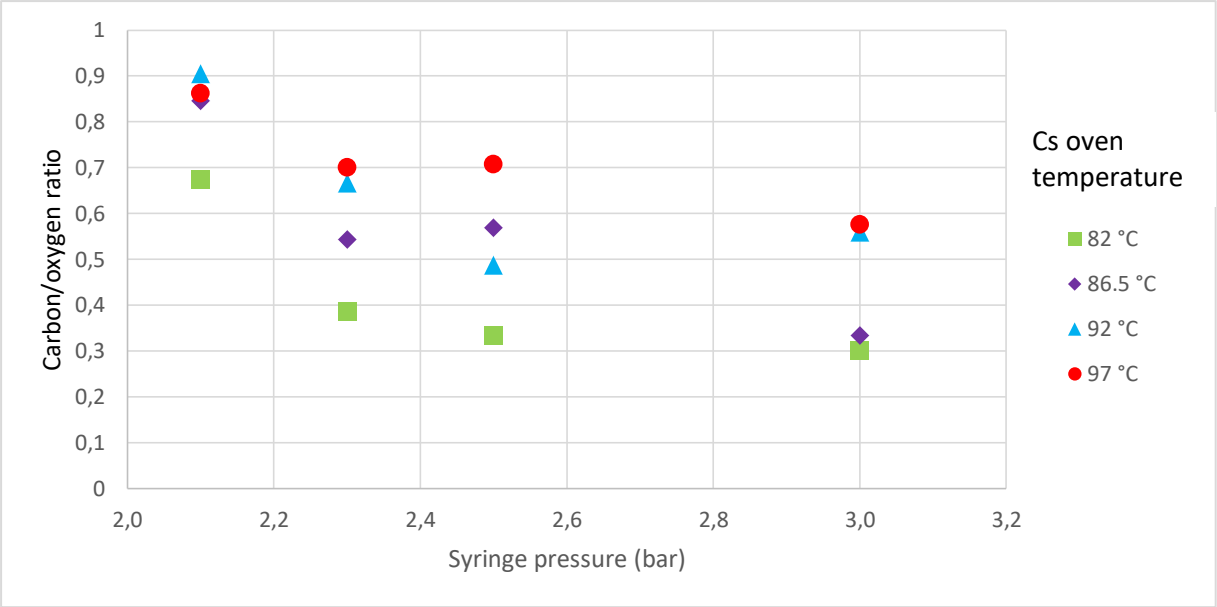

Figure 19: *Carbon/oxygen ratio as a function of syringe pressure (proportional to CO_2 flow) in different cesium oven temperatures.*

Overall, high cesium oven temperature is always preferable. Even higher temperatures than measured this time should be taken into account when doing actual experiments or further optimization as both the carbon current and relative carbon ionization efficiency might still be improved. With syringe pressure, high pressure increases the current but lowers the relative ionization efficiency. For large samples the lower efficiency does not have much downside but with small samples better relative ionization efficiency could be very useful as it allows the samples to be used better, therefore possibly allowing better accuracy.

Different syringe pressures cause the syringe to inject CO_2 with different speed. These speeds were measured by injecting CO_2 for long enough to get a stable volume decrease in the syringe. With known carbon mass inside the syringe, the carbon injection rate can be calculated. The syringe takes very long to stabilize the pressure especially with low pressures and the syringe is most likely not being able to keep a steady pressure inside of it as it should. This can be seen as fluctuating vacuum levels.

Table 3: *Measured injection speed as mass of carbon per minute with different syringe pressures.*

Syringe pressure	2.1 bar	2.3 bar	2.5 bar	3.0 bar
Carbon injection rate	5.8 µg/min	7.7 µg/min	9.5 µg/min	11.8 µg/min

In Figure 20, the injection rate of carbon is compared to the average carbon current. It can be seen that even though the injection rate at 2.1 bar is half of the rate of 3.0 bar, the carbon current of 2.1 bar syringe pressure is much less than half of current with 3.0 bar. This means that a large portion of the injected CO_2 is not getting ionized. Part of this can be explained by the very slow pressure stabilization of the syringe at 2.1 bar. But as the trendline in Figure 20 shows, the relation of carbon current and carbon injection rate is not ideal. With the linear trendline, the carbon current should become visible with injection rate of about 3 µg/min. This implies that low CO_2 injection rates do not show any carbon current until past a certain rate and after this rate, also the absolute ionization efficiency is significantly improved with higher injection rates.

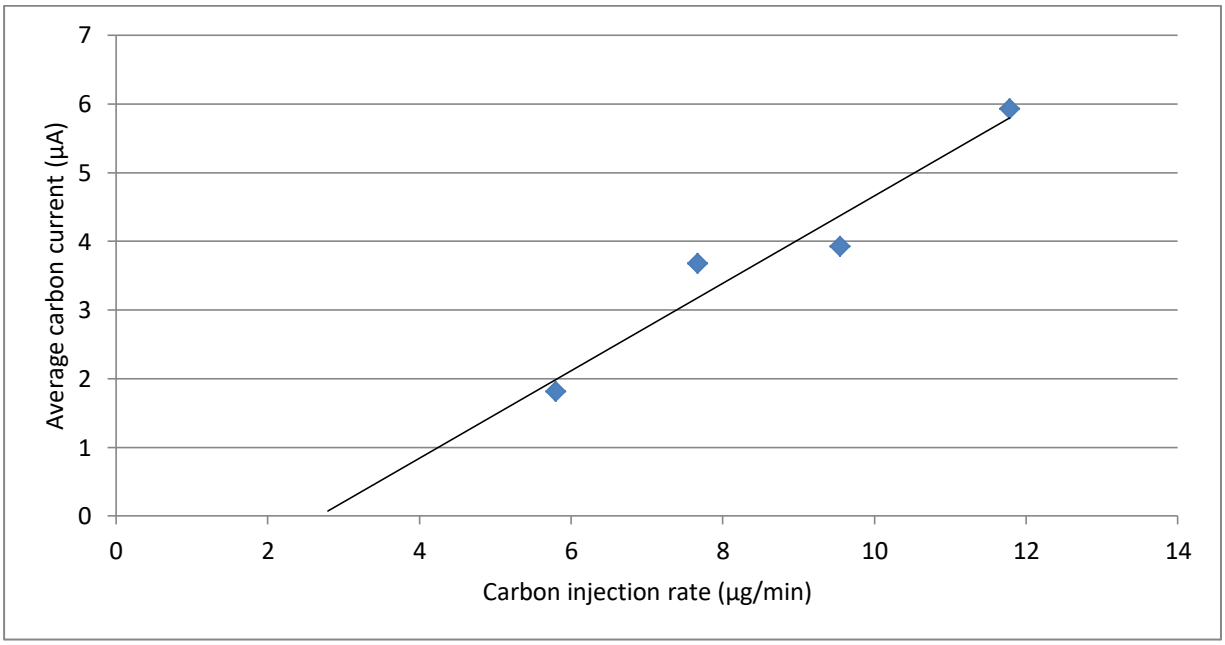

Figure 20: *Comparison of average carbon current and carbon injection rate.*

Another quantity measured with the syringe was how well it pressurized the CO_2 gas. Since the mass of CO_2 is always reported in the sample preparation procedure and therefore the amount of it in moles was known and the volume of the syringe was known and temperature was kept constant with heaters, the syringe was let to pressurize itself with different syringe pressures set. Using the volume of the syringe, ideal mass of carbon inside the syringe was calculated using the ideal gas law, assuming that the carbon dioxide inside was ideal gas. The results of measurements and calculations are listed in Table 4. High pressures and the gas being CO_2 instead of monatomic gas probably cause some of the

difference but the syringe and its slow and unstable pressurizing process might be causing most of the difference. Ideally, the volume after pressurizing should become much smaller which might imply that the friction in the syringe becomes too big for the syringe to pressurize to the wanted value and to small enough volumes. A better syringe or better pressurization system might significantly improve the pressurization by making it both faster and keep the pressure more stable. A higher pressure in syringe could also possibly fix the problem by reducing friction. This can be achieved easily by using a smaller capillary tube in the syringe to still keep the CO_2 flow the same as it is now.

Table 4: *Measured mass of carbon inside the full syringe when the pressure is constant compared to the calculated mass of carbon inside a full syringe using ideal gas law with CO_2 at 30 °C with the 1 ml syringe.*

Pressure in syringe	Measured mass of carbon (mg)	Calculated mass of carbon (mg)
3.0 bar	0.89	1.43
2.5 bar	0.74	1.19
2.3 bar	0.68	1.10
2.1 bar	0.62	1.00

6.3 Optimization of ion source

As most of the parameters of ion source can be tuned fast and automatically, the one that needed the most focus was cesium oven temperature. Changes in temperature of the oven are slow and its ionization greatly differs between solid and gas samples and therefore the temperature needs to be optimized to get a high enough carbon current and to improve the relative and absolute ionization efficiency of carbon. Some of the results related to the cesium oven temperature are already explained in the previous chapter with different gas system properties. This chapter shows some results only related to the cesium oven temperature and summarizes the results related to the ion source.

The cesium oven used in these measurements is used with much lower temperatures of around 80 °C when measuring solid graphite samples. This is because even with the low temperatures the carbon current is already high enough, about 20 µA. With CO_2 being used, the carbon currents are much lower and therefore a higher cesium oven temperature is used to increase the current. Figure 21 shows how the carbon current changes as cesium oven

temperature is raised with CO_2 gas samples. First properly measurable currents do not even show with less than 80 °C but the current increases rapidly after this. During these optimizations the highest cesium oven temperatures used were about 97 °C but even higher temperatures can be used to improve the carbon current and ionization rate in actual measurements or in further optimizations by increasing the amount of cesium available and causing the gas cathode to become more hot in the sputtering.

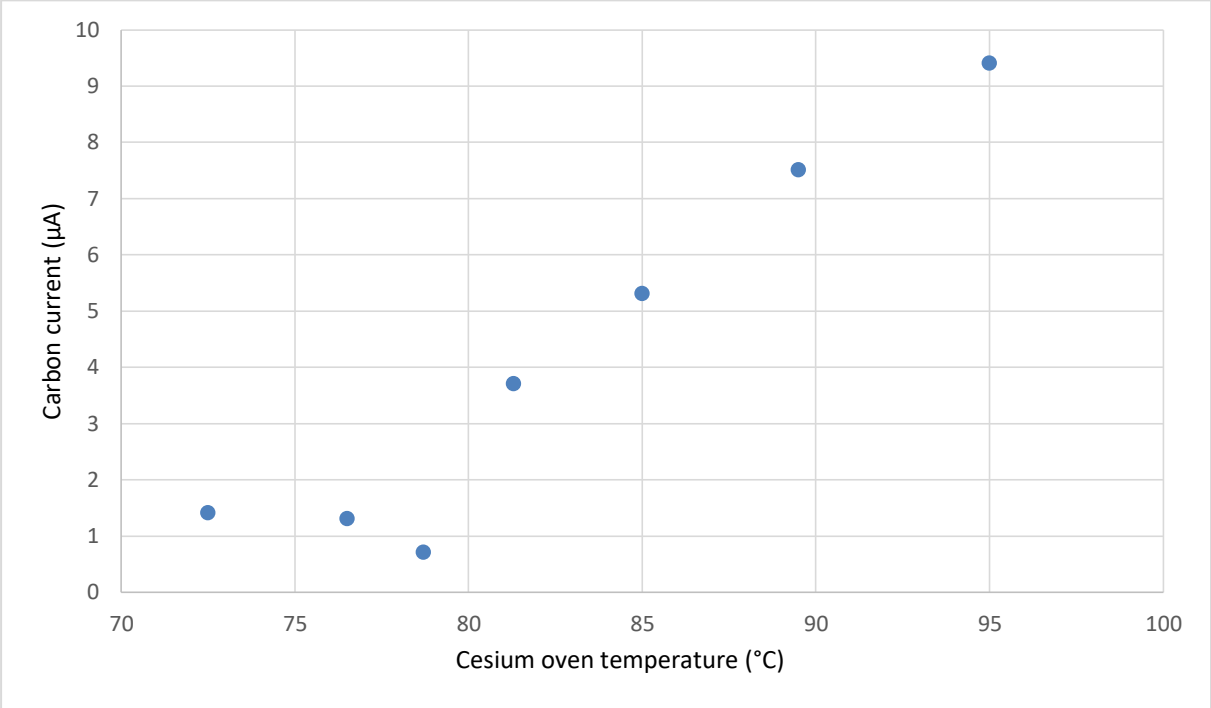

Figure 21: *Carbon current with different cesium oven temperatures.*

With helium pressure set to be a constant of 1.0 bar, the effect of syringe pressure and cesium oven temperature to carbon current can be seen. This is shown in Figure 22. The carbon current can be again seen to increase with higher syringe pressures and higher cesium oven temperatures. The effect of both is significant when trying to achieve a high carbon current. Increasing the syringe pressure gives the cathode more carbon to ionize and increasing the cesium oven temperature gives more cesium to ionize the carbon. Continuing the measurements further should reveal a visible maximum for syringe pressure in which there is no longer enough cesium to ionize all the injected carbon and also a maximum for cesium when it can no longer ionize more carbon. With the measurements done so far, no such visible maximum can yet be seen. With syringe pressure of 2.1 bar, the results seem to stay rather constant but this might be caused by the strange behavior of syringe with 2.1 bar.

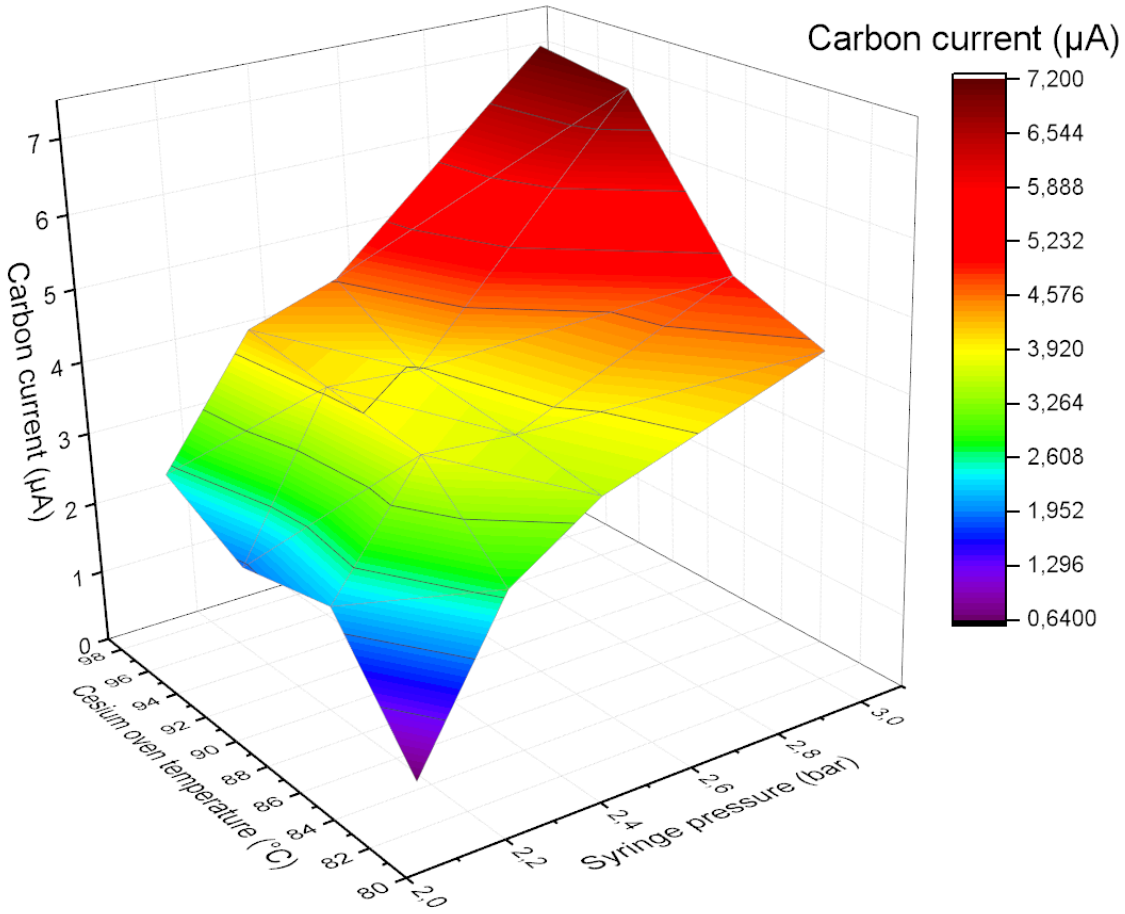

Figure 22: *Dependence of carbon current on syringe pressure and cesium oven temperature.*

Similarly, the carbon/oxygen ratio can be seen in Figure 23. Here again higher cesium oven temperature increases the relative carbon ionization efficiency but syringe pressure lowers it. This can be interpreted as high amounts of cesium and low amounts of CO_2 improve the carbon ionization. Overall, higher cesium oven temperatures seem to have only good sides by improving both efficiency and current with CO_2 so whether using a large sample with high syringe pressure or a small sample with low syringe pressure, high temperature should improve the results.

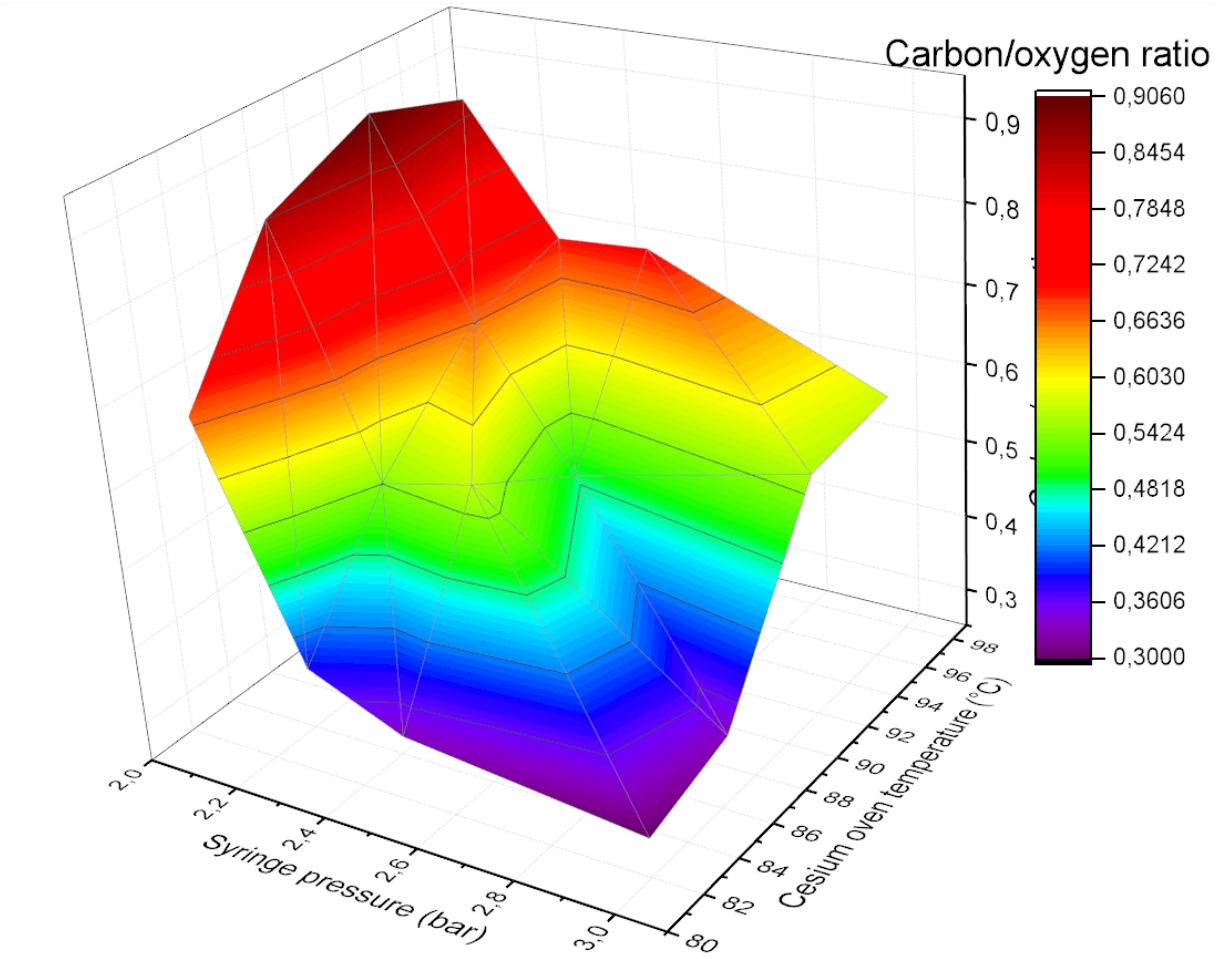

Figure 23: *Dependence of carbon/oxygen ratio on syringe pressure and cesium oven temperature.*

Aside from the carbon/oxygen ratio, which is the relative carbon ionization efficiency, also the absolute ionization efficiency of carbon should be calculated. This tells us how much of the carbon injected as CO_2 is actually ionized and detected. The number of particles detected per second can be calculated from the carbon current using the fact that one coulomb equals to $6.242 * 10^{18}$ elementary charges.

$$\left(\frac{N}{t}\right)_{det} = \frac{6.242 \times 10^{18} \frac{1}{\mathrm{C}} \times Q}{t} = 6.242 \times 10^{18} \frac{1}{\mathrm{C}} \times I$$

Here *I* is the carbon current in amperes, *Q* is charge as coulombs, *t* is time in seconds and *N* is the number of elementary charges. To get the absolute ionization efficiency, the amount of carbon injected per second is also required:

$$\left(\frac{N}{t}\right)_{inj} = \frac{N_A \times n}{t} = \frac{m \times N_A}{t \times M} = \frac{m \times 6.022 \times 10^{23} \frac{1}{\text{mol}}}{12.01 \frac{\text{g}}{\text{mol}} \times t} = 5.014 \times 10^{22} \frac{1}{\text{g}} \times \frac{m}{t},$$

in which N_A is Avogadro constant, *M* is molar mass of carbon and $\frac{m}{t}$ is injection speed in grams of carbon per second. This carbon injection rate can for example be taken from Table 3. By comparing these two values, the amount of carbon atoms injected and amount of carbon atoms detected, the absolute ionization efficiency can be calculated:

$$\frac{\left(\frac{N}{t}\right)_{det}}{\left(\frac{N}{t}\right)_{inj}} = \frac{6.242 \times 10^{18} \frac{1}{\text{C}} \times I}{5.014 \times 10^{22} \frac{1}{\text{g}} \times \left(\frac{m}{t}\right)_{inj}},$$

in which $\left(\frac{N}{t}\right)_{det}$ is the number of atoms per second detected, *I* is the carbon current measured in amperes, $\left(\frac{N}{t}\right)_{inj}$ is the number of atoms per second injected and $\left(\frac{m}{t}\right)_{inj}$ is the injection rate in grams per second, either calculated separately or taken for example from Table 3.

The equation here can be used for the carbon current before the accelerator because at this point the carbon atoms can be assumed to have -1 charge state and all the losses of carbon can be assumed to take place at the ion source. When calculating the efficiency after the accelerator, charge state of +3 of carbon atoms and losses inside the accelerator to the stripper must be taken into account in the calculations.

The absolute ionization efficiency of carbon with helium pressure of 1.0 bar is presented in Figure 24. High temperature improves the efficiency as there is more cesium available to ionize the CO_2. Unlike with relative ionization efficiency in Figure 19, the absolute efficiency mostly seems to be getting higher with higher syringe pressures. This result is similar to Figure 20 as very low injection rates do not give any carbon current but after a certain point, the current increases linearly. The gas cathode seems to use the CO_2 more efficiently when the CO_2 flow is increased. With the syringe pressures used in these measurements, no maximum can be seen yet. This gives promising results that both carbon current and absolute ionization efficiency can still be improved with higher CO_2 flow.

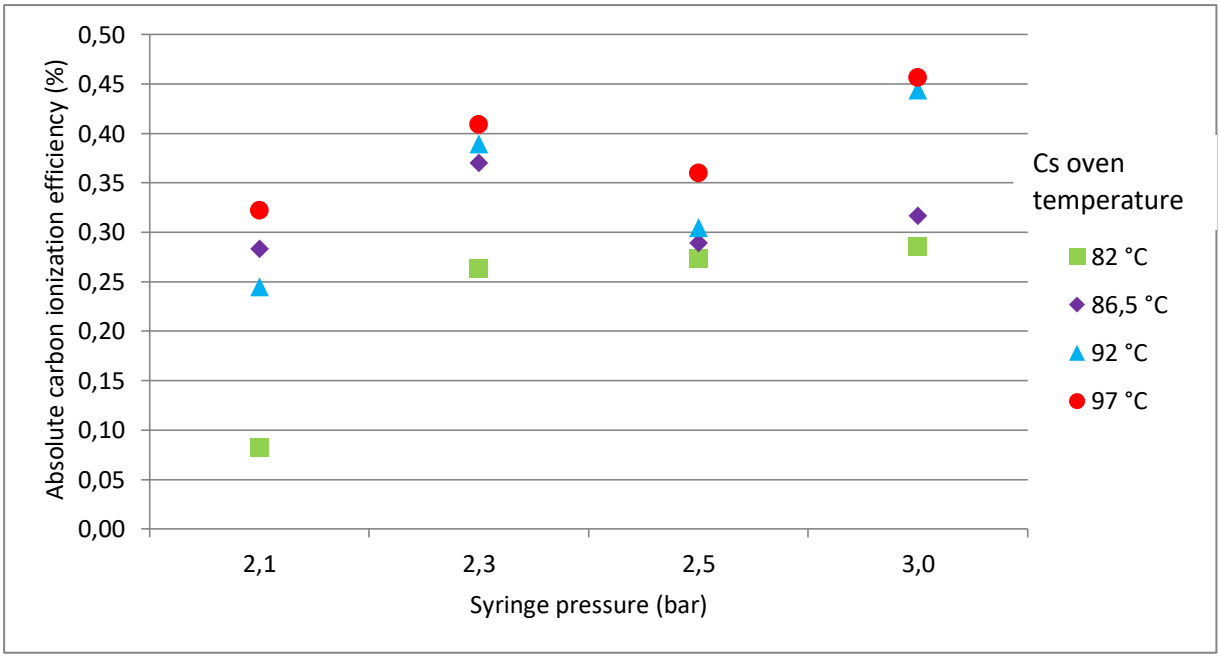

Figure 24: *Absolute ionization efficiency of carbon with different temperatures and syringe pressures. Higher temperatures increase the efficiency and increased syringe pressure also seems to be increasing the efficiency. No maximum is detected with these results. It is unclear why the efficiency is especially high with 2.3 bar syringe pressure but this may have to do with the syringe being unable to keep the pressure stable.*

The current gas system is still far behind in efficiency compared to for example the MICADAS (MIni CArbon DAting System) at ETH Zurich. MICADAS gas ion source can achieve up to 30 µA carbon current with only 2.5 µg/min carbon injection which is less than one fourth of the injection rates used to get high carbon currents with University of Helsinki's ion source [42]. Ionization efficiency at MICADAS is 6-11% which is over 10 times higher than with measurements done here. Other gas ion sources also report higher efficiencies such as 8% with 12 µA at SUERC in Scotland [43], 2.5% with 3.5 µA at Erlangen in Germany [44] and 3-4% with 15-20 µA at Oxford, United Kingdom [45]. Although these other hybrid ion sources have been in use for a longer time and have well been optimized for gas use, it can be seen that there is still much room for improvement for the Helsinki AMS gas setup, especially with the ionization efficiency. Much higher ionization efficiencies should be possible to get with much lower CO_2 injection rates by still keeping the carbon ion current as high at it is now with further optimizations and ion source upgrades.

6.4 Durability of gas cathode

As the titanium gas cathode is constantly being sputtered by the cesium ion source, longer usage times can cause a small hole to form in the middle, causing cesium to hit the stainless steel CO_2 injection tube. To prevent the tube opening from becoming obstructed, it is important to not to use the gas cathodes too long for the hole to form.

There are several ways to calculate the wearing of the cathode, for example by estimating the wearing of the surface caused by cesium sputtering. Here an estimate is made by using the cesium current to the cathode. A higher cesium current means higher wearing of the cathode. First, the load current was measured by only applying high voltage to the cathode and keeping other equipment off. With this, IV-curve of the background was got and the load resistance of the cathode circuit with different voltage was calculated. Results of this are shown in Figure 25. The nominal resistance of the cathode circuit is 2 MΩ but the measurements gave a smaller value and also showed a non-linear dependence on the voltage used.

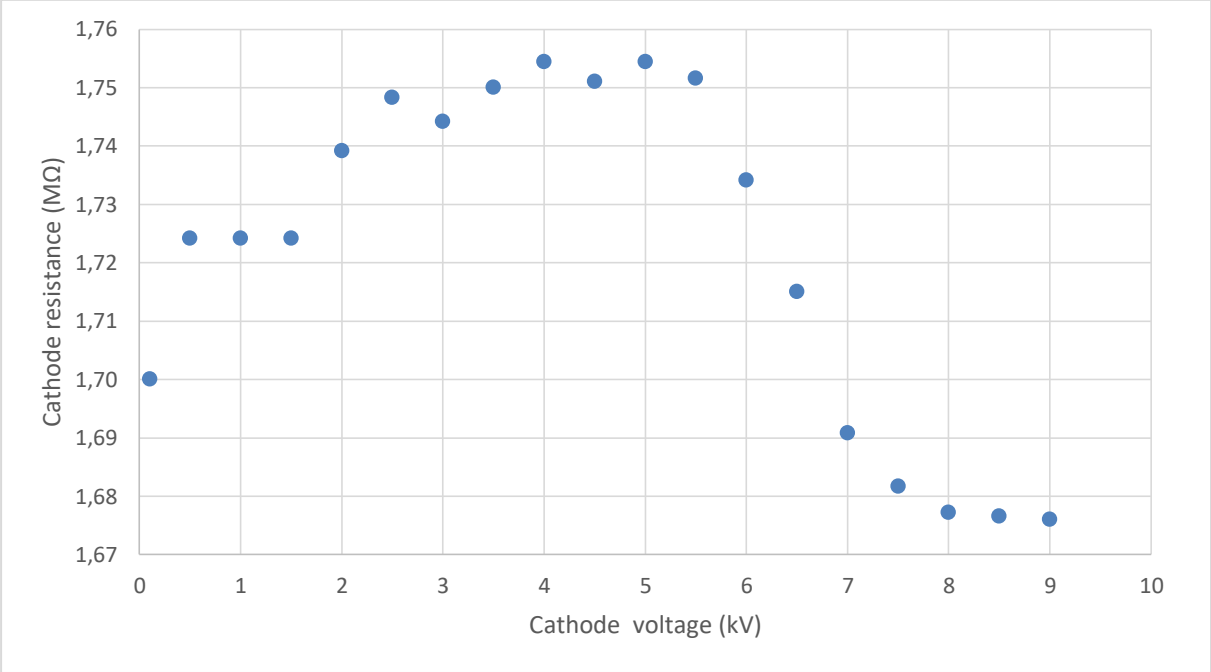

Figure 25: *Total resistance of cathode circuit with different voltage applied. Only the cathode had high voltage on and other equipment was off at the time of measurement.*

Cathode voltage used in the actual measurements was always 5.9 kV and the background current with this voltage was about 3.4 mA. Using data from the gas cathodes to which a

hole was formed, the average cathode current was calculated and background current subtracted from this to see the current caused by cesium. Then, the amount of cesium was estimated by using the total charge coming from the cesium with equation

$$Q = I \times t,$$

in which *Q* is the charge in coulombs, *I* is the current in amperes and *t* is time in seconds. The total charge until a hole is formed was estimated to be about 12 coulombs or 3.3 mAh. With 90 °C cesium oven temperature, the cesium current that is sputtering titanium off the cathode is about 1.2 mA. This means that it would be safe to use one gas cathode for around two hours but the exact time would always depend on the cathode current which is proportional to cesium oven temperature. Some of the current caused by cesium might be leakage current, causing the current to appear too high. To prevent the cathode wearing causing holes, it is still better to assume the cathode current too high.

6.5 Practicalities

There are several practical issues that should be taken into account when using the ion source with the gas system and with gas cathodes. This chapter describes some of these issues for more efficient use of the system.

Time it takes to insert a gas sample from a storage container to the syringe and pressurize it is usually at least 30 minutes. Pressurizing the syringe with a low pressure (2.1 bar – 2.3 bar) can however take much longer, up to one hour for the pressurizing process alone.

When the pinch valve of the CO_2 near the syringe is opened, it takes about 30 seconds for the current to increase. Closing the pinch valve near the ion source stops the flow within a few seconds.

A used gas cathode gets covered in carbon of the sample being used. This means that even after stopping the injection of CO_2 the current can stay high for a while. The gas cathode needs to be changed before measuring different samples to remove this effect.

When a new gas cathode is selected when the ion source is on, surface of the gas cathode is contaminated with very small amounts of modern carbon. A few minutes should be waited for the ion source to sputter it clean and for the carbon current to go down so it does not

affect the actual measurements. A wait time of three minutes decreased the carbon current from the new gas cathode significantly but five minutes gave a much better background. For precise measurements with minimal background, up to 10 minutes should be waited.

As previous samples seem to be leaving some residue to the capillary tubes, flushing the capillary tubes with helium by raising the helium pressure might be a way to get the background smaller. Pumping the syringe while heating removes some of the residue gas as some of this gas might still be inside the porous material of the syringe. Flushing not only the capillary tubes but also the syringe with helium can possibly remove the residue much better but this is not possible with the current gas system and requires improvements. It might still be required to do in order to improve the background of measurements.

7 Measurement of standard gases

Three gases were measured as normal samples: 1) OxII as standard gas with known $^{14}C/^{13}C$ ratio, 2) background fossil fuel sample and 3) humus sample with known Fraction Modern value from literature to see how accurately the gas system works. In this chapter the background measurements are shown and their meaning discussed. The results of standard gas and humus sample are presented with calculations.

Measurements were done with somewhat optimized settings to get a high carbon current. Therefore a high cesium oven temperature of around 96 °C was used and syringe pressure of 3.0 bar was used for the CO_2. Helium pressure was kept at 1.0 bar. Other AMS parameters were adjusted to usual values from Table 2 or to give as high carbon current as possible.

7.1 Background measurements

The background of the gas system, gas cathode and AMS system were measured with CO_2 gas of fossil origin. This way it can be assumed to have no ^{14}C isotope naturally and all the counted ^{14}C atoms can be assumed to be caused by contamination from modern sources. The background gas was prepared as other samples and measured normally.

Gas cathode with only helium being injected was also measured. The gas cathode has contamination from the atmosphere and thus has the $^{14}C/^{13}C$ ratio of modern atmosphere. This can be seen in Figure 26. But because there is no CO_2 flowing, the number of both ^{14}C and ^{13}C isotopes is low. When the background gas starts to flow, both ^{14}C and ^{13}C amounts get higher but because of the fossil origin, ^{13}C dominates and the $^{14}C/^{13}C$ ratio decreases as it should. In Figure 26, the ratio with background gas is first higher and stabilizes after a small decrease. This might be caused by remains of other, more modern CO_2 gases in capillary system or containment in the gas cathode.

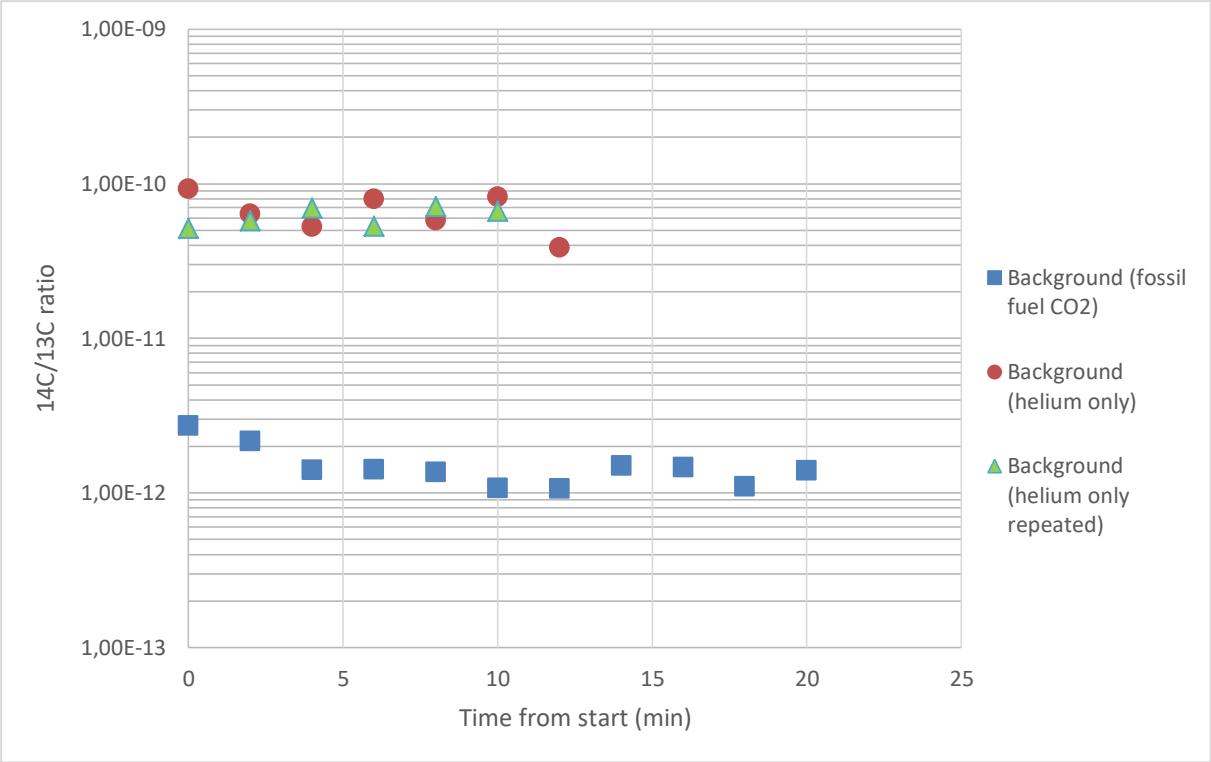

Figure 26: *The $^{14}C/^{13}C$ ratio of the background. Measurements were done with and without the fossil fuel CO_2 gas flowing. Helium was always flowing. Time is started from the change of cathode for the measurements with helium only and from the beginning of the CO_2 gas flow for the one with CO_2.*

When comparing the actual number of counts, it can be seen in Figure 27 that over half the number of ^{14}C might actually be caused by the gas cathode and residue slowly moving from the capillary tube with helium. Background contamination caused by the sample preparation should be visible as a higher number of ^{14}C counts in certain time when the background gas is injected. The increase in ^{14}C counts after the background gas injection however shows only a small increase. Initially a large burst of ^{14}C can be detected which might be caused by modern contamination in the syringe or the capillary tube near the syringe in which helium is not flowing. Once the number of ^{14}C counts stabilizes, the effect of the background gas itself can be seen.

Because most of the background ^{14}C counts seem to be caused by either the gas cathode or the residue in capillary tube, gas cathode cleanness might be important in reducing the background effect. Background caused by the gas itself is very small and biggest reductions could be achieved with better purging of the capillary or better cleaning of the gas cathode.

In this measurement, the titanium gas cathodes which had been inserted into the AMS system several times might have got more modern carbon contamination from the atmosphere than gas cathodes usually get before actual measurements. When inserting new gas cathodes into the device, the background of the gas cathode might be smaller. If this is the case, lower background effect overall is to be expected.

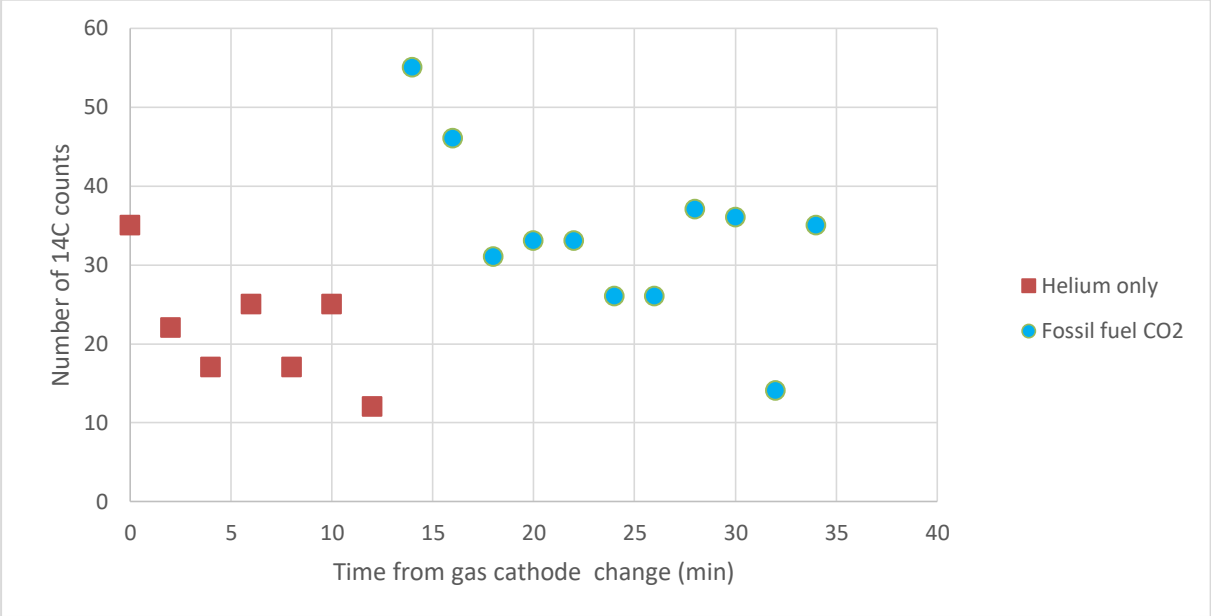

Figure 27: *Number of ^{14}C counts after changing the gas cathode to a new one. Number of counts means the number of counts registered during two minutes. First the gas cathode only had carrier gas helium flowing through it and all the counts measured were contamination from the cathode itself and from the capillary tube. After 12 minutes, the CO_2 fossil fuel background gas was injected. First, a high burst of ^{14}C was detected, but the flow soon stabilized after a few minutes.*

Background measurements were made after using different CO_2 gases. It was seen that gas used earlier will leave some residue inside the capillary tubes. As seen in Figure 28, the number of ^{14}C counts in background will at least briefly depend on the gas used before the change of cathode. In this measurement, the CO_2 gas flow of previous sample was stopped and only helium was let through for a few minutes before changing the gas cathode. Measurement time was started when cathode was changed. OxII (NOX) sample with Fraction Modern of about 1.3 being the previous sample, very high number of ^{14}C was detected up to 10 minutes. When previous sample was humus with Fraction Modern of about 0.66, the number of counts was significantly smaller. This kind of background can be reduced by waiting long enough or possibly by flushing the capillary tube with helium by momentarily

setting the helium pressure to a high value. The small section near the syringe in which helium does not flow is however hard to clean with the current gas system setup and most likely this section causes at least part of the high number of counts for a few minutes after injecting the background gas.

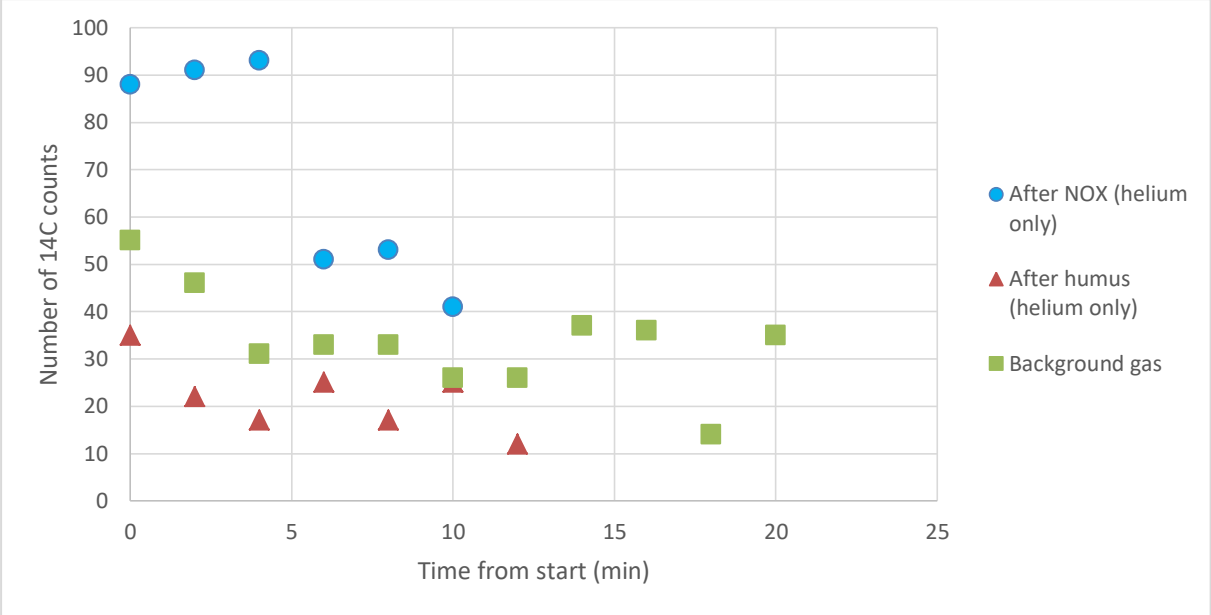

Figure 28: *Number of ^{14}C counts detected in the background. The helium only measurements were initiated after gas cathode change and the background gas measurement after flushing the capillary tube with helium.*

7.2 Standard gas

Measurements were conducted for about 30 minutes for OxII standard and humus and for about 15 minutes for the background gas. Gas cathode was changed between different samples and about 5 minutes were waited between gas cathode change and injection of next sample gas.

From the number of ^{14}C counts, the relative error of the measurement can be calculated by using equation (24). For example, for the humus sample, the statistical counting error is calculated by

$$err = \frac{1}{\sqrt{N}} = \frac{1}{\sqrt{24808}} = 0.0063$$

The $^{14}C/^{13}C$ ratio can be directly taken from the database within a certain time interval and then be used to calculate the $\delta^{13}C$ normalized $^{14}C/^{13}C$ ratio. This is done by using equation (20) for the sample and (21) for the OxII standard. $\delta^{13}C$ values used were -17.6 ‰ for OxII, -28.7 ‰ for humus and -25 ‰ for background gas. Examples with humus and OxII for the calculations are

$$\left(\frac{^{14}C}{^{13}C}\right)_{SN} = \left(\frac{^{14}C}{^{13}C}\right)_{S}\left(\frac{\left(1-\frac{25}{1000}\right)}{\left(1+\frac{\delta^{13}C}{1000}\right)}\right) = 5.14\times10^{-11}\times\left(\frac{\left(1-\frac{25}{1000}\right)}{\left(1+\frac{-28.7}{1000}\right)}\right) = 5.16\times10^{-11}$$

$$\left(\frac{^{14}C}{^{13}C}\right)_{ON} = 0.7459\left(\frac{^{14}C}{^{13}C}\right)_{OxII}\left(\frac{\left(1-\frac{25}{1000}\right)}{\left(1+\frac{\delta^{13}C_{\mathrm{OxII}}}{1000}\right)}\right)$$

$$= 0.7459\times1.02\times10^{-10}\times\left(\frac{\left(1-\frac{25}{1000}\right)}{\left(1+\frac{-17.6}{1000}\right)}\right) = 7.55\times10^{-11}$$

Because the background affects not only the sample but also the OxII standard by giving a too low value in measurements, the ratio of standard gas needs to be corrected for background before using it to calculate Fraction Modern for the actual sample. The Fraction Modern for OxII without activity normalization is 1.3407 and the background reduction is done to this value. First, the Fraction Modern for the background must be calculated. This is done with the non-background-reduced standard with equation (22):

$$F^{14}C_{bg} = \frac{\left(\frac{^{14}C}{^{13}C}\right)_{BGN}}{\left(\frac{^{14}C}{^{13}C}\right)_{ON}} = \frac{1.50\times10^{-12}}{7.55\times10^{-11}} = 0.01987$$

Now the background reduction to the standard can be done by using equation (23):

$$F^{14}C = F^{14}C_m\left[1-F^{14}C_{bg}\left(\frac{1}{F^{14}C_m}-1\right)\right] = 1.3407\times\left[1-0.01987\times\left(\frac{1}{1.3407}-1\right)\right]$$

$$= 1.3474$$

Using this value of Fraction Modern in equation (22), the background-corrected standard $^{14}C/^{13}C$ ratio can be calculated.

$$\left(\frac{^{14}\mathrm{C}}{^{13}\mathrm{C}}\right)_{SN} = \left(\frac{^{14}\mathrm{C}}{^{13}\mathrm{C}}\right)_{ON} \times F^{14}C = 7.55 \times 10^{-11} \times 1.3474 = 1.017 \times 10^{-10}$$

To get the background-corrected standard value, activity reduction still needs to be made:

$$0.7459 \times 1.017 \times 10^{-10} = 7.589 \times 10^{-11}$$

With these values, Fraction Modern can be calculated for the actual humus sample by using equation (22):

$$F^{14}C_m = \frac{\left(\frac{^{14}\mathrm{C}}{^{13}\mathrm{C}}\right)_{SN}}{\left(\frac{^{14}\mathrm{C}}{^{13}\mathrm{C}}\right)_{ON}} = \frac{5.16 \times 10^{-11}}{7.589 \times 10^{-11}} = 0.680$$

The background correction for this Fraction Modern value is done with equation (23):

$$F^{14}C = F^{14}C_m \left[1 - F^{14}C_{bg}\left(\frac{1}{F^{14}C_m} - 1\right)\right] = 0.680 \times \left[1 - 0.01987\left(\frac{1}{0.680} - 1\right)\right] = 0.674$$

The final Fraction Modern values with the measured values and calculated error are listed in Table 5.

Table 5: *The results of measurements with OxII as standard gas and humus as sample. The normalized OxII value is without activity normalization.*

	OxII (Standard gas)	Humus	Background gas
Number of ^{14}C counts	37337	24808	382
Relative error (%)	0.52	0.63	5.1
Measured $^{14}\mathrm{C}/^{13}\mathrm{C}$ ratio	1.02e-10	5.14e-11	1.50e-12
Normalized $^{14}\mathrm{C}/^{13}\mathrm{C}$ ratio	1.01e-10	5.16e-11	1.50e-12
Background-corrected Fraction Modern $F^{14}C$	1.3474	0.6735	0.01987

Fraction Modern value for the humus sample used is 0.658 from literature. The value measured is 2.4% higher than this so this test measurement can be taken as a success. A good number of ^{14}C counts was also got with the 30 minute measurement which made the relative error in the measurement as low as 0.63%.

To find out how much the background affects the measurement, one can compare the $^{14}C/^{13}C$ isotopic ratio of the standard gas with that of the background gas. With the entire part of the background taken into account, the background was 1.47% of the standard gas value. If there is enough gas to wait for a few minutes and let the background stabilize, the background effect was noticed to decrease to 1.28 %. As explained in chapter 7.1, this value might increase even more with normally prepared samples in actual measurements. Background of less than 1% compared to the standard might then be possible but with the measurements conducted this time, about 1.3% is to be expected.

8 Conclusions

The main objective of this thesis was to find out how the variation of different parameters affects the carbon ion current and ionization efficiency in the ion source of University of Helsinki AMS system with CO_2 gas being used as sample. Parameters such as temperature of cesium oven, helium pressure and CO_2 pressure were tested with multiple values and their dependency to each other discussed. Actual sample was measured to see how well the gas system currently works.

With the help of the results it is possible to get a good view on how the different parameters affect the carbon current and ionization efficiency. This helps with further optimization and actual use of the gas system for measurements as the carbon current is much lower with gas samples compared to solid graphite samples. This is why the current and efficiency should be maximized especially for the use of CO_2. When comparing the current system to other hybrid ion sources globally, especially the ionization efficiency seemed very low, implying that the current system still has a lot of room for improvement.

Increasing the amount of cesium was found to increase both carbon current and ionization efficiency in all situations at least up to the highest temperature measured. Increasing CO_2 flow was seen to increase the carbon current but decrease the relative carbon ionization efficiency compared to oxygen. Helium flow was seen to affect results mostly with low CO_2 pressures. Similar behavior with carbon current and ionization efficiency can be found in literature.

Gas system was used to find out practical improvements for easier, faster and more automated use in the future. Ideas to fix pressure problems found with syringe were discussed. Effect of background in AMS measurements was measured with different CO_2 gases, showing that the change of gas cathode and possibly a better flush of capillary tube can significantly reduce background left by previous samples. The level of background was found to be on tolerable levels but a large reduction is still possible to further improve the results.

The basic ideas in Vogel's model were reviewed. It is essential that neutral cesium atoms are excited and can thus give electrons to neutral carbon atoms in cesium plasma near the

cathode. Vogel presents many good points about his theory which explain many things left unclear by previous theories. Vogel's theory can explain some of the optimization results such as competitive ionization of carbon and oxygen. Conversion of CO_2 to CO could improve the ionization, as long as fractionation and loss of carbon can be avoided during the process. Initial plans to test laser excitation of cesium were done and some possible parts selected for the system.

If Vogel's theory is correct as it is, the results can also be applied to other rare isotopes such as ^{26}Al and ^{10}Be to improve their ionization efficiency and currents with better manipulation of excitation states of cesium. This can be achieved with 1) recesses with smaller diameter on cathodes, 2) using correct cathode materials to avoid competitive ionization and 3) with lasers with correct photon energies to excite suitable resonant electron states in cesium.

References

[1] Hua Q 2009 Radiocarbon: A chronological tool for the recent past *Quat. Geochronol.* **4** 378–90

[2] Tuniz C, Kutschera W, Bird J R, Fink D and Herzog G F 1998 Accelerator mass spectrometry: Ultrasensitive Analysis for Global Science *CRC Press, Boca Raton*

[3] Bronk Ramsey C and Hedges R E M 1997 Hybrid ion sources: Radiocarbon measurements from microgram to milligram *Nucl. Instruments Methods Phys. Res. Sect. B Beam Interact. with Mater. Atoms* **123** 539–45

[4] Middleton R 1984 A review of ion sources for accelerator mass spectrometry *Nucl. Instruments Methods Phys. Res. Sect. B Beam Interact. with Mater. Atoms* **5** 193–9

[5] Olsson I 1968 Modern aspects of radiocarbon datings *Earth-Science Rev.* **19** 203–18

[6] Bronk Ramsey C 2008 Radiocarbon dating: Revolutions in understanding *Archaeometry* **50** 249–75

[7] Pandow M, Mackay C and Wolfgang R 1960 The reaction of atomic carbon with oxygen: significance for the natural radio-carbon cycle *J. Inorg. Nucl. Chem.* **14** 153–8

[8] Bronk Ramsey C, Brenninkmeijer C A M, Jöckel P, Kjeldsen H and Masarik J 2007 Direct measurement of the radiocarbon production at altitude *Nucl. Instruments Methods Phys. Res. Sect. B Beam Interact. with Mater. Atoms* **259** 558–64

[9] Van Strydonck M 2017 Radiocarbon Dating *Top. Curr. Chem.* **374** 347–64

[10] Libby W F 1960 Radiocarbon dating *Nobel Lect.* 593–610

[11] Godwin H 1962 Half-life of Radiocarbon *Nature* **195** 984–984

[12] Currie L a. 2004 The remarkable metrological history of radiocarbon dating [II] *J. Res. Natl. Inst. Stand. Technol.* **109** 185

[13] Stenström K E, Skog G, Georgiadou E, Genberg J and Johansson A 2011 *A guide to radiocarbon units and calculations (*Unpublished laboratory report*)*

[14] Theodorsson P 1991 Gas Proportional Versus Liquid Scintillation Counting, Radiometric Versus AMS Dating *Radiocarbon* **33** 9–13

[15] Hua Q, Zoppi U, Williams A A and Smith A M 2004 Small-mass AMS radiocarbon analysis at ANTARES *Nucl. Instruments Methods Phys. Res. Sect. B Beam Interact. with Mater. Atoms* **223–224** 284–92

[16] Palonen V and Tikkanen P 2015 A novel upgrade to Helsinki AMS: Fast switching of isotopes with electrostatic deflectors *Nucl. Instruments Methods Phys. Res. Sect. B Beam Interact. with Mater. Atoms* **361** 263–6

[17] Stuiver M and Polach H A 1977 Radiocarbon *Radiocarbon* **19** 355–63

[18] Donahue D J, Linick T W and Jull a. J T 1990 Isotope-Ratio and Background Corrections for Accelerator Mass Spectrometry Radiocarbon Measurements *Radiocarbon* **32** 135–42

[19] Beta Analytic Inc. Introduction to Radiocarbon Determination by the Accelerator Mass Spectrometry Method *http://www.radiocarbon.com/PDF/Beta-AMS-Methodology.pdf*

[20] Muller R A 1977 Radioisotope Dating with a Cyclotron *Science* **196** 489–94

[21] Nelson D E, Korteling R G and Stott W R 1977 Carbon-14: Direct Detection at Natural Concentrations *Science* **198** 507–8

[22] Bennett C L, Beukens R P, Clover M R, Gove H E, Liebert R B, Litherland A E, Purser K H and Sondheim W E 1977 Radiocarbon Dating Using Electrostatic Accelerators: Negative Ions Provide the Key *Science* **198** 508–10

[23] National Electrostatics Corporation *http://www.pelletron.com/negion.htm*

[24] Tikkanen P, Palonen V, Jungner H and Keinonen J 2004 AMS facility at the University of Helsinki *Nucl. Instruments Methods Phys. Res. Sect. B Beam Interact. with Mater. Atoms* **223–224** 35–9

[25] Palonen V 2008 *Accelerator mass spectrometry and Bayesian data analysis* (Academic dissertation, University of Helsinki)

[26] Hofmann H J, Bonani G, Suter M and Wölfli W 1987 Charge state distributions and isotopic fractionation *Nucl. Instruments Methods Phys. Res. Sect. B Beam Interact. with Mater. Atoms* **29** 100–4

[27] Rantanen A 2014 *AMS-ionilähteen kaasunsyöttölinjan automatisointi* (Unpublished student report, in Finnish, Metropolia Ammattikorkeakoulu)

[28] Vogel J S, Giacomo J A and Dueker S R 2012 Measurement of Absolute Carbon Isotope Ratios: Mechanisms and Implications *AGU Fall Meet. Abstr.*

[29] Vogel J S 2013 Neutral resonant ionization in the high-intensity cesium sputter source *AIP Conf. Proc.* **1515** 89–98

[30] Middleton R and Klein J 1999 Production of metastable negative ions in a cesium sputter source: Verification of the existence of N 2 − and CO − *Phys. Rev. A* **60** 3786–99

[31] Vora R B, Turner J E and Compton R N 1974 Single-electron excitation and transfer in collisions of alkali-metal and oxygen atoms *Phys. Rev. A* **9** 2532–44

[32] Dutta N, Tkach R, Frohlich D, Tang C L, Mahr H and Hartman P L 1979 Resonance charge transfer from a photoexcited donor state *Phys. Rev. Lett.* **42** 175–8

[33] Vogel J S 2015 Anion formation by neutral resonant ionization *Nucl. Instruments Methods Phys. Res. Sect. B Beam Interact. with Mater. Atoms* **361** 156–62

[34] Weber K-H and Sansonetti C J 1987 Accurate energies of nS , nP , nD , nF , and nG levels of neutral cesium *Phys. Rev. A* **35** 4650–60

[35] National Institute of Standards and Technology NIST Energy Levels of Neutral Cesium (Cs I) *https://physics.nist.gov/PhysRefData/Handbook/Tables/cesiumtable5.htm*

[36] Vogel J S 2016 Anion formation in sputter ion sources by neutral resonant ionization *Rev. Sci. Instrum.* **87,** 02A504

[37] Vogel J S The " Negative Ion Cookbook " Viewed through Neutral Resonant Ionization *http://www.c-ad.bnl.gov/icis2015/abstracts/TuePE34%20Vogel%20John%20S.%20The%20Negative*

%20Ion%20Cookbook%20Viewed%20through%20Neutral%20Resonant%20Ionization%20C08%20Poster%20TuePE34.pdf

[38] Sansonetti J E 2009 Wavelengths, transition probabilities, and energy levels for the spectra of cesium (Cs I-Cs LV) *J. Phys. Chem. Ref. Data* **38** 761–923

[39] Schultz J T, Abend S, Doring D, Debs J E, Altin P a, White J D, Robins N P and Close J D 2009 Coherent 455 nm beam production in a cesium vapor *Opt. Lett.* **34** 2321–3

[40] Palonen V and Tikkanen P 2017 Automatic Optimization of AMS with LabVIEW *Radiocarbon* **59** 915–20

[41] Uhl T, Kretschmer W, Luppold W and Scharf A 2004 Direct Coupling of an Elemental Analyzer and a Hybrid Ion Source for AMS Measurements *Radiocarbon* **46** 65–75

[42] Fahrni S M, Wacker L, Synal H A and Szidat S 2013 Improving a gas ion source for 14C AMS *Nucl. Instruments Methods Phys. Res. Sect. B Beam Interact. with Mater. Atoms* **294** 320–7

[43] Xu S, Dougans A, Freeman S P H T, Maden C and Loger R 2007 A gas ion source for radiocarbon measurement at SUERC *Nucl. Instruments Methods Phys. Res. Sect. B Beam Interact. with Mater. Atoms* **259** 76–82

[44] Uhl T, Kretschmer W, Luppold W and Scharf A 2005 AMS measurements from microgram to milligram *Nucl. Instruments Methods Phys. Res. Sect. B Beam Interact. with Mater. Atoms* **240** 474–7

[45] Bronk Ramsey C, Ditchfield P and Humm M 2004 Using a Gas Ion Source for Radiocarbon Ams and Gc-Ams *Radiocarbon* **46** 25–32

Appendices

Appendix A Manual for Gas UI

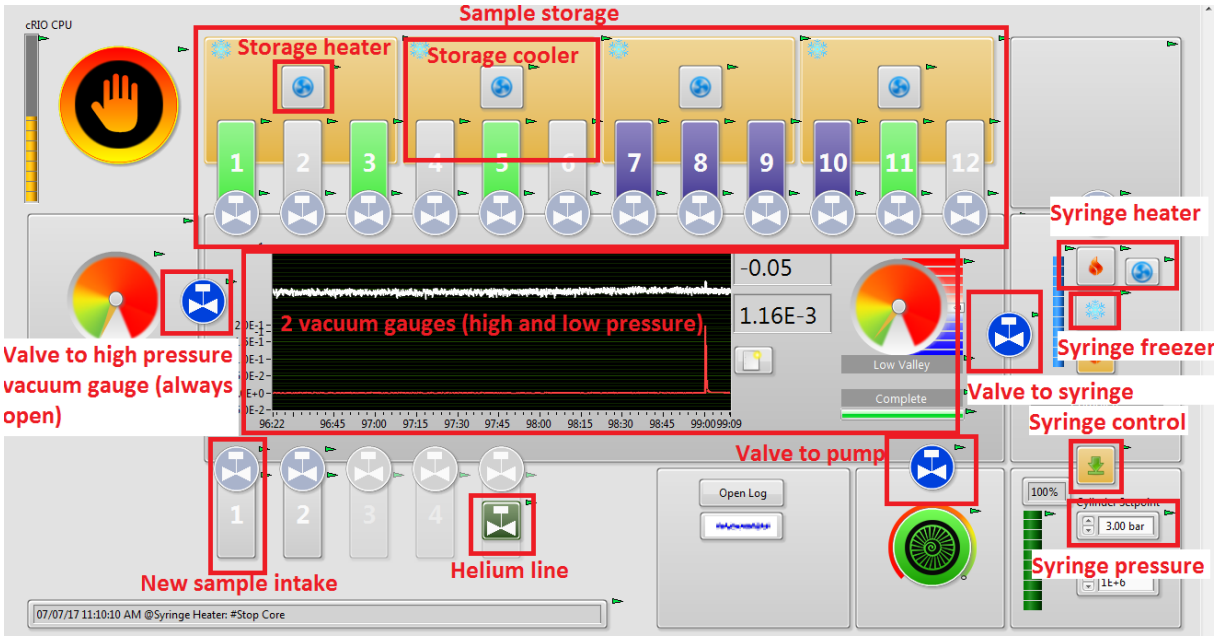

Appendix B Manual for starting and stopping the gas system

Starting up the equipment

1. Open the AMS Gas UI from the desktop (if not already open)
2. Close any active coolers so that they are all yellow (off)

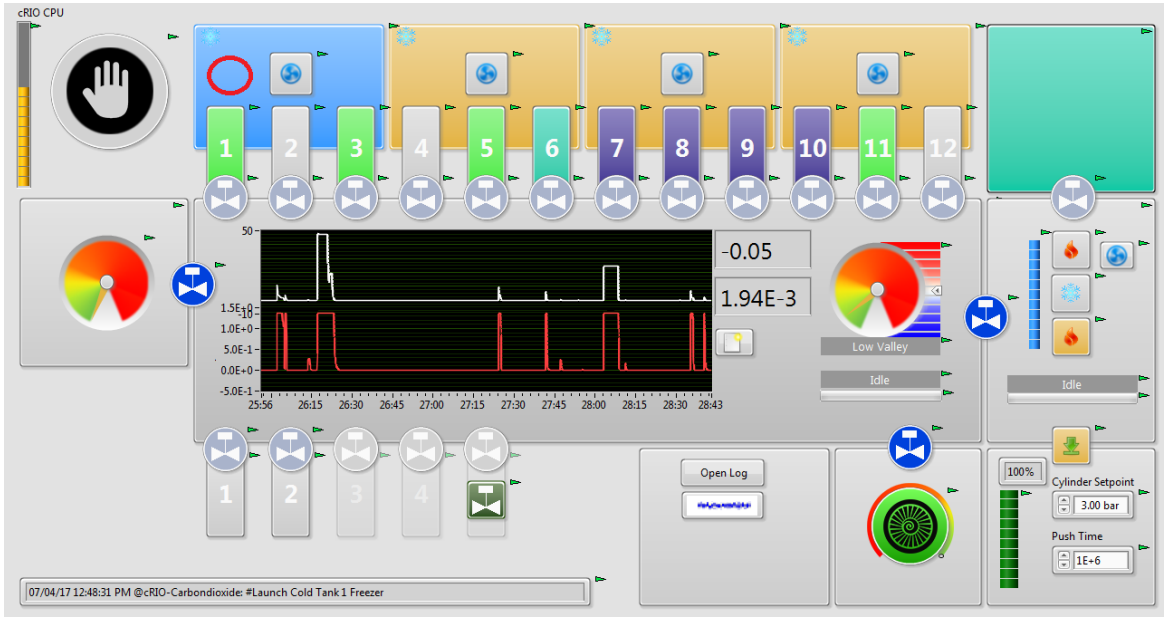

3. Open the manual liquid nitrogen valve
4. Close all valves except the ones to vacuum gauge and to turbo pump.

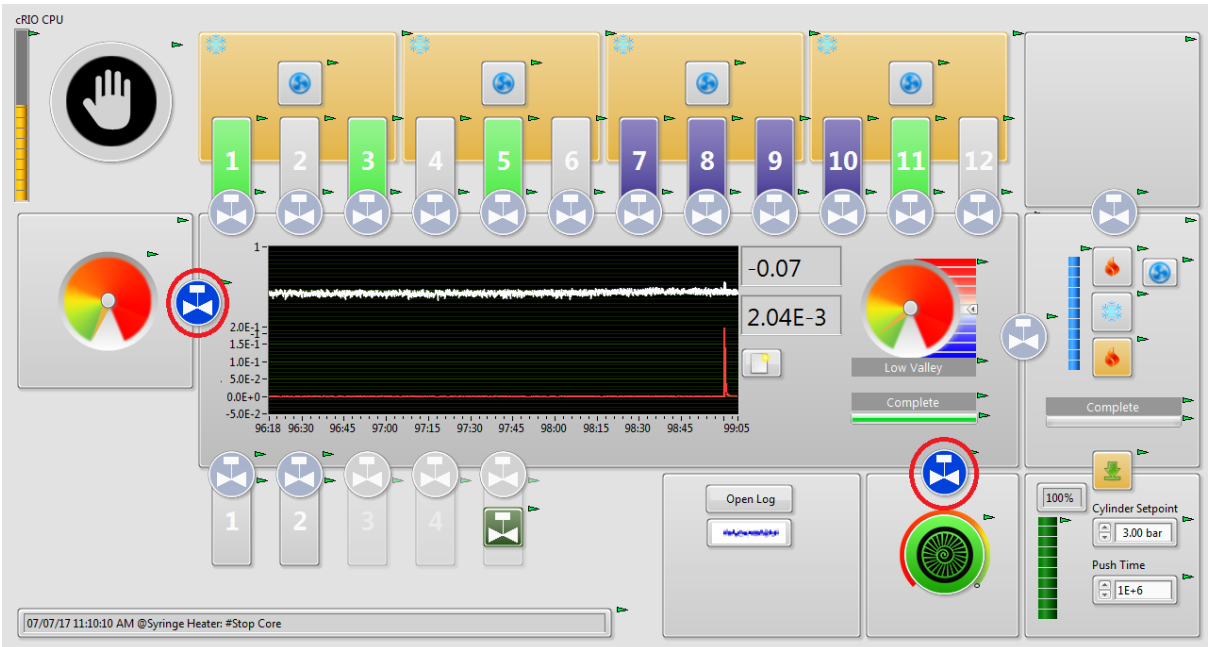

Shutting down the equipment

1. Open the valve between sample line and pressure gauge and the valve to syringe. Make sure all other valves are closed. Then open valve to pump.

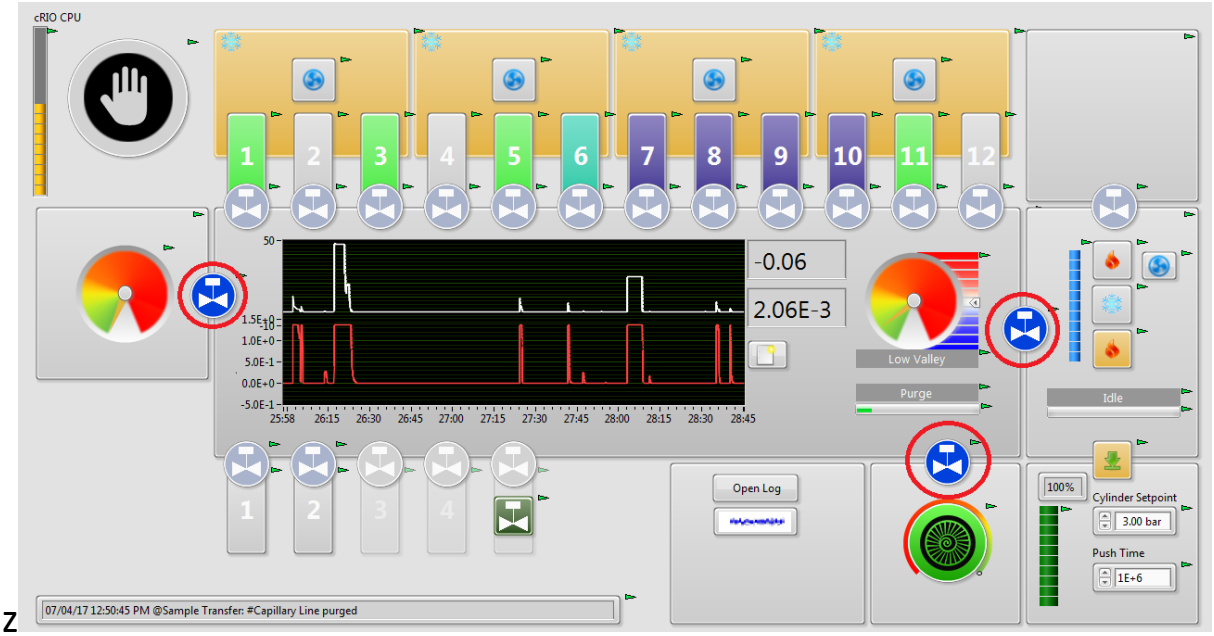

Z

2. Make sure all the coolers and heaters are off except the syringe bottom heater.
3. Close the manual valve to liquid nitrogen.
4. Open one cooler and leave it open.

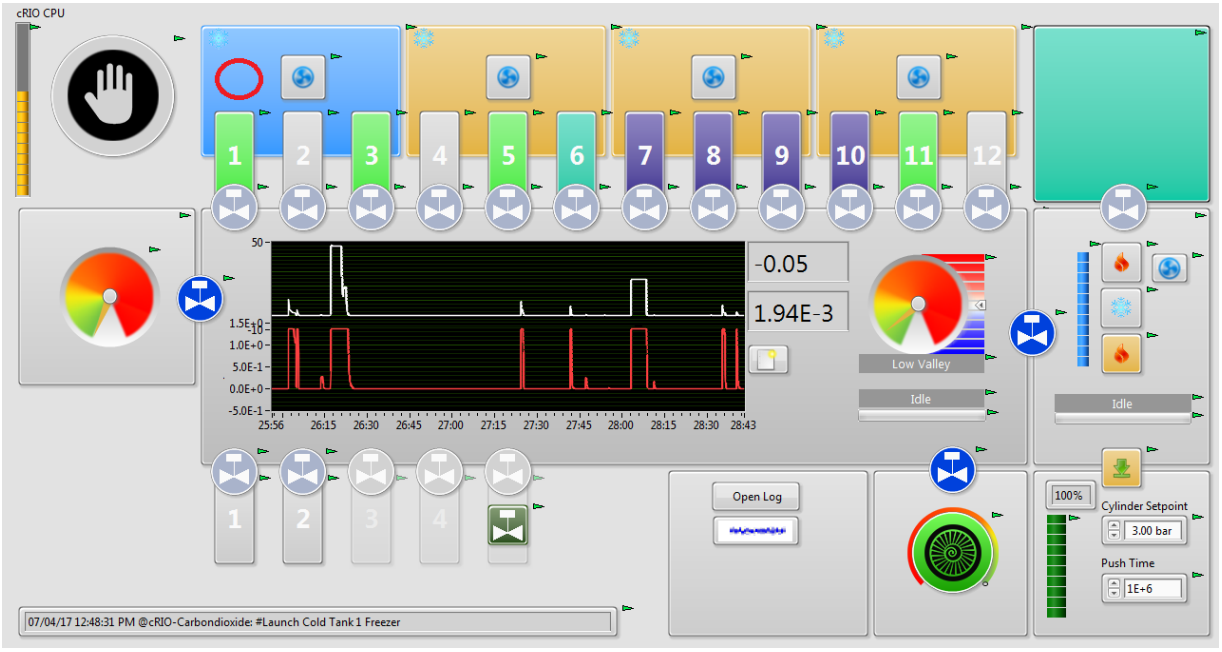

Moving a sample from container to storage:

1. Attach the container to intake. Do not open the container valve.
2. Choose an empty storage (grey). Click to open the valve between it and the sample line. Then open the valve to pump it clean. Once the pressure has dropped to around 1.0E-3 mbar and the color of storage and sample line have turned grey, close the 2 valves again.

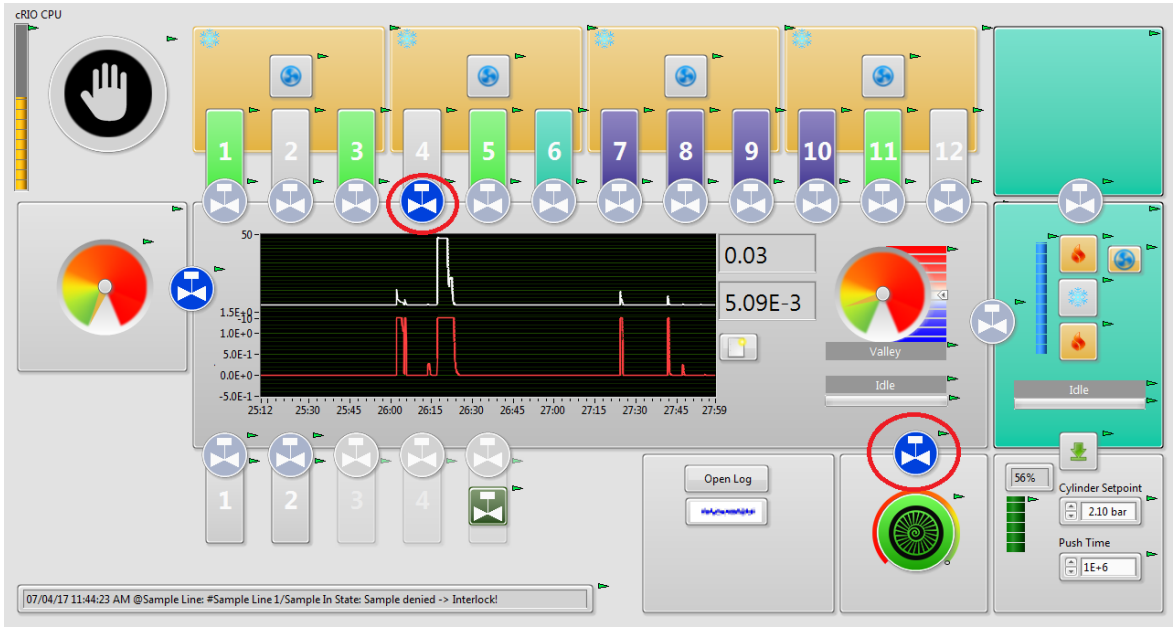

3. Make sure only the valve between pressure gauges is open.

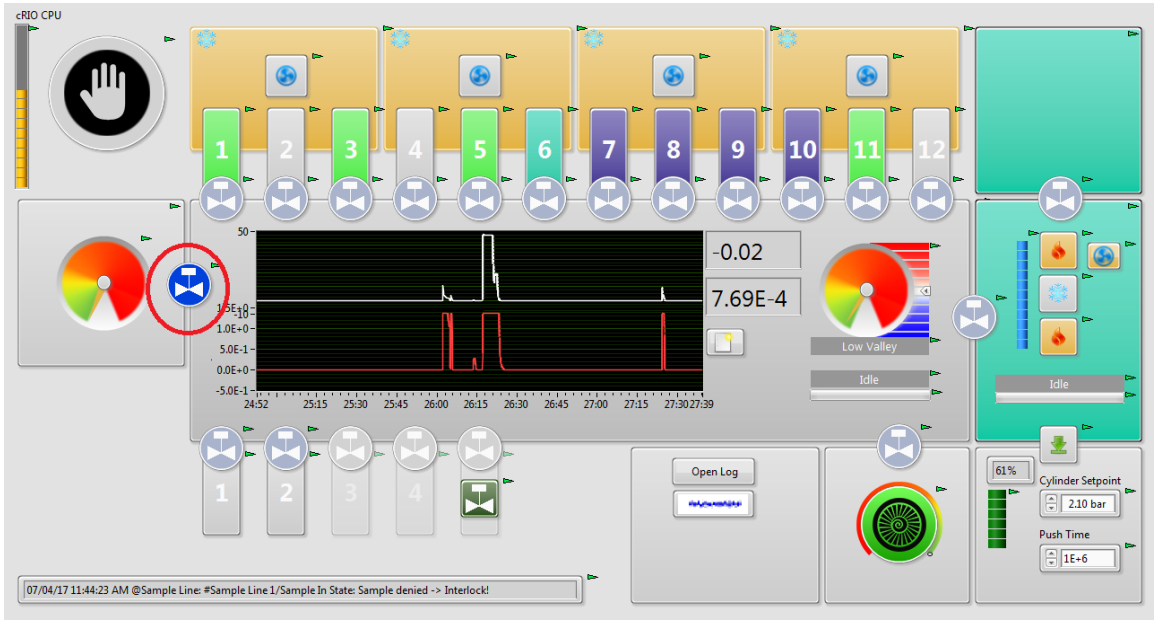

4. Click the sample container 1. Once a window opens, click the SampleIn button and then OK.

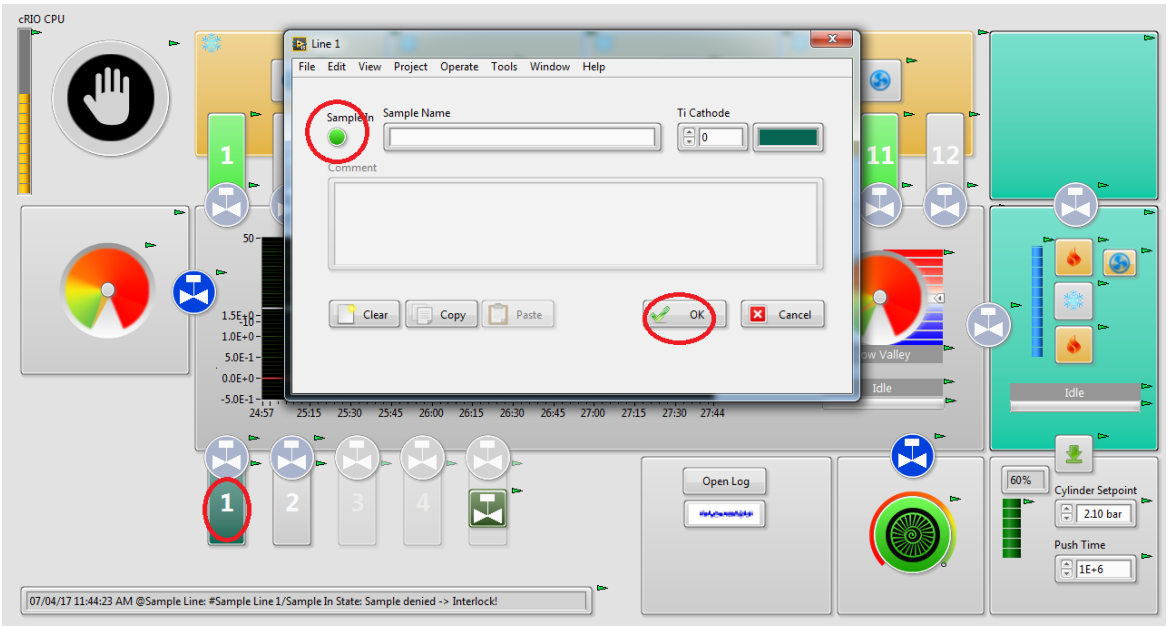

5. Click the valve between container and sample line. Keep the manual valve on the container closed. Then pump the sample line until it and the container turn grey.

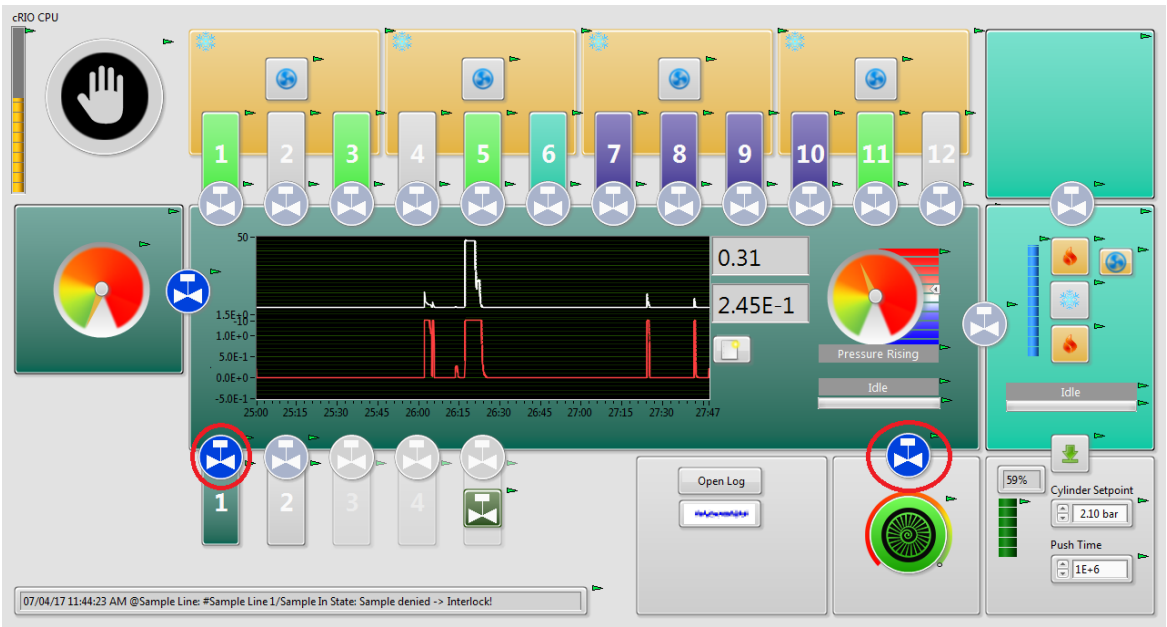

6. Once both the container and sample line are grey, close the two valves opened above. Then click container 1 and name the real sample and give it a color (Ti cathode number). Click OK.

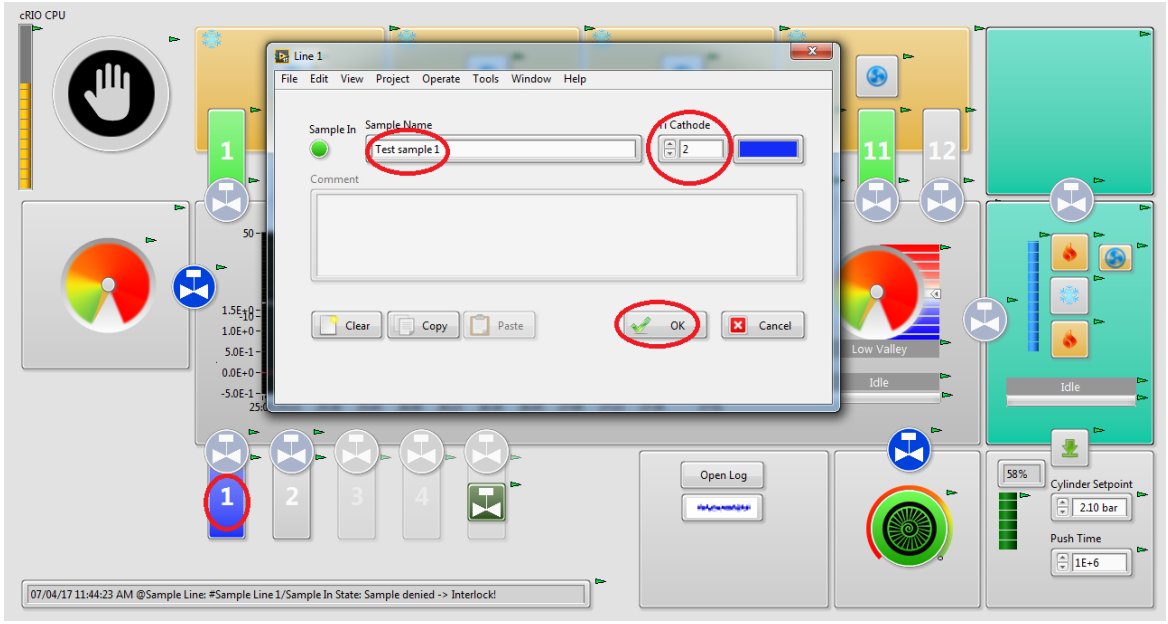

7. Open the manual valve on the container. Then click the valve between container and sample line. Make sure only this and the vacuum gauge valves are open.

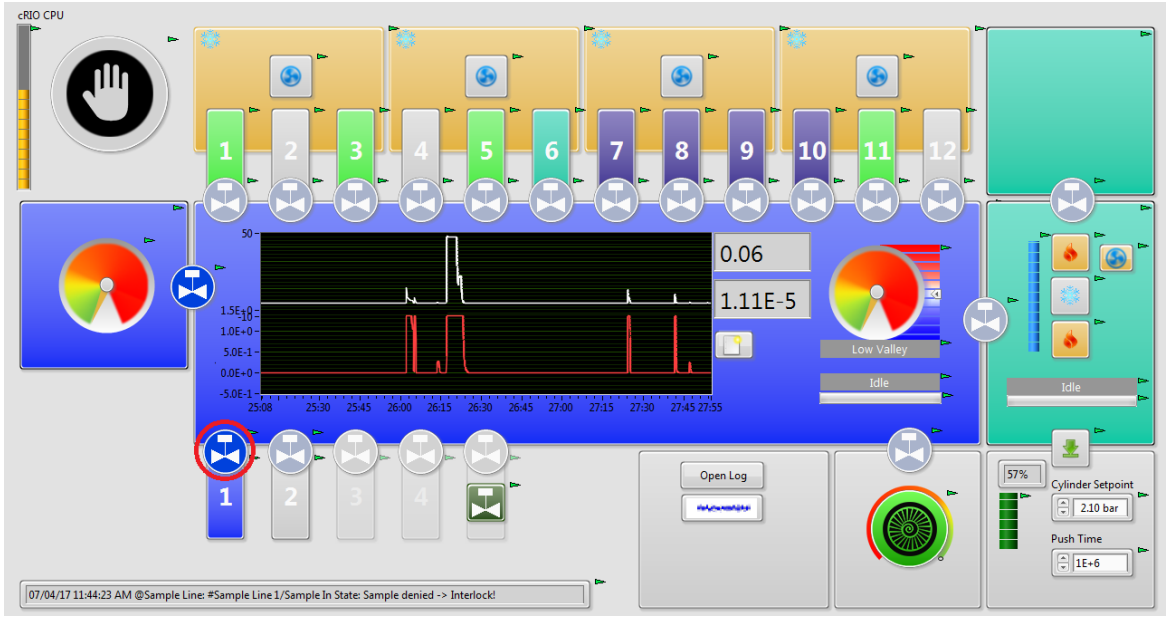

8. Open the storage valve which was pumped earlier. Start cooling for that container. Wait until the pressure has gone down and is stabilized. “Plateau” should appear next to the pressure values.

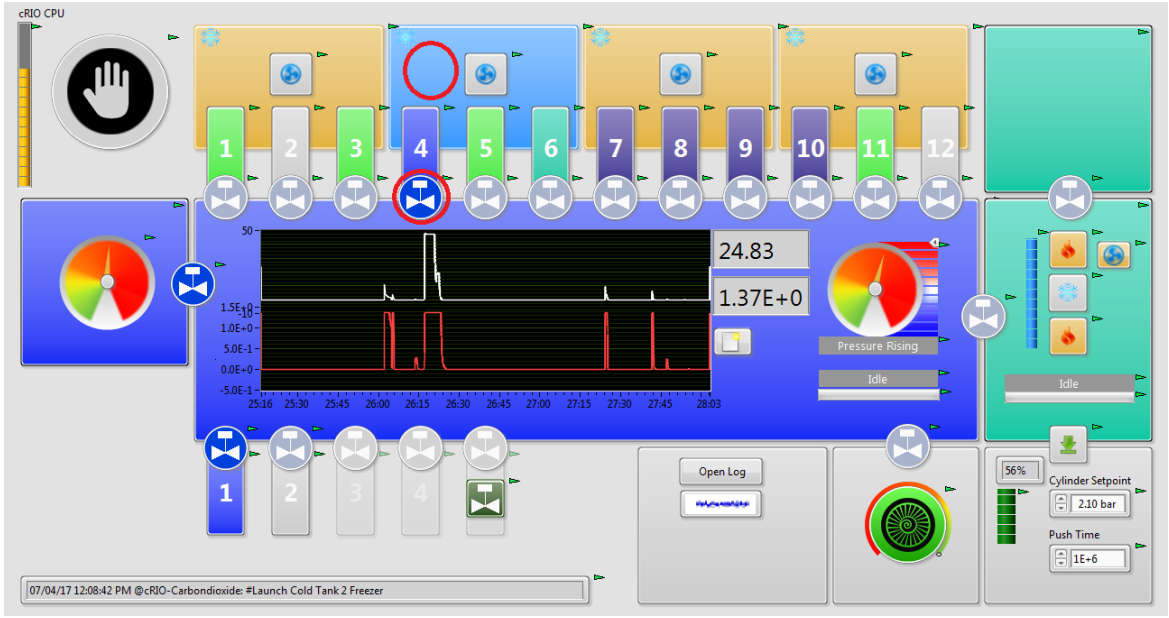

9. Once the all the sample has moved to the storage, close the two valves, stop the cooler and open the valve to pump the storage line.

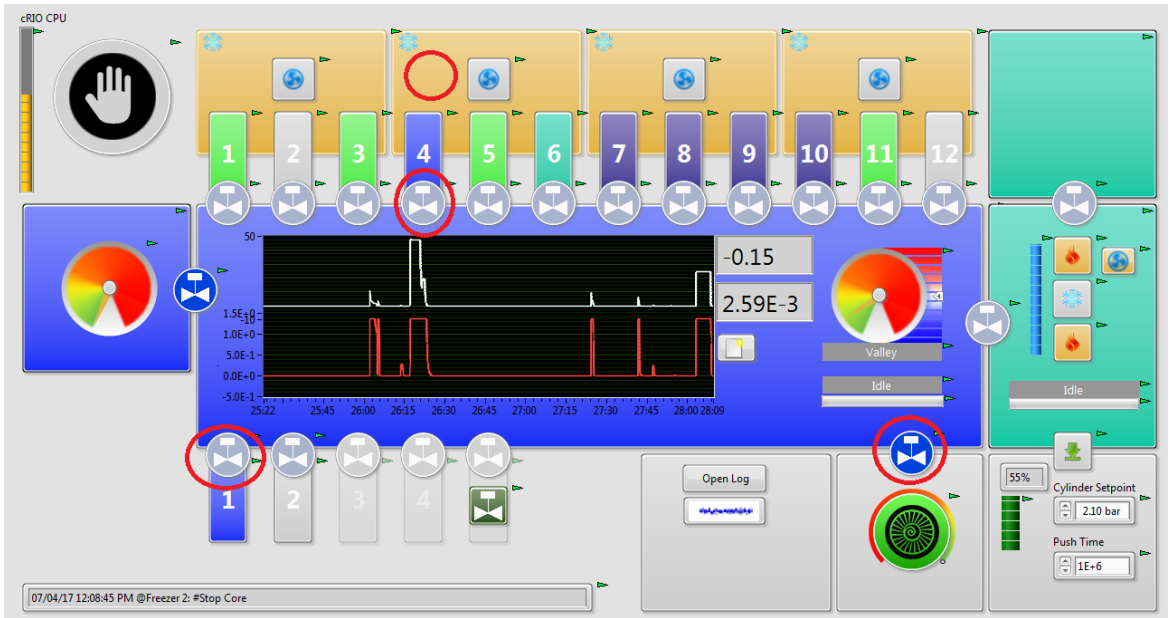

10. Click the container 1 and once the window opens, click clear and then OK. After this, close the manual valve on the container. Then you can remove the container from the intake.

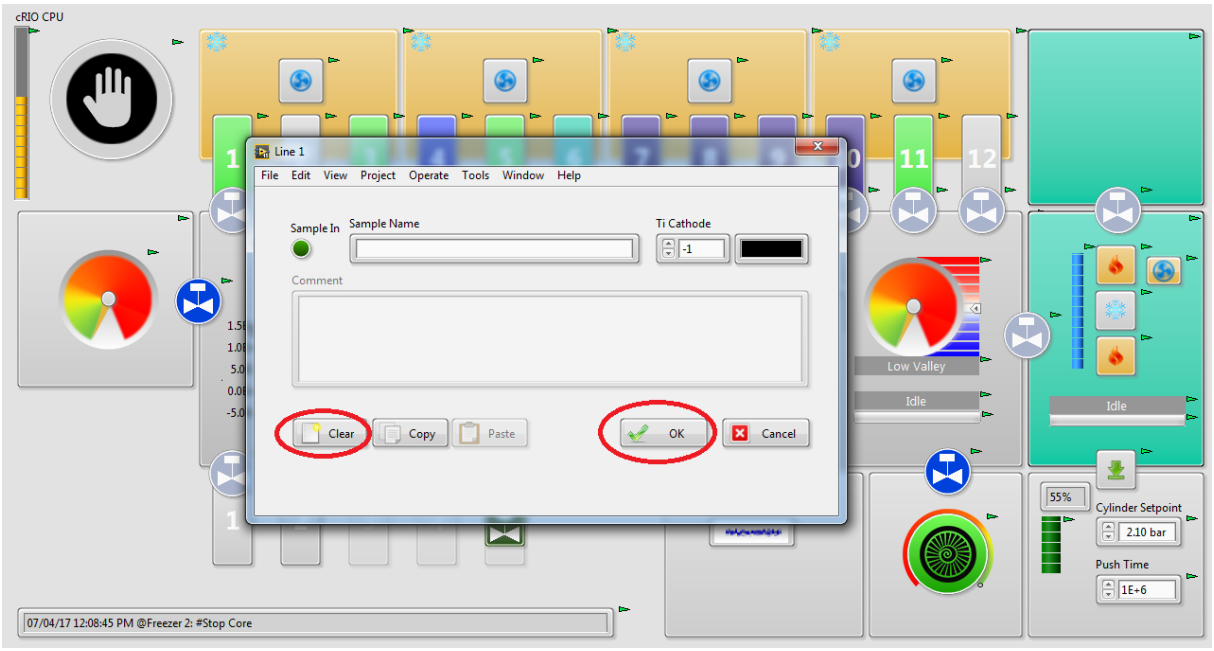

Manual to measure a sample from a storage

1. Open the Gas Transfer control (on desktop if not open already)
2. Make sure liquid nitrogen valve is open and ion source is ready or almost ready for measurements.
3. Check that helium pressure is correct (1 bar?) and adjust if needed
4. Choose correct pressure for syringe (Cylinder Setpoint). For example 3.0 bar for large samples, 2.3 bar for small samples.
5. Choose the sample you want to measure and insert it to Source Container. Make sure Target Container is Syringe.

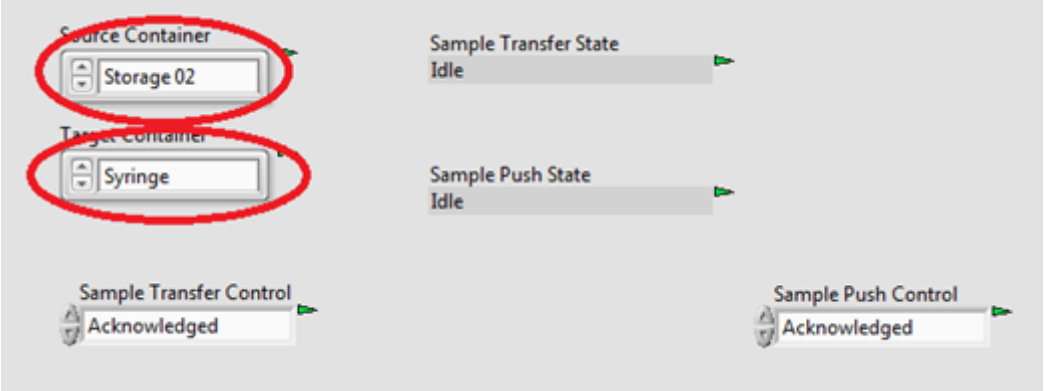

6. Click Sample Transfer Control and choose Transfer. This should take about 20 minutes.

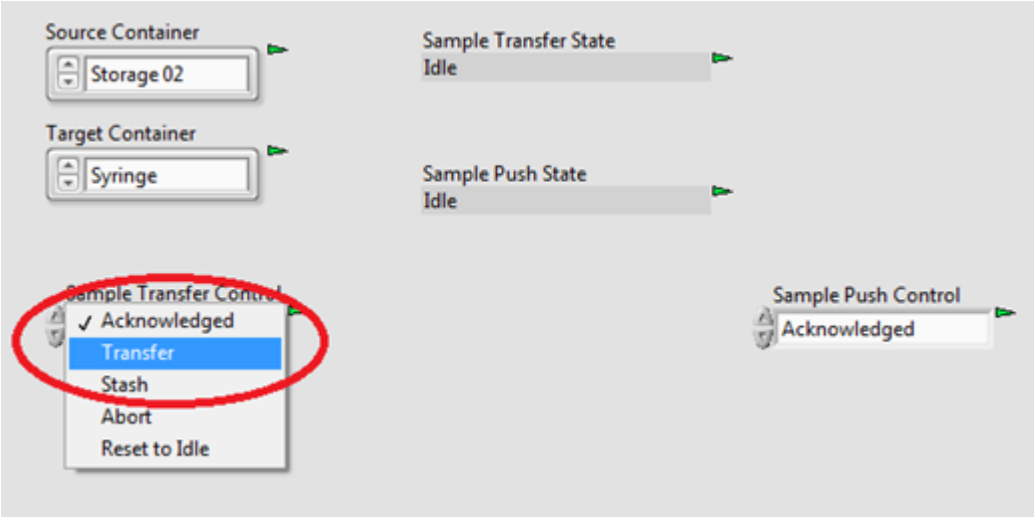

7. Once the transfer is complete, Sample Push State should say “Ready to push”. From the Sample Push Control, choose Push. The syringe will start pushing the gas towards the ion source.

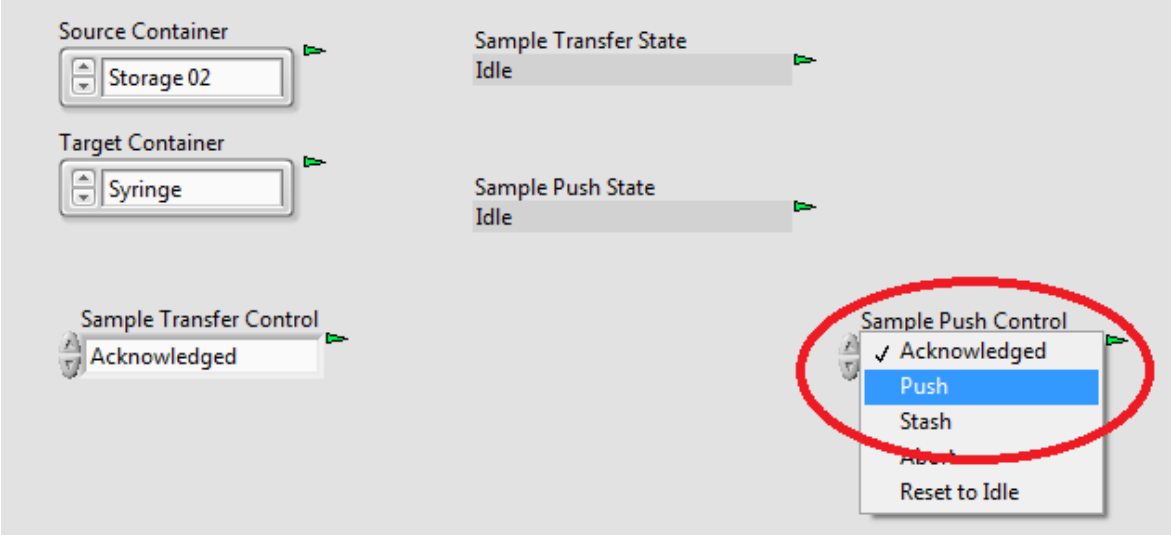

8. If you want to put the remaining sample back to storage, choose Stash from the Sample Push Control. After this you are ready.
9. If the syringe is empty or you want to remove the remaining sample, Choose Abort and then Reset to idle. Then on the UI, click to pull syringe down and open the valve to syringe and then to pump. Also close the top heater on the syringe.